

SIEMENS

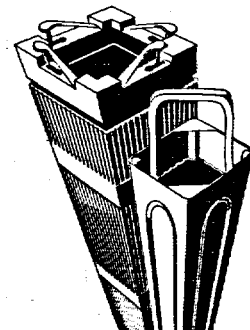
EMF-2310(NP)
Revision 0

SRP Chapter 15 Non-LOCA Methodology for Pressurized Water Reactors

November 1999

Siemens Power Corporation

Nuclear Division



**SRP Chapter 15 Non-LOCA Methodology for
Pressurized Water Reactors**

Prepared: Ken Greene 11/12/99
K. F. Greene, Staff Engineer
Safety Analysis Methods Date

Contributed: P. Boylan (Touch Base Computing), C. D. Fletcher, T. R. Lindquist, L. H. Nielson
(Rowe & Associates), W. T. Nutt, D. L. Redinger, B. A. Reeves, B. D. Stitt,
E. L. Tolman, G. S. Uyeda

Reviewed: J. M. Kelly 11/18/99
J. M. Kelly, Staff Engineer
Safety Analysis Methods Date

Concurred: J. F. Mallay Jr 11/15/99
J. F. Mallay, Director
Regulatory Affairs Date

Approved: R. E. Collingham 11/12/99
R. E. Collingham, Manager
Safety Analysis Methods Date

Approved: David M. Brown 11/17/99
D. M. Brown, Manager
PWR Neutronics Date

Approved: R. C. Gottula 11/17/99
R. C. Gottula, Manager
PWR Safety Analysis Date

Approved: Ralph Grummer 17 Nov 99
R. G. Grummer, Manager
Neutronic Analysis Methods Date

Approved: Polin L. Feuerbacher 11/15/99
R. L. Feuerbacher, Vice President
Engineering Date

**U.S. Nuclear Regulatory Commission
Report Disclaimer**

Important Notice Regarding the Contents and Use of This Document

Please Read Carefully

This technical report was derived through research and development programs sponsored by Siemens Power Corporation. It is being submitted by Siemens Power Corporation to the U.S. Nuclear Regulatory Commission as part of a technical contribution to facilitate safety analyses by licensees of the U.S. Nuclear Regulatory Commission which utilize Siemens Power Corporation fabricated reload fuel or technical services provided by Siemens Power Corporation for light water power reactors and it is true and correct to the best of Siemens Power Corporation's knowledge, information, and belief. The information contained herein may be used by the U.S. Nuclear Regulatory Commission in its review of this report and, under the terms of the respective agreements, by licensees or applicants before the U.S. Nuclear Regulatory Commission which are customers of Siemens Power Corporation in their demonstration of compliance with the U.S. Nuclear Regulatory Commission's regulations.

Siemens Power Corporation's warranties and representations concerning the subject matter of this document are those set forth in the agreement between Siemens Power Corporation and the Customer pursuant to which this document is issued. Accordingly, except as otherwise expressly provided in such agreement, neither Siemens Power Corporation nor any person acting on its behalf:

- a. makes any warranty, or representation, express or implied, with respect to the accuracy, completeness, or usefulness of the information contained in this document, or that the use of any information, apparatus, method, or process disclosed in this document will not infringe privately owned rights;

or

- b. assumes any liabilities with respect to the use of, or for damages resulting from the use of, any information, apparatus, method, or process disclosed in this document.

Nature of Changes

<u>Item</u>	<u>Page(s)</u>	<u>Description and Justification</u>
1.	All	This is a new document.

Contents

1.0	Introduction.....	1-1
2.0	Summary of Results	2-1
3.0	S-RELAP5 Modeling.....	3-1
3.1	System Modeling	3-1
3.2	Fuel Modeling	3-2
3.3	Summary of Code Differences Between S-RELAP5 and ANF-RELAP	3-5
4.0	LOFT Non-LOCA Transient Calculation.....	4-1
4.1	LOFT S-RELAP5 Model Description	4-1
4.2	LOFT L6-1 Loss of Load	4-4
4.3	LOFT L6-2 Loss of Primary Flow.....	4-16
4.4	LOFT L6-3 Excessive Steam Load.....	4-30
4.5	LOFT L6-5 Loss of Feedwater	4-42
4.6	LOFT Analysis Conclusions	4-53
5.0	Event-Specific Methodology	5-1
5.1	Scope of Application	5-1
5.2	Application Process.....	5-3
5.2.1	Disposition of Events.....	5-3
5.2.2	Analysis Assumptions	5-4
5.3	Biasing of Parameters.....	5-4
5.4	Main Steamline Break (MSLB)	5-6
5.4.1	Methodology Overview.....	5-7
5.4.2	Description of Methodology	5-10
5.4.3	S-RELAP5 NSSS Model	5-13
5.4.4	Core Neutronics Model.....	5-20
5.4.5	Core Thermal-Hydraulic Model.....	5-21
5.4.6	Reactivity Comparison	5-21
5.4.7	MDNBR and FCM Analysis	5-22
5.5	Steam Generator Tube Rupture (SGTR).....	5-27
5.6	CVCS Malfunction That Results in a Decrease in the Boron Concentration in the Reactor Coolant (Boron Dilution)	5-30
5.7	Inadvertent Loading and Operation of a Fuel Assembly in an Improper Location (Misloaded Assembly)	5-35
5.8	Control Rod Ejection	5-37
5.9	Radiological Consequences of the Failure of Small Lines Carrying Primary Coolant Outside Containment	5-38
6.0	Sample SRP Transients	6-1
6.1	Pre-Scram Main Steamline Break (MSLB)	6-8
6.2	Post-Scram Main Steamline Break (MSLB).....	6-22
6.3	Loss of External Load (LOEL)	6-38
6.4	Loss of Normal Feedwater (LONF) Flow	6-49
6.5	Loss of Forced Reactor Coolant Flow (LOCF).....	6-60

6.6	Uncontrolled Control Rod Bank Withdrawal (UCBW) at Power	6-70
6.7	Steam Generator Tube Rupture (SGTR).....	6-81
7.0	References.....	7-1

Tables

2.1	Applicable SRP Chapter 15 Events	2-3
2.2	Summary of Key Parameters.....	2-5
4.1	LOFT L6-1 Event Sequence	4-7
4.2	LOFT L6-2 Event Sequence	4-19
4.3	LOFT L6-3 Event Sequence	4-32
4.4	LOFT L6-5 Event Sequence	4-44
6.1	Sample Problem Initial Conditions	6-2
6.2	Pre-Scram MSLB Event Summary.....	6-11
6.3	Post-Scram MSLB Event Summary	6-26
6.4	LOEL/TT Event Summary.....	6-41
6.5	LONF Event With Offsite Power Available Event Summary	6-53
6.6	LOCF Event Summary.....	6-63
6.7	DNB-Limiting UCBW at Power Event Summary.....	6-73
6.8	SGTR Event Summary	6-84

Figures

4.1	S-RELAP5 Nodalization Schematic for LOFT Experiments	4-3
4.2	LOFT L6-1 Steam Generator Level.....	4-8
4.3	LOFT L6-1 Pressurizer Liquid Level	4-9
4.4	LOFT L6-1 Pressurizer Pressure	4-10
4.5	LOFT L6-1 Steam Generator Secondary Pressure	4-11
4.6	LOFT L6-1 Reactor Power.....	4-12
4.7	LOFT L6-1 Hot Leg Temperature	4-13
4.8	LOFT L6-1 Cold Leg Temperature.....	4-14
4.9	LOFT L6-1 Steam Generator Steam Flow	4-15
4.10	LOFT L6-2 Reactor Coolant Mass Flow Rate	4-20
4.11	LOFT L6-2 Steam Generator Liquid Level	4-21
4.12	LOFT L6-2 Pressurizer Liquid Level	4-22
4.13	LOFT L6-2 Pressurizer Pressure	4-23
4.14	LOFT L6-2 Steam Generator Secondary Pressure	4-24
4.15	LOFT L6-2 Reactor Power.....	4-25
4.16	LOFT L6-2 Hot Leg Temperature	4-26
4.17	LOFT L6-2 Cold Leg Temperature.....	4-27
4.18	LOFT L6-2 Steam Generator Steam Flow Rate	4-28
4.19	LOFT L6-2 RCP Speed	4-29
4.20	LOFT L6-3 Secondary Feedwater Flow Rate.....	4-33
4.21	LOFT L6-3 Steam Generator Secondary Side Liquid Level	4-34
4.22	LOFT L6-3 Pressurizer Liquid Level	4-35
4.23	LOFT L6-3 Pressurizer Pressure	4-36
4.24	LOFT L6-3 Steam Generator Secondary Pressure	4-37
4.25	LOFT L6-3 Reactor Power.....	4-38
4.26	LOFT L6-3 Hot Leg Temperature	4-39
4.27	LOFT L6-3 Cold Leg Temperature.....	4-40
4.28	LOFT L6-3 Steam Generator Steam Flow	4-41
4.29	LOFT L6-5 Steam Generator Secondary Side Liquid Level	4-45
4.30	LOFT L6-5 Pressurizer Liquid Level	4-46
4.31	LOFT L6-5 Pressurizer Pressure	4-47
4.32	LOFT L6-5 Steam Generator Secondary Pressure	4-48
4.33	LOFT L6-5 Reactor Power.....	4-49
4.34	LOFT L6-5 Hot Leg Temperature	4-50
4.35	LOFT L6-5 Cold Leg Temperature.....	4-51
4.36	LOFT L6-5 Steam Generator Steam Flow	4-52
5.1	SPC Steamline Break Methodology.....	5-9
5.2	Core Model for CE Plant.....	5-24
5.3	Core Model for Three-Loop Westinghouse Plant	5-25
5.4	[] for Three-Loop Westinghouse Plant.....	5-26
6.1	Sample Problem Vessel Nodalization	6-3
6.2	Sample Problem Reactor Coolant System Piping Nodalization.....	6-4
6.3	Sample Problem SG and Secondary Nodalization	6-5
6.4	Sample Problem Vessel Nodalization for MSLB	6-6
6.5	Sample Problem Steam Generator and Secondary Nodalization for MSLB	6-7
6.6	Pre-Scram MSLB Break and Turbine Steam Flow Rates.....	6-12
6.7	Pre-Scram MSLB Steam Generator Pressures.....	6-13

6.8	Pre-Scram MSLB Steam Generator Heat Transfer Rates.....	6-14
6.9	Pre-Scram MSLB Calculated Reactor, Indicated Nuclear, and Indicated Thermal Core Powers.....	6-15
6.10	Pre-Scram MSLB Average Fuel Rod Heat Flux.....	6-16
6.11	Pre-Scram MSLB Peak Fuel Centerline Temperature.....	6-17
6.12	Pre-Scram MSLB RCS Hot Leg and Cold Leg Temperatures.....	6-18
6.13	Pre-Scram MSLB Pressurizer Pressure.....	6-19
6.14	Pre-Scram MSLB Reactivity Components.....	6-20
6.15	Pre-Scram MSLB Core Inlet Flow Rate.....	6-21
6.16	Post-Scram MSLB Break Flow Rates.....	6-27
6.17	Post-Scram MSLB Steam Generator Pressures.....	6-28
6.18	Post-Scram MSLB Steam Generator Heat Transfer Rates.....	6-29
6.19	Post-Scram MSLB Feedwater Flow Rates.....	6-30
6.20	Post-Scram MSLB Steam Generator Total Mass Inventories.....	6-31
6.21	Post-Scram MSLB Core Inlet Temperatures.....	6-32
6.22	Post-Scram MSLB Pressurizer Pressure.....	6-33
6.23	Post-Scram MSLB Pressurizer Liquid Level.....	6-34
6.24	Post-Scram MSLB Total HPSI Flow Rate.....	6-35
6.25	Post-Scram MSLB Reactivity.....	6-36
6.26	Post-Scram MSLB Core Power.....	6-37
6.27	LOEL/TT Steam Generator Pressures.....	6-42
6.28	LOEL/TT RCS Temperatures.....	6-43
6.29	LOEL/TT Pressurizer and SRV Inlet Pressures.....	6-44
6.30	LOEL/TT Reactor Power.....	6-45
6.31	LOEL/TT Total Reactivity.....	6-46
6.32	LOEL/TT Pressurizer Level.....	6-47
6.33	LOEL/TT Pressure at Bottom of Reactor Vessel.....	6-48
6.34	LONF (With Offsite Power) Reactor Power Level.....	6-54
6.35	LONF (With Offsite Power) RCS Temperatures.....	6-55
6.36	LONF (With Offsite Power) Pressurizer Pressure.....	6-56
6.37	LONF (With Offsite Power) Pressurizer Liquid Level.....	6-57
6.38	LONF (With Offsite Power) Steam Generator Pressure.....	6-58
6.39	LONF (With Offsite Power) Steam Generator Inventory.....	6-59
6.40	LOCF Reactor Power Level.....	6-64
6.41	LOCF Core Average Heat Flux.....	6-65
6.42	LOCF RCS Temperatures.....	6-66
6.43	LOCF Pressurizer Pressure.....	6-67
6.44	LOCF Reactivity.....	6-68
6.45	LOCF Reactor Coolant Flow Rate.....	6-69
6.46	DNB-Limiting UCBW at Core Power and VHP Trip Setpoint.....	6-74
6.47	DNB-Limiting UCBW at Power Reactivity.....	6-75
6.48	DNB-Limiting UCBW at Power Average Fuel Rod Heat Flux.....	6-76
6.49	DNB-Limiting UCBW at Power RCS Temperatures.....	6-77
6.50	DNB-Limiting UCBW at Power Pressurizer Pressure and TM/LP Trip Setpoint.....	6-78
6.51	DNB-Limiting UCBW at Power Pressurizer Liquid Level.....	6-79
6.52	DNB-Limiting UCBW at Power Steam Generator Pressure.....	6-80
6.53	SGTR Reactor Power.....	6-85
6.54	SGTR Pressurizer Pressure.....	6-86

6.55	SGTR Pressurizer Liquid Level.....	6-87
6.56	SGTR RCS Temperatures.....	6-88
6.57	SGTR Steam Generator Pressures	6-89
6.58	SGTR Steam Generator Levels	6-90
6.59	SGTR Steam Generator Mass.....	6-91
6.60	SGTR Active Core Mass Flow Rate.....	6-92
6.61	SGTR MFW Flow Rates	6-93
6.62	SGTR Break Flow Rate	6-94
6.63	SGTR Integrated Break Flow.....	6-95
6.64	SGTR Integrated ADV Flows	6-96
6.65	SGTR Integrated MSSV Flows	6-97

Nomenclature

<u>Acronym</u>	<u>Definition</u>
2-D	two-dimensional
3-D	three dimensional
ADVs	atmospheric steam dump valves
AFW	auxiliary feedwater
ANF	Advanced Nuclear Fuels Corporation
AOOs	Anticipated Operational Occurrences
ASME	American Society of Mechanical Engineers
BOC	beginning-of-cycle
CE	Combustion Engineering
CEA	control element assembly
CFR	Code of Federal Regulations
CHF	critical-heat-flux
CRGT	control rod guide tube
CVCS	chemical and volume control system
DNB	departure from nucleate boiling
DNBR	departure from nucleate boiling ratio
EAB	exclusion area boundary
ECC	emergency core coolant
ECCS	emergency core cooling system
ENC	Exxon Nuclear Company
EOC	end-of-cycle
EOP	emergency operating procedure
EPRI	Electric Power Research Institute
ESFAS	Engineered Safeguard Feature Actuation System
FCM	fuel centerline melt
FSAR	final safety analysis report
HFP	hot full power
HPSI	high pressure safety injection
HTP	High Thermal Performance
HZP	hot zero power
LBLOCA	large break loss-of-coolant accident
LHGR	linear heat generation rate
LOCA	loss-of-coolant accident
LOCF	Loss of Forced Reactor Coolant Flow
LOEL	Loss of External Load
LOFT	Loss of Fluid Test Facility
LONF	Loss of Normal Feedwater

LPD	local power density
LPZ	low population zone
MDNBR	minimum departure from nucleate boiling ratio
MFW	main feedwater
MSFCV	main steam flow control valve
MSIS	main steam isolation signal
MSIVs	main steam isolation valves
MSSVs	main steam safety valves
MSLB	main steamline break
MTC	moderator temperature coefficient
NI	nuclear instrumentation
non-LOCA	non-loss-of-coolant accident
NRC	United States Nuclear Regulatory Commission
NSSS	Nuclear Steam Supply System
OD	outside diameter
PAs	Postulated Accidents
PORV	power operated relief valve
PWR	pressurized water reactor
RCCA	rod cluster control assembly
RCP	reactor coolant pump
RCS	reactor coolant system
RHR	residual heat removal
RPS	reactor protection system
RWST	refueling water storage tank
SAFDLs	specified acceptable fuel design limits
SCS	secondary coolant system
SDCS	shutdown cooling system
SER	Safety Evaluation Report
SGs	steam generators
SGTR	steam generator tube rupture
SIS	safety injection system
SPC	Siemens Power Corporation
SRP	Standard Review Plan
SRV	safety relief valve
TMLP	thermal margin/low pressure
TT	turbine trip
UCBW	uncontrolled bank withdrawal
UPTF	Upper Plenum Test Facility
VHP	variable high power

Abstract

A revised Pressurized Water Reactor (PWR) non-Loss-of-Coolant Accident (non-LOCA) transient analysis methodology is presented that incorporates S-RELAP5 as the systems analysis code in place of ANF-RELAP. The methodology applies to all PWR non-LOCA transients, including Main Steamline Break (MSLB). The methodology retains the previously approved XCOBRA-IIIC methodology for predicting the event-specific minimum departure from nucleate boiling ratio (MDNBR). The methodology is robust, providing assurance that the event-specific acceptance criteria specified in the United States Nuclear Regulatory Commission (NRC) Standard Review Plan (SRP) are met.

Loss of Fluid Test Facility (LOFT) calculations demonstrate that S-RELAP5 is capable of modeling the non-LOCA transients for which a systems analysis is required. Sample problem calculations for a PWR demonstrate how the methodology can be applied to analyze events from the major categories of SRP Chapter 15.

1.0 Introduction

Siemens Power Corporation (SPC) plans to use the S-RELAP5 (Reference 1) code for analysis of all events in the SRP (Reference 2) for PWRs that require a system analysis. The NRC has reviewed and accepted the SPC methodology using the ANF-RELAP code for analyzing non-LOCA transients (Reference 3), the MSLB event (Reference 4), and small break loss-of-coolant accident (LOCA) event (Reference 5) for PWRs. S-RELAP5 is an updated version of ANF-RELAP.

The purpose of this report is to demonstrate the adequacy of the revised SPC non-LOCA methodology, including the replacement of ANF-RELAP by S-RELAP5. In addition, References 3 and 4 have been combined into a single non-LOCA transients analysis methodology document in a manner that removes all restrictions placed on Reference 3. The report also incorporates events that do not require a systems analysis. This non-LOCA transient analysis methodology will be applied to all PWR plant types designed by Combustion Engineering (CE) and Westinghouse.

The objective in using S-RELAP5 is to apply a single advanced, industry recognized code for all analyses, including LOCA and non-LOCA events. Using a single code that has had extensive review permits the development of one base input deck for the analysis of all events for a particular application. The benefits of using a single code include ease of use by engineers, reduced maintenance requirements on developers, improved quality of both code and applications, and reduction of resources for the NRC review of associated methodology.

S-RELAP5 is a modification of ANF-RELAP. The modifications were made primarily to accommodate large and small break LOCA modeling. S-RELAP5 remains essentially equivalent to ANF-RELAP for non-LOCA applications.

The XCOBRA-IIIC code (Reference 6) will continue to be used to obtain the final predicted MDNBR for each transient event. That is, the core conditions from the S-RELAP5 reactor coolant system (RCS) calculations will be used as input to the existing XCOBRA-IIIC core and subchannel methodology to predict the event-specific MDNBR.

This report describes :

- Transient modeling
- LOFT non-LOCA transient calculations
- Event-specific application methodology
- Sample SRP events.

2.0 Summary of Results

The non-LOCA transient analysis methodology was developed to apply to all of the SRP Chapter 15 events listed in Table 2.1. The methodology is robust, providing assurance that the event-specific acceptance criteria specified in the NRC SRP are met. The Disposition of SRP Chapter 15 Events (Disposition of Events) provides a rigorous assessment of a reactor's existing Chapter 15 analyses of record to determine which analyses must be updated to support a new reload. The strategy for biasing of parameters, consistent with the SRP, provides realistic event simulation while maintaining sufficient conservatism in the calculated results.

Non-LOCA event-specific LOFT calculations are described in Section 4.0 to demonstrate that S-RELAP5 is capable of capturing the essential features of modeling non-LOCA transients for those SRP Chapter 15 events which require a system analysis. Key parameters, such as reactor power, primary and secondary system pressures, mass flow rates in the primary and secondary systems, and levels in the pressurizer and steam generator (SG), all compare well with the results from ANF-RELAP (the currently approved code) and with data from LOFT.

Sample problems for selected events are provided for a CE 2x4 plant. These events include Main Steamline Break (MSLB), Loss of External Load (LOEL), Loss of Forced Reactor Coolant Flow (LOCF), Loss of Normal Feedwater (LONF), Uncontrolled Bank Withdrawal at Power, and Steam Generator Tube Rupture (SGTR). These sample problems demonstrate the application of the methodology to events representing the major categories of Chapter 15 except for category 15.5, which are normally bounded by the other Condition II events.

Differences in key parameters for the events are summarized in Table 2.2. In both the LOFT calculations and the sample problem calculations, the S-RELAP5 predictions are compared to those of ANF-RELAP. They show that S-RELAP5 is essentially equivalent to ANF-RELAP for the modeling of non-LOCA transients.

This report includes additional information on the following subjects:

- Inclusion of upper head heat structures in system model nodalizations (Figure 4.1, Figure 6.1, and Figure 6.4);
- MSLB event-specific methodology (Section 5.4) and associated sample problems (Section 6.1 and 6.2);
- SGTR event-specific methodology (Section 5.5) and sample problem (Section 6.7);

- Boron dilution event-specific methodology (Section 5.6);
- Misloaded assembly event-specific methodology (Section 5.7);
- Control rod ejection event-specific methodology (Section 5.8);
- Radiological Consequences of the Failure of Small Lines Carrying Reactor Coolant Outside Containment (Section 5.9); and
- Fuel rod modeling for fast and slow transients (Section 3.2).

Table 2.1 Applicable SRP Chapter 15 Events

Event	SRP No.	Typical Condition
CATEGORY 15.1 – Increase in Heat Removal by the Secondary System		
Decrease in Feedwater Temperature	15.1.1	II
Increase in Feedwater Flow	15.1.2	II
Increase in Steam Flow	15.1.3	II
Inadvertent Opening of Steam Generator (SG) Relief/Safety Valve ^a	15.1.4	II
Steam System Piping Failures Inside and Outside Containment ^a	15.1.5	IV
CATEGORY 15.2 – Decrease in Heat Removal by Secondary System		
Loss of Outside External Load (LOEL)	15.2.1	II
Turbine Trip (TT)	15.2.2	II
Loss of Condenser Vacuum	15.2.3	II
Closure of Main Steam Isolation Valve (MSIV)	15.2.4	II
Steam Pressure Regulator Failure	15.2.5	II
Loss of Non-Emergency AC Power to the Station Auxiliaries	15.2.6	II
Loss of Normal Feedwater (LONF) Flow	15.2.7	II
Feedwater System Pipe Breaks Inside and Outside Containment	15.2.8	IV
CATEGORY 15.3 – Decrease in Reactor Coolant Flow Rate		
Loss of Forced Reactor Coolant Flow (LOCF)	15.3.1	II
Flow Controller Malfunctions	15.3.2	II
Reactor Coolant Pump (RCP) Rotor Seizure	15.3.3	IV
RCP Shaft Break	15.3.4	IV

^a This event is analyzed with the Steam Line Break methodology described in Section 5.4.

Table 2.1 Applicable SRP Chapter 15 Events (Continued)

Event	SRP No.	Typical Condition
CATEGORY 15.4 – Reactivity and Power Distribution Anomalies		
Uncontrolled Rod Cluster Control Assembly (RCCA) Bank Withdrawal From a Subcritical or Low Power Startup Condition	15.4.1	II
Uncontrolled RCCA Bank Withdrawal at Power	15.4.2	II
RCCA Misoperation	15.4.3	
Dropped Rod/Bank	15.4.3.1	II
Single Rod Withdrawal	15.4.3.2	III
Statically Misaligned RCCA	15.4.3.3	II
Startup of an Inactive Loop at an Incorrect Temperature	15.4.4	II
Chemical and Volume Control System (CVCS) Malfunction That Results in a Decrease of Boron Concentration (Boron Dilution)	15.4.6	II
Inadvertent Loading and Operation of a Fuel Assembly in an Improper Position (Misloaded Assembly)	15.4.7	III
Spectrum of Rod Ejection Accidents	15.4.8	IV
CATEGORY 15.5 – Increase in Reactor Coolant Inventory		
Inadvertent Operation of the Emergency Core Cooling System (ECCS) That Increases Reactor Coolant Inventory	15.5.1	II
CVCS Malfunction That Increases Reactor Coolant Inventory	15.5.2	II
CATEGORY 15.6 – Decreases in Reactor Coolant Inventory		
Inadvertent Opening of a Pressurizer Pressure Relief Valve	15.6.1	II
Radiological Consequences of the Failure of Small Lines Carrying Primary Coolant Outside Containment	15.6.2	II
Radiological Consequences of Steam Generator (SG) Tube Failure	15.6.3	IV

Table 2.2 Summary of Key Parameters

Sample Problem				
Event	Parameter	S-RELAP5	ANF-RELAP	Difference
Pre-Scram MSLB	Peak Power (%) ^a	137.6	137.6	< 0.1
Post-Scram MSLB	Peak Power (%) ^a	8.8	8.9	0.1
LOEL	Peak Pressure (psia)	2691.4	2692.2	0.8
LONF	Minimum SG Mass (%) ^b	20.1	27.4	7.3
LOCF	MDNBR	1.58	1.54	0.04
UCBW at Power	Peak Power (%) ^a	112.2	112.2	< 0.1
SGTR	Affected SG Release (lb _m)	100,800	100,200	600
LOFT				
L6-1 LOEL (LOFT: 15.86 MPa) ^c	Peak Pressure (MPa)	16.02	16.01	0.01
L6-2 LOCF (LOFT: 23.0 s)	Natural Circulation Established (s)	22.6	22.4	0.2
L6-3 Excess Steam Flow (LOFT: 42.6 MW)	Peak Fission Power (MW)	41.6	40.3	0.3
L6-5 LONF (LOFT: 2.14 m)	SG Level (m)	2.05	1.83	0.22
<p>^a Relative to rated power</p> <p>^b Relative to initial mass</p> <p>^c LOFT measurement is for pressurizer; calculated values are for bottom of reactor vessel</p>				

3.0 S-RELAP5 Modeling

3.1 System Modeling

The system analysis is performed with S-RELAP5. A description of S-RELAP5 is provided in Reference 1. The reactor vessel nodalization provides modeling of the key components in the reactor vessel using junctions, volumes, and heat structures. The secondary side includes the tube bundles, feedwater system, separators, steamlines, and turbine simulator.

Nodalizations for specific plant analyses are necessarily different from each other to capture unique design and hardware features (for example, the CE design of the reactor system piping is different than that for Westinghouse). These plant differences are reflected in the nodalization. When the nodalization needs to be revised, consideration is made for realistic modeling of significant phenomena and the need for conservatism. Also, existing nodalization studies are evaluated to determine if additional studies are warranted. Sample nodalizations are provided for LOFT (Figure 4.1) and a sample problem based on a CE 2x4 plant (Figure 6.1 to Figure 6.5).

A complete reactor point kinetics model simulates the production of nuclear power in the core. The model computes both the immediate fission power and the power generated from decay of fission fragments and actinides. The model provides capability to include feedback due to moderator density and fuel temperature changes.

The control systems coincide with the model's nodalization so that the transient initiation requires a minimum amount of user input. The typical main control systems modeled for these events are:

- Automatic rod control
- RPS control
- Pressurizer heater and spray control
- Steam flow and turbine control
- SG liquid level and feedwater control
- Primary and secondary relief valve control
- Safety injection

The RPS controller trip functions include the trip function and the uncertainties and time delay associated with it. The RPS trips incorporated into the model (for a typical CE plant) are:

- Low SG pressure
- Low pressurizer pressure
- High pressurizer pressure
- Thermal Margin/Low Pressure (TM/LP)
- VHP
- Low RCS flow
- SG low level
- Engineered Safeguard Feature Actuation System (ESFAS) signals

The control logic is versatile enough to establish and maintain steady-state operating conditions. It will also initiate and analyze transients. The transient events typically initiate as restart runs from the established steady-state run.

3.2 Fuel Modeling

The approach to fuel modeling is changed from that described in Reference 3. It is still based on RODEX2 (References 7 and 8), however.

Fuel modeling contributes to the determination of the power and heat flux for the core. The heat flux determines the core coolant heating rate and, ultimately, the temperature response of the RCS to power changes. The power is affected by changes in fuel temperature, that determines the Doppler feedback, and by the change in the core coolant temperature, that determines the moderator feedback. Studies of the relevant fuel parameters using SPC's fuel design code, RODEX2 (Reference 7), are described below.

The reactor core is typically modeled as a single hydraulic channel with axial volumes, each of which is coupled to a heat structure. These heat structures model axial segments of the fuel. The heat structures represent the fuel, cladding, and fuel-to-cladding gap by a series of concentric cylinders. The radial mesh points of the heat structures are characterized by radial locations of the boundaries, relative power in the volume, heat capacity, and thermal conductivity. Most of the radial mesh points represent the fuel pellet stack. The gap is represented by one radial mesh point, and the cladding by two or more.

Fuel Design Studies

The average core behavior and hot rod behavior for PWR fuel designs were evaluated using RODEX2. The effects of gap conductance, heat capacity, thermal conductivity, porosity, and exposure were assessed and are discussed here.

The gap conductance varies significantly throughout the cycle. However, it is not strongly dependent on the fuel design. All four fuel designs show similar variations in gap conductance with power (fuel temperature) and burnup. Near the beginning-of-cycle (BOC), the average value of gap conductance at full power is about 1200 Btu/hr-ft²-°F, independent of the fuel design. It increases until the end-of-cycle (EOC), where it is greater than 5000 Btu/hr-ft²-°F. At higher powers, the fuel temperature increases, and both the contact pressure between the pellet-cladding and the gap conductance also increase.

Heat capacity and thermal conductivity models from RODEX2 were evaluated over a range of temperatures. The heat capacity for a fuel pellet varies with temperature and, to a very small extent, pellet densification. The thermal conductivity of a fuel pellet varies with temperature and with porosity. Pellet porosity is radially distributed and varies throughout the cycle. The RODEX2 evaluation shows that pellet porosity and its changes throughout the cycle are relatively independent of the fuel design. Burnup adjustments can be incorporated in both uranium dioxide (UO₂) and (when appropriate) Gd₂O₃ properties to conservatively represent the time in cycle.

The model applies to PWR fuel designs. Significant changes in fuel design, that fall outside the study, require reassessment to determine if the model remains applicable. The characteristics which determine when re-evaluation is required are free volume to fuel ratio, cladding type (creepdown behavior), porosity, a change in certain RODEX2 properties (pellet resintering, pellet cracking, porosity), cycle exposure, and/or a change in the fuel rod code (use of a code other than RODEX2).

The impact of fuel modeling on transient heat flux and fuel temperature is discussed below. Slow transients and fast transients are considered separately.

Slow Transients

Most of the transients to be evaluated using this methodology are considered to be slow transients. In almost all cases, a power transient is associated with the event. During a complete operating cycle, the effective time constant ranges from about 5 seconds at BOC to about 3 seconds at EOC. For slow transients, this range of responses results in a relatively minor, but noticeable, difference in the heat flux from the core. For the average core, SPC uses average fuel rod properties based on the fuel design studies, which represent the appropriate time in the cycle. By so doing, SPC's transient analysis captures the transient response of the fuel in the core and results in heat fluxes that are consistent with the fuel rod thermal properties in the fuel design code.

The challenge to the fuel centerline melt (FCM) limit is generally evaluated statically for these slower transients, although it may be evaluated using the more mechanistic hot spot model described below. In the static evaluation, the maximum effective linear heat generation rate (LHGR) (based on rod surface heat flux rather than neutron power) for a UO₂ pellet is compared to a bounding melt limit to determine whether FCM has occurred.

Fast Transients

Fast transients, such as Control Rod Ejection or Uncontrolled Bank Withdrawal from Hot Zero Power (HZP), are characterized by rapidly changing power levels. The power changes so rapidly that the rod surface heat flux bears little resemblance to the power. The modeling of the transient response of the fuel can result in significantly different peak heat flux and fuel temperature. This transient response depends on the mass, heat capacity, and thermal conductivity of the fuel and on the gap conductance; therefore, determining appropriate values for these parameters requires more care than for slow transients.

In a fast transient, the average core response will depend on the average fuel properties. The heat capacity of the average fuel rod depends almost entirely on the fuel temperature. The effect of densification on the heat capacity is small (less than 2 percent) and can be ignored. Thermal conductivity depends on the fuel porosity and the fuel temperature. It can change by about 8 to 10 percent over the range of porosities experienced by regions of a fuel pellet during operation. Fuel porosity varies radially in the pellet and changes with burnup. The thermal

conductivity is adjusted to account for the porosity distribution of the average core at the burnup of interest.

Gap conductance varies with burnup and fuel temperature. When the event is initiated from HZP, the gap conductance will range from several hundred Btu/hr-ft²-°F at the beginning of the transient to several thousand Btu/hr-ft²-°F at the time of the peak fuel temperature. The power transient for such an event will be arrested by negative Doppler. [

Hot Spot Model

To demonstrate protection against FCM dynamically, an additional heat structure is added to the model. This heat structure, called the hot spot, represents the axial segment of the hot rod that has the maximum power. The physical modeling, except for the length and the total power, is the same as the average fuel rod. It is attached to the uppermost volume of the average core, to obtain the highest coolant temperature.

The thermal properties used for the hot spot heat structure are consistent with the exposure of the hot rod. For fuel designs in which the rods with burnable poison (Gd₂O₃) can reach a power close to that of the limiting UO₂ rod in the core, the properties of the Gd₂O₃ rod are used. The thermal conductivity and heat capacity, which are obtained using the models in RODEX2, are significantly different for Gd₂O₃.

The hot spot model provides a conservative calculation of the fuel centerline temperature, which is then compared to the fuel melt temperature.

3.3 Summary of Code Differences Between S-RELAP5 and ANF-RELAP

The S-RELAP5 code evolved from SPC's ANF-RELAP code, a modified RELAP5/MOD2 version, used at SPC for performing PWR plant licensing analyses including small break LOCA analysis, steamline break analysis, and PWR non-LOCA Chapter 15 event analyses. The code structure for S-RELAP5 was modified to be essentially the same as that for RELAP5/MOD3, with the similar code portability features. The coding for reactor kinetics, control systems and

trip systems were replaced with those of RELAP5/MOD3. Most of the modifications to S-RELAP5 were undertaken to improve its applicability for the realistic calculation of Large Break LOCA (LBLOCA) and are irrelevant to the analysis of PWR Non-LOCA events.

In Section 1.1 of the S-RELAP5 Models and Correlations Manual (Reference 1) there is a list summarizing major modifications and improvements in S-RELAP5 that is reproduced below:

(1) Multi-Dimensional Capability

Full two-dimensional treatment was added to the hydrodynamic field equations. The 2-D capability can accommodate the Cartesian, and the cylindrical (z,r) and (z, θ) coordinate systems and can be applied anywhere in the reactor system. Thus far SPC has applied 2-D modeling to the downcomer, core, and upper plenum. Some improvements were also made to the RELAP5/MOD2 cross flow modeling. If necessary, 3-D calculations can be approximated by 2-D plus one direction of cross flow. The application of a 2-D component in the downcomer is essential for simulating the asymmetric ECC water delivery observed in the Upper Plenum Test Facility (UPTF) downcomer penetration tests. Note that the 2-D component was not used in the Non-LOCA event analyses.

(2) Energy Equations

The energy equations of RELAP5/MOD2 and RELAP5/MOD3 have a strong tendency to produce energy error when a sizable pressure gradient exists between two adjacent cells (or control volumes). This deficiency is a direct consequence of neglecting some energy terms which are difficult to handle numerically. Therefore, the energy equations were modified to conserve the energies transported into and out of a cell (control volume). For LOCA calculations, no significant differences were calculated in the key parameters such as clad surface temperature, break mass flow rate, void fraction, and others between the two formulations of the energy equations. For analyses involving a containment volume, the new approach is more appropriate. This code improvement had only a minor effect on the Non-LOCA event analyses. Specifically, a small effect on critical flow for steamline breaks was observed.

(3) Numerical Solution of Hydrodynamic Field Equations

The reduction of the hydrodynamic finite-difference equations to a pressure equation is obtained analytically by algebraic manipulations in S-RELAP5, but is obtained numerically by using a Gaussian elimination system solver in RELAP5/MOD2 and MOD3. This improvement aids computational efficiency and helps to minimize effects due to machine truncation errors.

(4) State of Steam-Noncondensable Mixture

Computation of state relations for the steam-noncondensable mixture at very low steam quality (i.e., the ratio of steam mass to total gas phase mass) was modified to allow the presence of a pure noncondensable gas below the ice point (0°C). The ideal gas approximation is used for both steam and noncondensable gas at very low steam quality. This modification is required to correctly simulate the accumulator depressurization and to prevent code failures during the period of accumulator ECC water injection.

(5) Hydrodynamic Constitutive Models

Significant modifications and enhancements were made to the RELAP5/MOD2 interphase friction and interphase mass transfer models. The constitutive models are flow regime dependent and are constructed from the correlations for the basic elements of flow patterns such as bubbles, droplets, vapor slugs (i.e., large bubbles), liquid slugs (i.e., large liquid drops), liquid film and vapor film. Some flow regime transition criteria of RELAP5/MOD2 were modified to make them consistent with published data. When possible and applicable, literature correlations are used as published. A constitutive formulation for a particular flow regime may be composed of two different correlations. Transition flow regimes are introduced for smoothing the constitutive models. Partition functions for combining different correlations and for transitions between two flow regimes are developed based on physical reasoning and code-data comparisons. Most of the existing RELAP5/MOD2 partition functions were not modified or only slightly modified. The vertical stratification model implemented in ANF-RELAP was further improved. Also, the RELAP5/MOD2 approximation to the Colebrook equation of wall friction factor is known to be inaccurate and is, therefore, replaced by an accurate explicit approximate formulation of Jain.

No major effects on non-LOCA event analyses resulted from these code improvements. However, as discussed in the LOFT benchmark and PWR sample problem analyses, some effects are noticeable due to the effects of wall drag on SG tube pressure drop and due to the effects of interfacial friction on SG secondary side liquid distribution.

(6) Heat Transfer Model

The use of a different set of heat transfer correlations for the reflood model in RELAP5/MOD2 was eliminated. Some minor modifications were made to the selection logic for heat transfer modes (or regimes), single phase liquid natural convection and condensation heat transfer. The Lahey correlations for vapor generation in the subcooled nucleate boiling region were implemented. No changes are made to the RELAP5/MOD2 CHF correlations.

(7) Choked Flow

The computation of the equation of state at the choked plane was modified. Instead of using the previous time step information to determine the state at the break, an iterative scheme is used. This modification was also implemented in ANF-RELAP. Some minor modifications were also made to the under-relaxation scheme to smooth the transition between subcooled single phase critical flow and two-phase critical flow. Moody critical flow model is also implemented, but not used for the realistic LBLOCA calculations though it is used for the Appendix K analyses.

(8) Counter-Current Flow Limiting

A Kutateladze type CCFL correlation was implemented in ANF-RELAP. This was replaced in S-RELAP5 by the Bankoff form, which can be reduced to either a Wallis type or a Kutateladze type CCFL correlation. RELAP5/MOD3 also uses the Bankoff correlation form.

(9) Component Models

The EPRI pump performance degradation data was included in the S-RELAP5 pump model. The computation of pump head in the fluid field equations was modified to be more implicit. A containment model was added. With this model, the containment

pressure boundary conditions are provided by the approved EXEM/PWR evaluation model code, ICECON, which is run concurrently with S-RELAP5 using realistic values for parameter input. The accumulator model was eliminated because of its well-known problems. With S-RELAP5, the accumulator is to be modeled as a pipe with nitrogen or air as noncondensable gas. The ICECON containment model is not used in non-LOCA transient analyses.

(10) Fuel Model

Initial fuel conditions are supplied by the SPC realistic fuel performance code, RODEX3. The fuel deformation and conductivity models of RODEX3 were included in S-RELAP5. The plastic strain and metal-water reaction models were taken from RELAP5/MOD3 with minor modifications. RODEX2 has also been incorporated into S-RELAP5. The internal RODEX2 and RODEX3 models are not used for non-LOCA transients.

Despite this extensive list of modifications, only three model changes were discerned to be responsible for the relatively minor differences observed in the S-RELAP5 and ANF-RELAP calculations for the PWR Non-LOCA event sample problems. Specifically, it was found that changes to the single-phase wall drag, the interfacial shear package, and the energy equation affected the results. Nevertheless, no significant differences in the parameters that directly affect the specified acceptable fuel design limits (SAFDLs) were observed in these sample problems. Each of the LOFT calculations and PWR sample problems are discussed in Sections 4.0 and 6.0 and differences in the code-to-code predictions are examined with respect to these code modifications.

4.0 LOFT Non-LOCA Transient Calculation

This section presents the S-RELAP5 simulation of the LOFT L6-1, L6-2, L6-3, and L6-5 experiments. The S-RELAP5 calculations are compared to ANF-RELAP calculations to demonstrate the similarity of the two codes for non-LOCA analysis. ANF-RELAP was evaluated against the experimental data in Reference 3. LOFT measured data are provided also. ANF-RELAP results are provided for comparison, but unless specifically stated, the discussion of results is based on S-RELAP5 predictions.

The LOFT integral test facility was designed to simulate the major components of a four-loop, commercial PWR, thereby producing data on the hydraulic, thermal, nuclear, and structural processes expected to occur during anticipated or postulated accidents in a PWR. A general description of the LOFT facility and tests is given in Reference 9. References 10 and 11 provide detailed descriptions of test configurations, instrumentation, experimental procedures and results for L6-1, L6-2, L6-3, and L6-5. The information for simulating the LOFT facility and L6 experimental conditions was obtained from References 12, 13, and 14 and the electronic data received from the NRC databank.

4.1 LOFT S-RELAP5 Model Description

The LOFT control system, similar to a large PWR, contains many active subsystems, such as the feedwater control system, High Pressure Safety Injection (HPSI), pressurizer pressure control system, main steam flow control valve (MSFCV) control system, and reactor scram controls.

This section outlines the structure of the S-RELAP5 base deck that was used in the LOFT L6 series calculation. The schematic of the S-RELAP5 model displaying the thermal-hydraulic components and heat structures for the LOFT L6 experimental series is shown in Figure 4.1. The numbering scheme for components in this model is:

<u>Major Component</u>	<u>Numbering</u>
loop one	100 - 199
reactor	200 - 299
loop two	300 - 399
pressurizer	400 - 499

secondary side of SG	500 - 599
ECC system	600 - 699
containment	800 - 899

Heat Structures are included in the model also. The systems with heat structures include the reactor, SG, piping, and pressurizer.

The steady-state control section contains a reactor coolant flow rate control system, pressurizer pressure control system, pressurizer liquid level control system, SG temperature control system, and SG liquid level control system. These systems systematically adjust the RCS flow rate, pressurizer pressure and liquid level, SG temperature and liquid level, and reactor power to the specified initial conditions for a given experiment. The transient control system consists of a RCS pump control, reactor control, pressurizer control, SG control, and emergency core cooling system (ECCS) control systems.

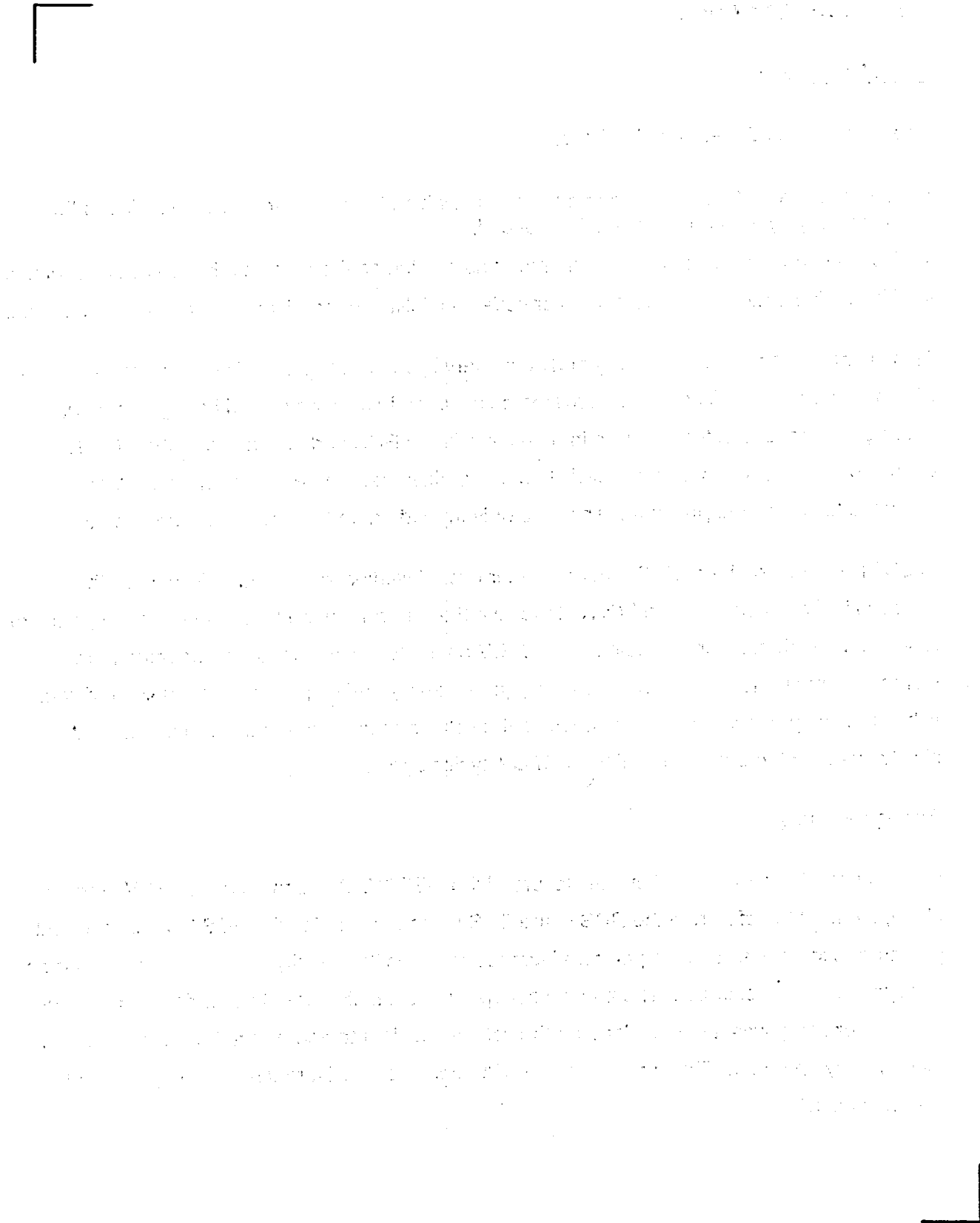


Figure 4.1 S-RELAP5 Nodalization Schematic for LOFT Experiments

4.2 LOFT L6-1 Loss of Load

Event Description

The objectives of Experiment L6-1 are:

- To investigate plant response to a transient in which the heat removal capabilities to the secondary system are significantly reduced.
- To evaluate the automatic recovery methods in bringing the plant to a hot-standby condition.
- To provide data to evaluate computer code capabilities to predict secondary initiated events.

This event challenges both primary and secondary system over pressurization limits. The loss of heat removal capability creates a mismatch between heat removal and heat generation, leading to increases in temperature in both the primary RCS and secondary of the SG. The expansion of the primary coolant leads to a pressurizer insurge. Pressurizer sprays are activated to control the pressure. The reactor is tripped on an RCS high pressure signal.

In LOFT, the role of the MSFCV changes after event initiation and closure. The valve then behaves like a secondary side PORV, to relieve the pressure in the SG. When the SG pressure reaches the high pressure setpoint, the MSFCV opens to relieve pressure. Opening the valve increases heat removal from the secondary (and primary), driving the system pressure down. When the low pressure setpoint is reached, the valve closes. Stored heat and decay heat slowly increase the pressure until the MSFCV cycles again.

Analysis Results

Experiment L6-1 was initiated by the closure of the MSFCV. As soon as the MSFCV starts to close, the heat transfer from the RCS to the SCS decreases forcing the RCS temperature and pressure to increase. The temperature increase changes the density of the coolant causing an insurge into the pressurizer. The pressurizer spray was initiated at 8.8 seconds. Because the pressurizer spray was much cooler than the cold leg coolant temperature, the pressure rise is momentarily reversed. The pressure of the RCS increases until it reaches the high pressure scram setpoint.

As the primary system temperature increases, the reactor power decreases due to the moderator temperature and Doppler feedbacks. The reactor scrams at 22.3 seconds on high primary system pressure. Maximum pressure is reached at 23.0 seconds.

The pressure in the SG reaches the high pressure setpoint at 20.2 seconds causing the MSFCV to begin to open. The removal of energy from the secondary, in conjunction with decreased energy production in the primary following reactor scram drives the pressure downward. The pressurizer level reaches its maximum at 26.7 seconds. The decrease in pressure turns the spray off at 26.8 seconds. The depressurization continues causing an outsurge from the pressurizer as the primary volume shrinks. The backup pressurizer heaters come on at 27.8 seconds. The MSFCV is closed at 43.0 seconds and the system begins to stabilize. Because of stored heat in the system structures and decay heat from the reactor, the pressure in the SG slowly creeps upward until the high pressure setpoint is again reached. The MSFCV opens at 104 seconds and closes again at 117 seconds. The simulation is terminated at 200 seconds.

The transient event sequence is shown in Table 4.1. Key system parameters are plotted in Figure 4.2 to Figure 4.9. This table and these figures include calculation results from ANF-RELAP for comparison. The LOFT measured results are provided also.

This event challenges both primary and secondary over-pressurization limits. The peak pressures, for both the primary and secondary, are very close for the S-RELAP5 and ANF-RELAP calculations. Nevertheless, there is a noticeable difference in the event chronology for the calculations of the two codes. Specifically, the S-RELAP5 code predicts the reactor trip on high pressurizer pressure to occur at 22.3 seconds whereas it occurs 3.3 seconds earlier in the ANF-RELAP calculation. After this time, differences between the two codes are affected by this timing difference and so are not examined below.

Examining Figures 4.3 and 4.4 shows that the peak pressurizer pressure occurs earlier in the ANF-RELAP calculation and occurs at a lower pressurizer level. The difference between the two calculations is then the result of a difference in the effect of the pressurizer spray. The pressurizer spray is initiated by a high pressure setpoint (15.25 MPa) at about 8.8 seconds in both calculations. This leads to an initially rapid pressure decrease before the pressurizer insurge overwhelms this effect and the pressure resumes rising towards its peak value.

In the ANF-RELAP calculation, the pressure decrease due to condensation upon the spray causes the pressure to fall slightly below a low pressure setpoint (14.90 MPa) at about 11.4 seconds that shuts off the spray. The pressurizer spray remains off until the pressure once again rises above the high pressure setpoint at about 13.1 seconds. In the S-RELAP5 calculation, however, the pressurizer pressure reaches an initial minimum slightly above (~0.015 MPa) the low pressure setpoint, so that the spray remains on. This interval without the pressurizer spray is responsible for the early reactor trip in the ANF-RELAP calculation. In turn, the more rapid decrease in pressure upon spray initiation is due to a difference in the interfacial heat transfer package between the two codes for the annular/mist regime.

Conclusions

In summary, the S-RELAP5 code compares very well against ANF-RELAP calculated results and provides a satisfactory calculation of the LOFT L6-1 experiment. S-RELAP5 adequately captures the effects of pressurizer insurges, outsurges, condensation due to pressurizer spray, expansion and contraction of the reactor coolant, primary-to-secondary heat transfer, core heat generation, SG pressure, and steam flow. S-RELAP5 is essentially equivalent to ANF-RELAP in modeling this event.

Table 4.1 LOFT L6-1 Event Sequence





Figure 4.2 LOFT L6-1 Steam Generator Level



Figure 4.3 LOFT L6-1 Pressurizer Liquid Level



Figure 4.4 LOFT L6-1 Pressurizer Pressure



Figure 4.5 LOFT L6-1 Steam Generator Secondary Pressure



Figure 4.6 LOFT L6-1 Reactor Power



Figure 4.7 LOFT L6-1 Hot Leg Temperature



Figure 4.8 LOFT L6-1 Cold Leg Temperature

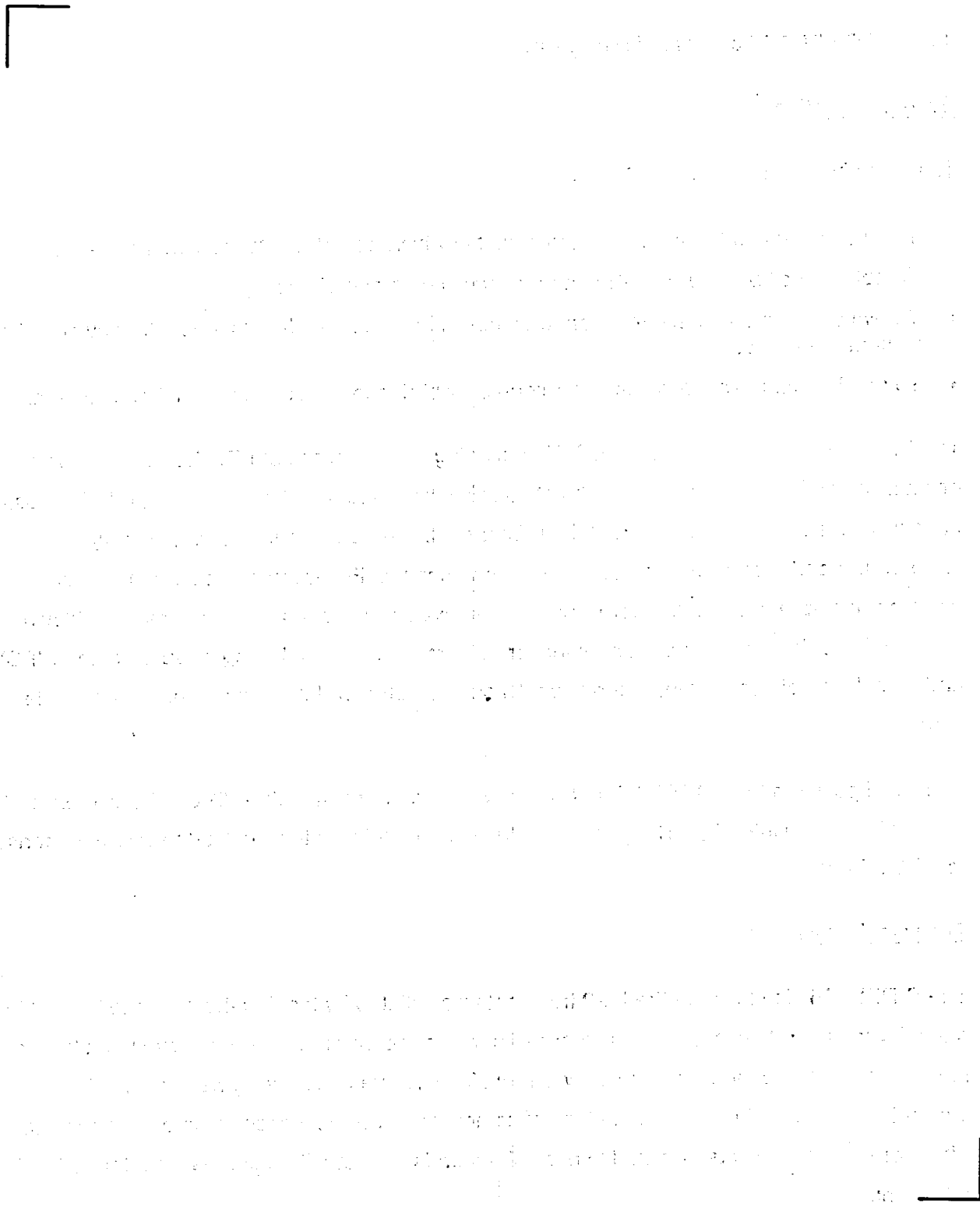


Figure 4.9 LOFT L6-1 Steam Generator Steam Flow

4.3 *LOFT L6-2 Loss of Primary Flow*

Event Description

The objectives of Experiment L6-2 are:

- To investigate plant response to a transient in which forced reactor coolant flow is lost.
- To obtain additional data on the natural circulation mode of cooling.
- To evaluate the automatic recovery methods in bringing the plant to a hot-standby condition, without the RCPs.
- To provide data to assess computer code capabilities to predict primary initiated events.

The LOCF event was simulated in LOFT by tripping the power to both RCPs. A flow coastdown begins. When low flow is detected, the reactor is scrammed and the turbine tripped. The loss of flow diminishes heat transfer from the primary to the secondary, increasing primary temperature and pressure. A pressurizer insurge occurs. Following scram, the mismatch between heat generated in the core and heat removed by the secondary causes a cooldown, resulting in coolant shrinkage. A pressurizer outsurge occurs. Following closure of the MSFCV, and completion of coastdown, natural circulation is initiated and the system reaches a stable state.

The initial power in the LOFT L6-2 test was reduced to approximately 75% of full power so as to not challenge fuel integrity. The purpose of the experiment was to investigate system response to a LOCF event.

Analysis Results

The S-RELAP5 simulation of the L6-2 transient was initiated by tripping the power to both RCPs and allowing them to coastdown. The experiment was scrammed by the detection of a low flow rate in the RCS. No measured low flow scram signal (value of flow rate) was given in the available documents but instead the time of scram was given as 2 seconds into the transient. Therefore, the scram was modeled to occur 2 seconds after the RCS pumps were tripped in the L6-2 simulation.

With reactor trip, the MSFCV began to close at 2.0 seconds, and was fully closed at 14.6 seconds.

The flow rate begins to decrease rapidly. Following an initial slight rise in temperature and, pressure, the pressure begins to drop rapidly, due to continued heat removal from the secondary. The low pressure setpoint is reached at 4.5 seconds, causing the backup heaters to come on to mitigate the pressure decrease. The feedwater control valve begins to close at the time of reactor trip and becomes fully closed at 4.1 seconds.

At 18.2 seconds, the RCPs decouple from the motor sets and complete the coastdown. An increasing difference in temperature between the upper and lower plenum is first detected at 22.6 seconds as significant natural circulation cooling begins. The decrease in heat removal from the primary, in conjunction with decay heat and stored heat, terminates primary coolant shrinkage at 28.3 seconds, when the minimum level in the pressurizer is reached. The pressure gradually recovers and the pressurizer backup heaters turn off at 48.6 seconds.

The calculation is terminated at 200 seconds with the system in a stable state. The transient event sequence is summarized in Table 4.2. Key system parameters are plotted in Figure 4.10 through Figure 4.19. This table and these figures include calculation results from ANF-RELAP for comparison. The LOFT measurements are provided also.

The calculated transient response of the S-RELAP5 and ANF-RELAP codes is nearly identical for this event. Only minor differences are observed for a transient that included periods of pressurizer insurge, pressurizer outsurge, and loop natural circulation. The one apparently significant difference is the timing for the shutoff of the pressurizer backup heaters as the RCS pressure is recovered. S-RELAP5 calculates that the RCS pressure will reach this setpoint (15.07 MPa) at about 98.6 seconds and ANF-RELAP calculates it to occur at about 117 seconds. At the time the S-RELAP5 calculation reaches this setpoint, the difference in RCS pressure between the two codes is less than 0.038 MPa (5.5 psia). The event timing difference results because the RCS pressurization rate is very slow ($\sim 1.8 \times 10^{-3}$ MPa/s). The observed differences in the calculations for this event are so small that no effect of code modeling differences can be discerned.

Conclusions

In summary, S-RELAP5 compares very well against ANF-RELAP calculated results and provides a satisfactory calculation of the LOFT L6-2 experiment. S-RELAP5 adequately

captures RCP coastdown behavior and natural circulation flow rate. In addition, the calculations show overall good agreement with experimental data.

Table 4.2 LOFT L6-2 Event Sequence





Figure 4.10 LOFT L6-2 Reactor Coolant Mass Flow Rate



Figure 4.11 LOFT L6-2 Steam Generator Liquid Level



Figure 4.12 LOFT L6-2 Pressurizer Liquid Level



Figure 4.13 LOFT L6-2 Pressurizer Pressure



Figure 4.14 LOFT L6-2 Steam Generator Secondary Pressure



Figure 4.15 LOFT L6-2 Reactor Power



Figure 4.16 LOFT L6-2 Hot Leg Temperature



Figure 4.17 LOFT L6-2 Cold Leg Temperature



Figure 4.18 LOFT L6-2 Steam Generator Steam Flow Rate

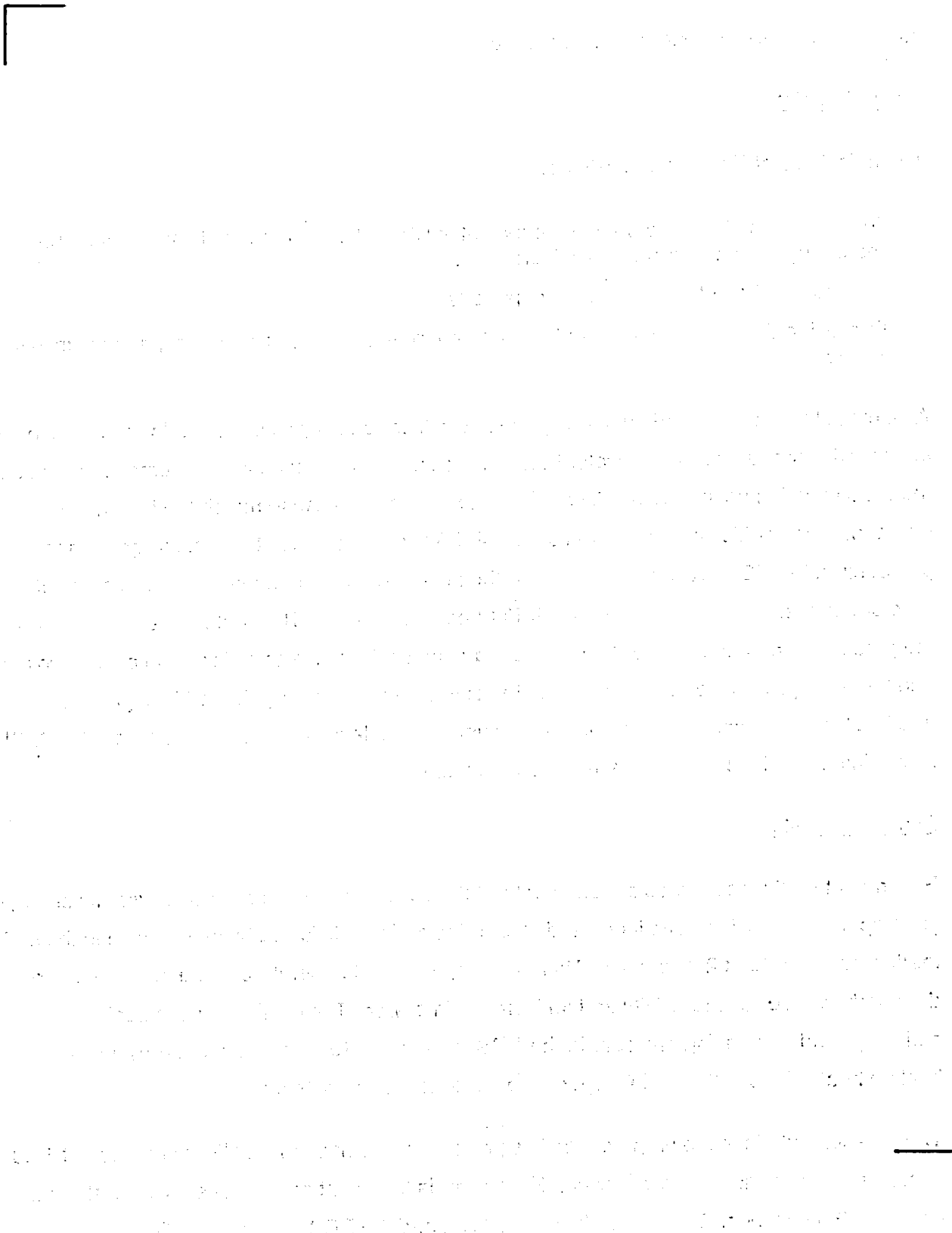


Figure 4.19 LOFT L6-2 RCP Speed

4.4 *LOFT L6-3 Excessive Steam Load*

Event Description

The objectives of Experiment L6-3 are:

- To investigate plant response to a transient in which the heat removal capability of the secondary system is significantly increased.
- To evaluate the automatic recovery methods.
- To provide data to assess computer code capabilities to predict secondary system initiated events.

An excess load is simulated by opening the MSFCV to its full open position. In response to the increased steam demand, feedwater flow increases. The increased energy removal rate cools the RCS inducing positive reactivity and the power begins to rise to match the increased demand. The cooldown of the RCS causes shrinkage of the coolant and outsurge from the pressurizer, the RCS pressure falls. When the pressure drops to the low pressure setpoint, the reactor scrams. Following scram, the MSFCV begins to close. The cooldown continues and the pressure drops further. HPSI pumps are automatically activated to increase coolant volume and keep the pressurizer from emptying. In conjunction with closing the MSFCV, the pressure and level reach a minimum and begin to recover. As the level and pressure recover, the HPSI is terminated and the system reaches a stable state.

Analysis Results

Experiment L6-3 was initiated by ramping the MSFCV to the fully open position from its steady-state operating position. The increased steam demand was followed by an increase in the main feedwater flow rate at 2.2 seconds. Within 6 seconds, the temperature in the core begins to drop, inducing positive reactivity and an increase in power. The cooling causes coolant shrinkage and decreasing pressure in the RCS system. At 10.4 seconds, the pressurizer backup heaters are activated in response to the decreasing pressure.

The pressure continues to drop and the low pressure setpoint of 14.12 MPa is reached at 18.3 seconds, causing the reactor to scram. Feedwater is tripped at scram. The MSFCV starts to close at 20.5 seconds. The pressurizer liquid level and the RCS pressure continues to fall. HPSI pumps are activated at 26.7 seconds. At this point, steam demand is decreasing because

the MSFCV is being ramped closed. Minimum RCS pressure is reached at 34.6 seconds and minimum pressurizer level is reached at 37.3 seconds. The MSFCV is fully closed at 40.6 seconds. The pressure and level begin to recover and the HPSI flow is terminated at 53.0 seconds. As the level continues to recover, the pressurizer backup heaters turn off at 82.0 seconds. The transient calculations are terminated at 200 seconds, with the system in a stable state.

A sequence of events summary is provided in Table 4.3. Key parameters are plotted in Figure 4.20 to Figure 4.28. ANF-RELAP calculated results are provided for comparison to S-RELAP5. LOFT measurements are provided also.

The calculated response of the S-RELAP5 and ANF-RELAP codes is nearly identical for this event up to the time of reactor trip. Reactor scram occurs on a low cold leg pressure setpoint (14.12 MPa) and is predicted at 15.3 seconds in the ANF-RELAP calculation and at 19.0 seconds in the S-RELAP5 calculation. The post-scram differences between the two calculations are primarily due to the additional energy deposition that occurs during this 3.7 second period in the S-RELAP5 calculation. During the RCS cooldown that results from the increase of steam load, the calculated SG heat transfer rate and the shrinkage of the RCS is almost the same for the two codes. However, differences in the interfacial heat transfer package affect the behavior in the pressurizer during the outsurge so that the pressure in the S-RELAP5 calculation reaches the low pressure setpoint later. At this time, the difference in calculated pressure is less than 0.06 MPa (8.7 psia).

Conclusions

In summary, S-RELAP5 compares very well against ANF-RELAP calculated results and provides a satisfactory calculation of the LOFT L6-3 experiment. S-RELAP5 adequately captures the effects of system cooldown, HPSI injection, pressurizer modeling, and primary-to-secondary heat transfer. In addition, the calculations show reasonable agreement with the experimental data.

Table 4.3 LOFT L6-3 Event Sequence

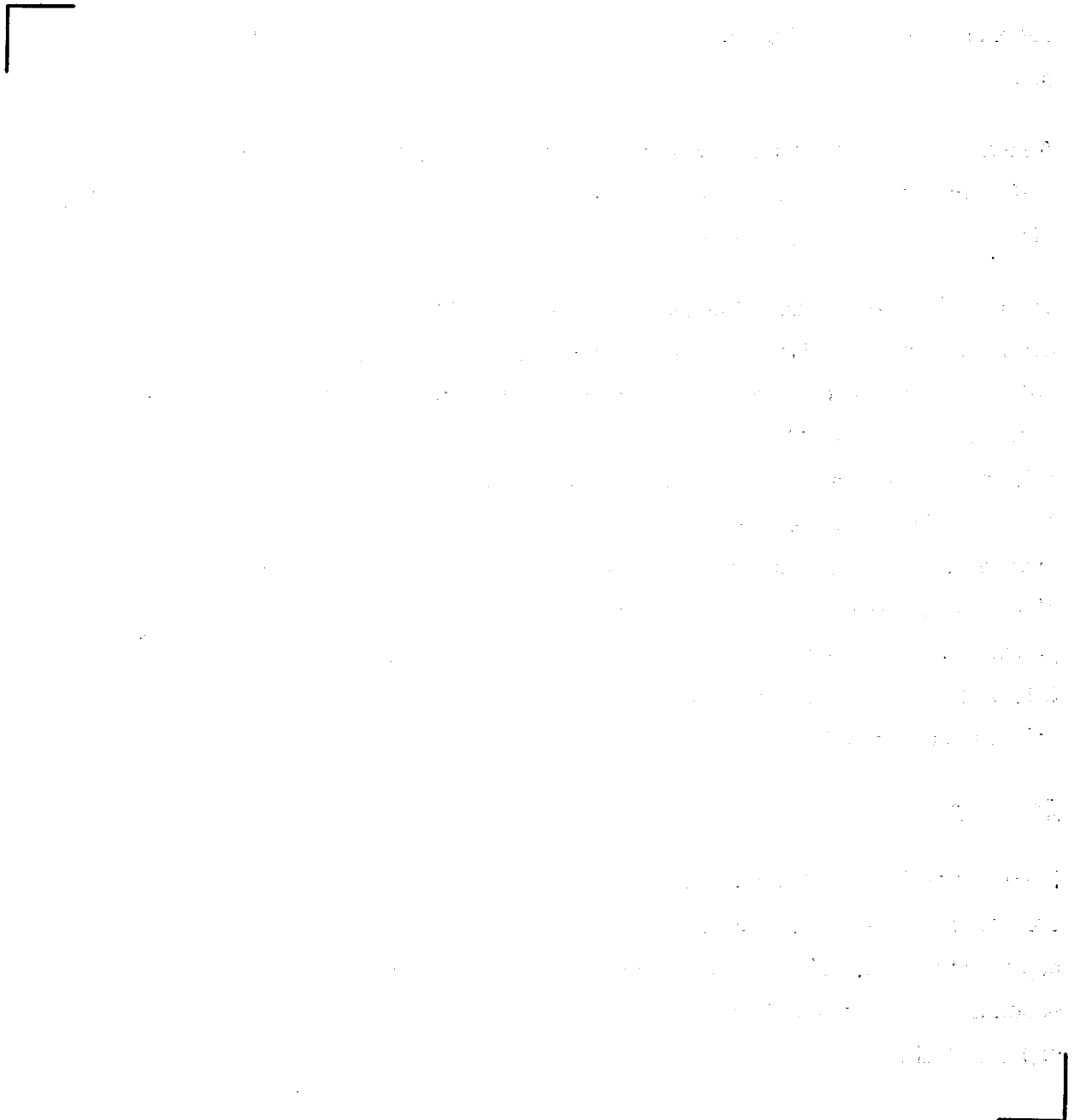




Figure 4.20 LOFT L6-3 Secondary Feedwater Flow Rate



**Figure 4.21 LOFT L6-3 Steam Generator Secondary Side Liquid
Level**



Figure 4.22 LOFT L6-3 Pressurizer Liquid Level



Figure 4.23 LOFT L6-3 Pressurizer Pressure



Figure 4.24 LOFT L6-3 Steam Generator Secondary Pressure



Figure 4.25 LOFT L6-3 Reactor Power



Figure 4.26 LOFT L6-3 Hot Leg Temperature



Figure 4.27 LOFT L6-3 Cold Leg Temperature

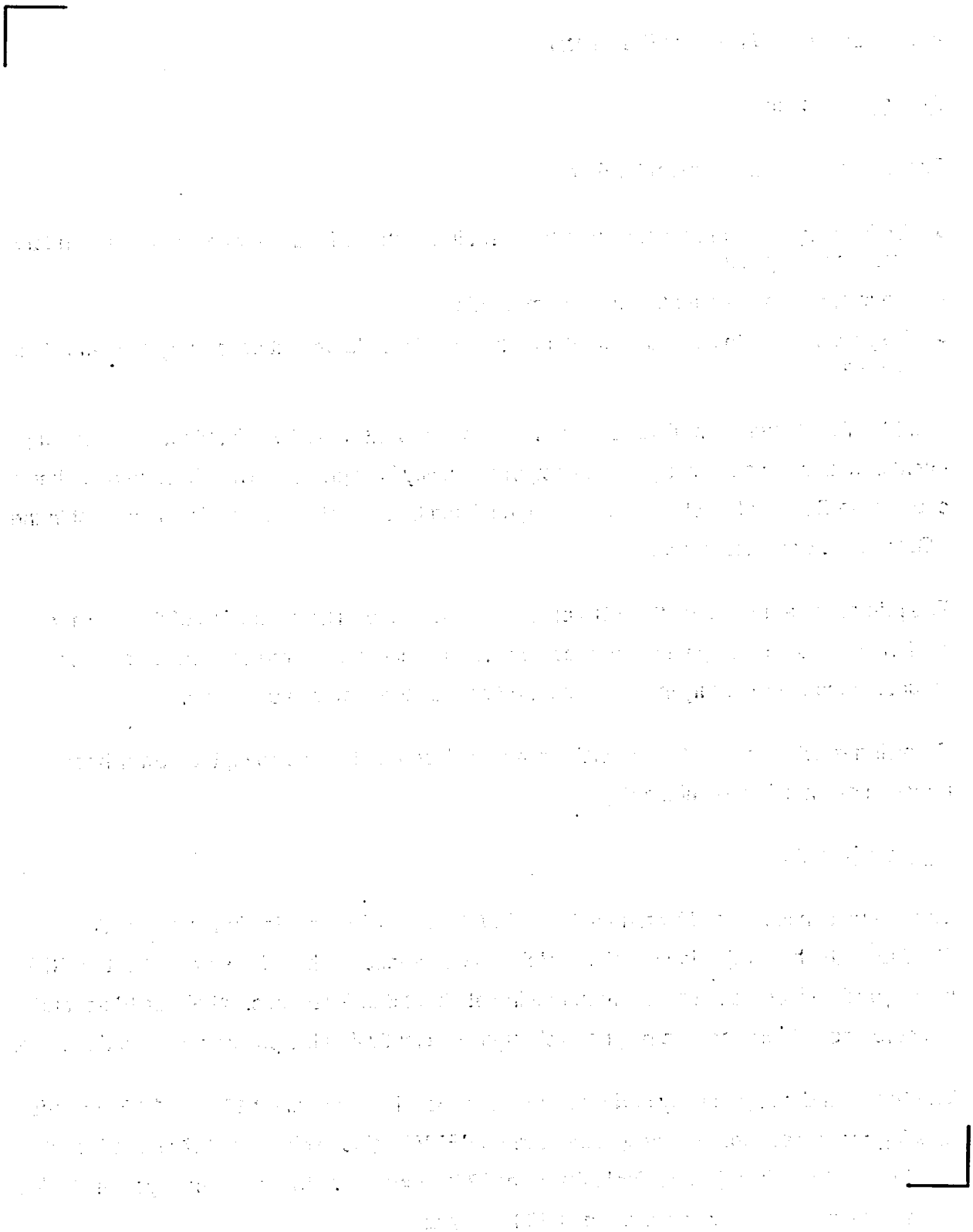


Figure 4.28 LOFT L6-3 Steam Generator Steam Flow

4.5 *LOFT L6-5 Loss of Feedwater*

Event Description

The objectives of Experiment L6-5 are:

- To investigate plant response to a transient in which the feedwater flow to the secondary system is stopped.
- To evaluate the automatic recovery methods.
- To provide data to assess computer code capabilities to predict secondary system initiated events.

The LOFT L6-5 event simulates a loss of feedwater event with AFW disabled. It is a heatup event because the secondary heat rejection capability is degraded. The absence of makeup causes the SG liquid level to drop. When the liquid level reaches the low level setpoint in the SG, the reactor is scrammed.

The primary heatup causes the RCS pressure to increase. The expansion of the primary coolant causes an insurge into the pressurizer. The increase in core coolant temperature induces negative reactivity in the reactor and causes the power to decrease.

Following reactor scram, the MSFCV is ramped closed and at this point, the power-heat rejection mismatch is terminated.

Analysis Results

The calculation is initiated by terminating MFW flow. AFW is disabled in the calculation. Gradually, the heat rejection capability of the SG decreases. The effects are felt in the RCS with a gradual increase in pressure beginning at about 6 to 8 seconds. At about 10 seconds, the core coolant temperature begins to change sufficiently that the power begins to decrease.

The SG level drops gradually and reaches the low level setpoint of -0.13 m at 19.5 seconds, causing reactor scram. Following scram, the MSFCV begins to close at 20.7 seconds and terminates steam flow (except for leakage) at 32.2 seconds. At this point, the system stabilizes and the calculations were terminated at 200 seconds.

A summary of the event sequence is provided in Table 4.4. Plots of key parameters are provided in Figure 4.29 to Figure 4.36. The table and figures include results of ANF-RELAP calculations for comparison. LOFT measured data are included also.

The calculated response of the S-RELAP5 and ANF-RELAP codes is very close for this event up to the time of reactor trip. Reactor scram occurs on a low SG level setpoint (2.824 m) and is predicted at 19.5 seconds in the S-RELAP5 calculation and at 21.9 seconds in the ANF-RELAP calculation. After the time of reactor scram, the calculated results are affected by the additional energy deposition during this 2.4 second interval, consequently, only code-to-code differences leading up to this difference in scram time will be examined.

After the termination of the main feedwater, the steam generator mass decreases at almost exactly the same rate for the two calculations. The response of the SG level, however, is somewhat different due to a difference in the initial SG void fraction profiles. Modifications to the interfacial drag package in S-RELAP5 affect the void profile both in the SG boiler region and at the top of the downcomer. In the boiler region, the interfacial drag is reduced and the initial SG mass is ~2.5 percent greater in the S-RELAP5 calculation for the same indicated level.

The difference in interfacial drag packages also affects the transient SG downcomer behavior. For S-RELAP5, a sharper liquid-vapor interface is calculated and when the SG downcomer volume at the feedwater junction starts to drain, condensation begins that temporarily reduces the downcomer-to-boiler flow rate. The subcooling at the boiler inlet decreases, vapor generation increases, and the SG level begins to drop faster than that of the ANF-RELAP calculation. The result is that S-RELAP5 predicts a reactor trip on low SG level about 2.4 seconds earlier than ANF-RELAP. During this initial heatup period, until the time of reactor trip for S-RELAP5, no significant differences were observed in the calculated response for either the reactor power or the SG heat removal rate.

Conclusions

In summary, S-RELAP5 agrees reasonably with the ANF-RELAP calculations and provides a satisfactory calculation of the LOFT L6-5 LONF experiment. The code adequately captures secondary side heat transfer and inventory changes. The results are consistent with the LOFT measurements.

Table 4.4 LOFT L6-5 Event Sequence





Figure 4.29 LOFT L6-5 Steam Generator Secondary Side Liquid Level



Figure 4.30 LOFT L6-5 Pressurizer Liquid Level



Figure 4.31 LOFT L6-5 Pressurizer Pressure



Figure 4.32 LOFT L6-5 Steam Generator Secondary Pressure



Figure 4.33 LOFT L6-5 Reactor Power



Figure 4.34 LOFT L6-5 Hot Leg Temperature



Figure 4.35 LOFT L6-5 Cold Leg Temperature



Figure 4.36 LOFT L6-5 Steam Generator Steam Flow

4.6 LOFT Analysis Conclusions

The results of these analyses of the LOFT L6 experiments indicate good agreement between the S-RELAP5 calculated results and ANF-RELAP calculated results. The analyses test both the component and heat structure nodalization and the simulation capabilities of S-RELAP5. The simulation capabilities tested include the modeling of automatic control components and systems, such as MSFCV, pressurizer spray, pressurizer heaters, feedwater control, pressure control, SG liquid level control, and reactor scram. The S-RELAP5 thermal-hydraulic components and heat structure nodalization provide information on the adequacy of the reactor coolant loop flow dynamics, pressurizer pressure adjustments, core kinetics, reactor coolant loop thermal transport, SG heat transfer, and secondary system thermal-hydraulic behaviors.

5.0 Event-Specific Methodology

This section describes the application of this methodology. It describes the SRP Chapter 15 events for which the methodology is to be applied, the Disposition of Events Review process for both initial and follow-on reloads, and the biasing of parameters. It also includes a discussion of events that were either not described in the previously approved methodology (Reference 3) or that need further clarification.

The MSLB methodology (Reference 4) is merged into this report to replace ANF-RELAP with S-RELAP5 and to have one report that covers non-LOCA transients. The Boron Dilution and Misloaded Assembly events were not described in Reference 3 and are included here for completeness. They are also events which do not require system models. The Control Rod Ejection event is added to describe the thermal-hydraulic evaluation of the event. The Radiological Consequences of the Failure of Small Lines Carrying Primary Coolant Outside Containment event is included to address an Safety Evaluation Report (SER) restriction on Reference 3. The SGTR event is discussed explicitly to address an SER restriction on the Reference 3 methodology.

5.1 Scope of Application

The methodology is applicable to all CE and Westinghouse plant designs and all modes of plant operation. The methodology is related to the thermal-hydraulic aspects of the SRP events and does not include analysis of radiological dose consequences. However, this methodology provides input to radiological consequence analyses.

The methodology is applicable to the SRP Chapter 15 non-LOCA events listed in Table 2.1. The events are listed according to the event categories given in the SRP. The methodology is applicable to Condition I, II, III, and IV events. The event frequency classifications are:

- **CONDITION I:** events expected to occur frequently in the course of power operation, refueling, maintenance, or plant maneuvering.
- **CONDITION II:** events expected to occur on a frequency of once per year during plant operation.
- **CONDITION III:** events expected to occur once in the lifetime of the plant.
- **CONDITION IV:** events not expected to occur that are evaluated to demonstrate the adequacy of the design.

The Condition I events, in part, establish the initial conditions for the analysis of more severe events, while the Condition II through IV events normally constitute the licensing analyses. The Condition II events are Anticipated Operational Occurrences (AOOs), and the Condition III and IV events are Postulated Accidents (PAs). The classification of a given SRP Chapter 15 event may vary depending on a given plant's licensing basis.

Licensing analyses are performed to support plant operation. This is demonstrated by meeting the applicable acceptance criteria for each event. The acceptance criteria are defined in each plant's licensing basis and may differ from the criteria specified by the SRP. The acceptance criteria for Condition II, III, and IV events, as specified in the SRP, are:

Condition II Events (AOOs):

- Pressures in the RCS and main steam system are less than 110 percent of design values.
- Fuel cladding integrity is maintained by ensuring that SAFDLs are not exceeded.
- Radiological consequences are less than the 10 CFR 20 guidelines.
- The event does not generate a more serious plant condition without other faults occurring independently.

Condition III Events (PAs):

- Pressures in the RCS and main steam system are less than 110 percent of design values.
- A small fraction of fuel failures may occur, but these failures do not hinder core coolability.
- Radiological consequences are a small fraction of the 10 CFR 100 guidelines (generally less than 10 percent).
- The event does not generate a limiting fault or result in the consequential loss of the reactor coolant or containment barriers.

Condition IV Events (PAs):

- Radiological consequences do not exceed 10 CFR 100 guidelines.
- The event does not cause a consequential loss of the required functions of systems needed to maintain the reactor coolant and containment systems.

Additional event-specific criteria are described, as required, in the appropriate section.

5.2 *Application Process*

All events listed in Table 2.1 that constitute the licensing basis for a given plant may be analyzed using this methodology. A Disposition of Events may be performed to limit the number of events that are analyzed.

5.2.1 Disposition of Events

The purpose of a Disposition of Events review is (1) to evaluate the impact of changes to key parameters on the safety-related analyses supporting a plant's licensing basis, and (2) to determine the scope of analyses that need to be performed. A Disposition of Events review may be performed for the first SPC reload in a given plant, for each subsequent reload, and at other times due to changes in plant configuration or operation. The Disposition of Events evaluates changes in (1) plant configuration, operating conditions, Technical Specifications, and reactor protection system (RPS) and other equipment setpoints, (2) fuel design, and (3) neutronics parameters. Additional factors considered in the Disposition of Events include (1) the plant licensing basis, (2) all modes of operation, (3) core exposure, and (4) event initiators.

The Condition II, III, and IV events are divided into event categories in the SRP that have similar characteristics, such as heatup events, cooldown events, and reactivity events. Each SRP event category is considered to determine which events within each category, or events with similar characteristics, are limiting for the specific licensing application.

The Disposition of Events typically disposes Condition II events and PAs (Condition III and IV events) separately since the acceptance criteria are different for Condition II events and PAs. However, if a Condition III or IV event is analyzed to meet the acceptance criteria of a Condition II event, a Condition III or IV event analysis may bound a given Condition II event in the same category or with similar characteristics.

The Disposition of Events review classifies each event into one of the following categories:

- Event must be reanalyzed.
- Event is bounded by another event.
- Event is bounded by a previous analysis.
- Event is outside the licensing basis of the plant.

5.2.2 Analysis Assumptions

When analyses of the various SRP Chapter 15 events are performed, the analyses will consider the following items:

[

]

5.3 *Biasing of Parameters*

[

The following text is extremely faint and largely illegible. It appears to be a technical description or procedure, possibly related to the methodology mentioned in the header. The text is organized into several paragraphs, but the specific details are difficult to discern due to the low contrast and resolution of the scan.

1

5.4 Main Steamline Break (MSLB)

The methodology described below replaces that described in Reference 4. Detail has been added on how mixing in the reactor pressure vessel is modeled and how event parameters are biased. A description of how the pre-scrum portion of the MSLB event is modeled has also been added. S-RELAP5 is used in place of ANF-RELAP for MSLB. Except for these changes, the methodology for MSLB analyses is unchanged from Reference 4.

In a PWR, accidental occurrence of an MSLB, coincident with a negative moderator coefficient and the most reactive control rod stuck in the withdrawn position, can lead to a critical core and a return to power from a previous subcritical state. Analysis of this event is conducted as part of safety analyses required by the NRC for operation of PWR nuclear power plants. Guidelines for NRC review and acceptance of MSLB safety analyses are presented in SRP 15.1.5.

The MSLB event is analyzed to assess the potential for fuel failure from either DNB or FCM. Acceptance criteria allow fuel failure, but require the radiological consequences for an MSLB with the highest worth control rod stuck out of the core and an assumed pre-accident iodine spike to be within 10 CFR Part 100 guideline values. For an MSLB with equilibrium iodine concentrations for continuous full power operation and an assumed accident-initiated iodine spike, the calculated doses must be a small fraction of the 10 CFR Part 100 guideline values.

The SPC MSLB analytical methodology utilizes S-RELAP5 (Reference 1) for the NSSS calculation, an approved neutronics code for the detailed core neutronics calculation, and XCOBRA-IIIC (Reference 6) for the detailed core thermal-hydraulic calculation.

The use of S-RELAP5, combined with the various assumptions described in Section 5.4.3, provides a conservative simulation of an MSLB accident. The use of a steam-only-out-the-break model, the inclusion of upper head flashing, a point kinetics core model, [minimal mixing] between the affected and unaffected coolant loops, and the conservative representation of plant systems combine to ensure a very conservative S-RELAP5 model. [

]

There is flexibility in the methodology to accommodate vendor and reactor type differences, as well as different approaches to various aspects of MSLB analysis, such as reactivity feedback and mixing within the reactor pressure vessel.

Although the related containment analysis methodology is not part of the methodology described below, the worst case MSLB NSSS calculation may serve as the basis of the mass and energy history sources in the containment calculation for an MSLB transient.

5.4.1 Methodology Overview

The SPC MSLB methodology is illustrated by the flow diagram in Figure 5.1. The methodology uses S-RELAP5 to calculate the plant transient response to an MSLB, based on a detailed hydraulic model of the reactor coolant and steam systems and a point kinetics model of the core. Fuel failure from either departure from nucleate boiling (DNB) or FCM is assessed, based on the conditions calculated by XCOBRA-IIIC and the neutronics code for the highest powered fuel assemblies.

Core power, core boundary conditions, other primary system conditions, and secondary conditions are computed during the transient with S-RELAP5. At selected points in time during the transient, the power distribution and reactivity are computed with the neutronics code, based on the core power and core boundary conditions from S-RELAP5. At the same points in time, the PWR open lattice (i.e., open channel) core flow distribution is calculated with XCOBRA-IIIC, based on the power distribution from the neutronics code and the core boundary conditions from S-RELAP5.

The MDNBR is determined by using approved correlations such as the XNB (Reference 15), high thermal performance (HTP) (Reference 16), modified Barnett (Reference 17), or Biasi

correlation (Reference 18). The potential for fuel failure from DNB is assessed by comparing the calculated MDNBR to the applicable departure from nucleate boiling ratio (DNBR) safety limit.

The peak fuel rod LHGR which occurs during the transient is calculated using the core power from S-RELAP5 and the power distribution from the neutronics code. The potential for fuel failure from FCM is assessed by comparing the calculated peak LHGR to an LHGR limit for FCM, determined with RODEX2 or other approved fuel rod thermal-mechanical computer codes.

The S-RELAP5 calculation includes a sectorized core and allows for flashing in the upper head of the reactor pressure vessel. Asymmetric thermal-hydraulic and related reactivity feedback effects are accounted for with the sectorized core. Upper head flashing capability retards the pressure decay in the reactor coolant system and thus both delays the time of initial delivery and decreases the delivery rate of boron to the core from the Safety Injection System (SIS).

In some cases the complete computation string is not required. For example, in cases where there is no return to power, or where the return to power is extremely small, DNBR and FCM calculations are not necessary.

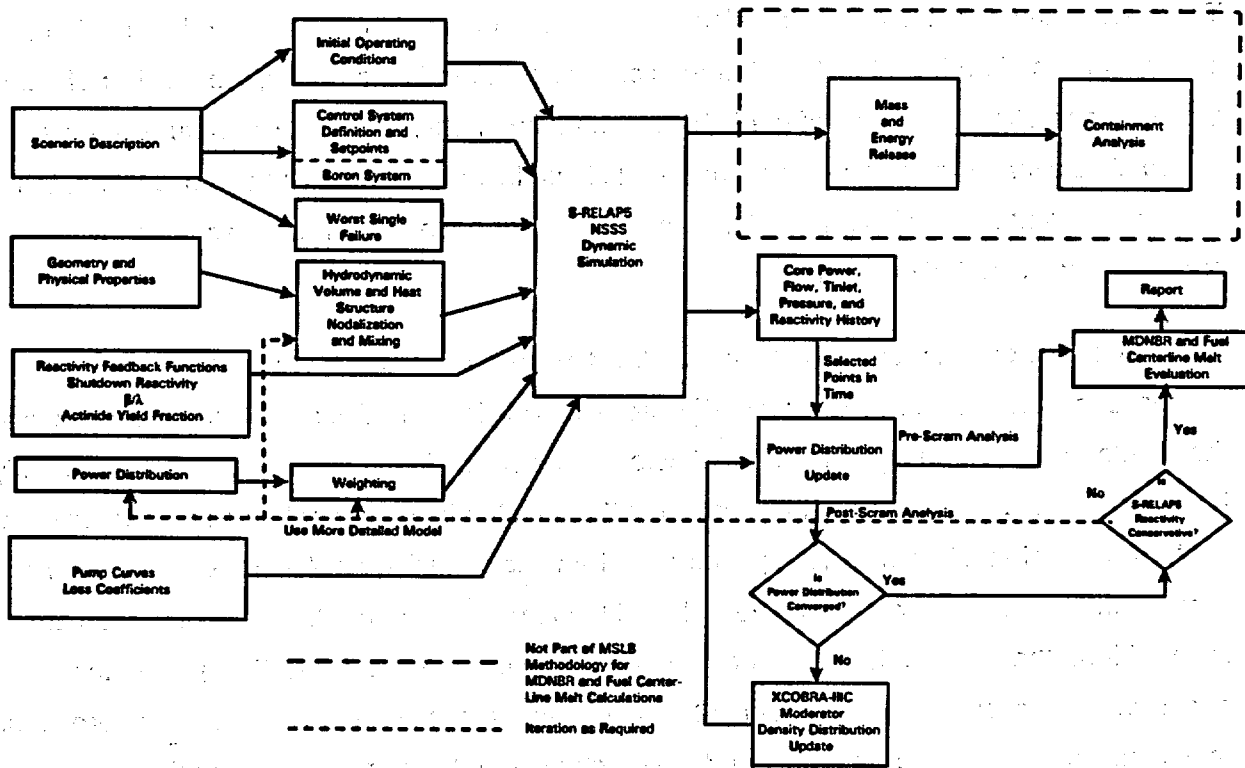


Figure 5.1 SPC Steamline Break Methodology

5.4.2 Description of Methodology

5.4.2.1 Transient Characteristics

There are many possible MSLB transient scenarios. Factors of importance in determining the consequences of an MSLB include the reactor vendor related differences, the number of loops, the initial operating conditions of the NSSS, availability of offsite power (i.e., natural versus forced circulation of reactor coolant), the worst single failure, the break size and location, the cycle dependent neutronics parameters, and whether or not a stuck rod is assumed in connection with the iodine spiking.

In all large break scenarios, with extended blowdown from one SG, there will be a rapid depressurization and cooldown of the affected SG. This in turn will lead to a rapid cooldown in the reactor coolant loop containing the affected SG and also in the core sector cooled primarily by water entering the core from the cold leg of the affected loop. Other loops and related core sectors will cool at a lesser rate, depending on the various mixing and/or crossflow phenomena present within the reactor pressure vessel, and the time delay before the remaining SGs are isolated from the break with closure of the main steam isolation valves (MSIVs). Due to the cooldown, the reactor system coolant will contract. In the case of a severe steamline break this may cause the pressurizer to empty and the reactor coolant system pressure to decrease rapidly. Water in the reactor pressure vessel upper head may flash if this region is fairly stagnant. Upper head flashing will act to delay the reactor coolant system pressure decay once the saturation pressure of the upper head is reached. This may delay the initiation of borated water injection by the SIS. Higher reactor coolant system back pressure will also result in lower flow from the SIS, further lengthening the time it takes for boron to enter the core.

5.4.2.2 Post-Scram MSLB

The core will be subcritical shortly after initiation of the MSLB, due to a scram at power, a scram at critical HZP, or as a consequence of initiating the transient from subcritical conditions. Shortly after the break, both Doppler and moderator reactivity feedback will be positive at EOC core conditions, due to cooldown of both the fuel and the moderator throughout the entire core.

With the most reactive control rod assumed to be stuck out of the core, the radial neutron flux (and therefore power) distribution will be highly peaked in the region of the stuck control rod.

Under this condition, both positive reactivity feedback effects during cooldown and negative feedback effects during heatup will be dominated by the region around the stuck control rod. If the core sector with the stuck control rod is also the sector being cooled primarily with coolant delivered by the cold leg of the affected loop, positive feedback due to cooldown of the fuel and moderator will be accentuated due to the flux distribution. If criticality is reached and the reactor begins a power excursion, negative Doppler feedback will tend to reduce the core reactivity. In certain regions of the core the moderator feedback may also be negative, due to heatup of the coolant in that region, thereby further reducing the total core reactivity. This is particularly true for the highest power peaked assemblies near the stuck control rod, where, if power levels are high enough, voiding will occur, which will result in significant reductions in total core reactivity. If boron is not injected into the core and if the affected SG does not dry out for an extended period of time into the transient, a quasi-steady-state power level will be reached, as reactivity feedback effects equilibrate and the steam flow rate out the break equilibrates with core power. Eventually, as the affected SG begins to dry out, reactor coolant system temperatures will rise, reactivity feedback effects will reduce power, and a new equilibrium power level will result, with the break steam flow rate equal to the AFW flow rate.

If the boron injected into the core is from a high concentration boric acid tank, then the power excursion will be terminated upon the first pass of borated safety injection water through the core. If the concentrated boric acid tank has been removed, or the boric acid has been removed from the tank, and boron is supplied from the more dilute RWST, then the power excursion will terminate more slowly. Delivery of significant quantities of boron into the core is dependent on (1) the time delay between the SIS signal and the time required to bring the pumps to rated speed, (2) the time delay between actuation of the SIS and decay of the reactor coolant system pressure below the safety injection pump shutoff head, (3) the time delay required to transport the boron from the boron source to the core, and (4) dilution of the boron between the source and the core. Other important factors are the number and characteristics of injection pumps assumed operational.

Main and AFW characteristics also have an impact on the MSLB transient. The higher the feedwater flow rate, the longer the period of flow, and the lower the enthalpy of the feedwater sources—the greater will be the severity of the reactor coolant system cooldown. If the MFW is on, it will be terminated after a short delay following receipt of a main steam isolation signal (MSIS).

Two RCP cases are typically considered in the MSLB analysis. These are (1) offsite power available—with the RCPs operating throughout the transient—and (2) offsite power lost when the transient is initiated—with the RCPs tripped at initiation.

The maximum break size is the most limiting, since it maximizes the rate and extent of cooldown. For plants with integral flow restrictors in the SG heads, the worst break location is either immediately downstream of the flow restrictor or between the flow meter and the MSIV. For plants without integral flow restrictors, the worst break location is between the SG head and the flow meter. In order to bound radiological consequences, break locations both inside and outside containment are considered.

The worst single failure is determined on a plant specific basis. Typically, the worst single failure for the Post-Scram MSLB analysis has been found to be the failure of a single safety injection pump. Failure of an MSIV to close will have no effect on the worst transient scenario, due to the location of the break.

5.4.2.3 Pre-Scram MSLB

The pre-scram phase of an MSLB event can challenge acceptance criteria due to harsh containment conditions and power decalibration. Power decalibration is caused by density-induced changes in the reactor pressure vessel downcomer shadowing the power-range excore detectors during heatup or cooldown transients. The nuclear power level indicated by the excore detectors is lower than the actual reactor power level when the coolant entering the reactor pressure vessel is cooler than the normal full power temperature (and higher when the inlet coolant is warmer than the normal full power temperature). This effect is taken into account in the modeling of any power-dependent reactor trips credited in the analysis.

A break located downstream of a main steamline check valve will allow steam to flow to the break from all SGs prior to MSIV closure and will be referred to as a "symmetric" break. An "asymmetric" break is located upstream of a check valve and allows steam to flow to the break from the upstream SG only (because the check valve precludes backflow to the break from the downstream SGs).

The worst single failure for an asymmetric break is the failure of one nuclear instrumentation (NI) channel. There are typically four channels of NI, using excore detectors located around the

reactor which provide power indication to the RPS. Since the power in the affected region will always be higher than in the unaffected region, the NI channel closest to the affected sector is conservatively assumed to be failed. If plant operation allows one NI channel to be out-of-service, it is selected from the remaining NI channels as that closest to the affected region. The response of the remaining excore detectors are conservatively modeled, and provide the signal for initiation of a reactor trip on an over-power condition.

There is no single failure which could worsen the event consequences for a symmetric break. A full range of break sizes, up to a double-ended guillotine break of a main steamline, is considered. The moderator temperature coefficient (MTC) is varied over each break size analyzed to sufficiently bound the timing effects between a Low SG Pressure trip (dependent on break size) and an over-power trip (dependant on the primary side cooldown and the value of the MTC).

5.4.3 S-RELAP5 NSSS Model

5.4.3.1 General Overview

The general input requirements for S-RELAP5 include a description for the primary and secondary systems in terms of hydrodynamic volumes and the structures which interact with these volumes from a heat transfer standpoint. A typical nodalization is provided in Figure 6.2, Figure 6.4 and Figure 6.5. (This nodalization is specific to the sample problem and is meant to illustrate how the sample problem was modeled. In general, nodalizations differ for each specific application due to differences in reactor design.)

Reactor kinetics, power distributions, and reactivity feedback weighting are all required as part of the input. Pump curves and hydraulic loss coefficients are also part of the input. Additional input information required to describe the transient scenario of interest to MSLB analysis can be specified through the control system model integral to S-RELAP5.

Items of particular importance to the S-RELAP5 NSSS model are discussed in detail in the following sections.

5.4.3.2 Sectorized Core and Other Reactor Pressure Vessel Components

In order to simulate the asymmetric thermal-hydraulic and reactivity feedback effects that can occur during an MSLB transient, the core is divided into two sectors. The division is made between the core sector which is directly impacted by the affected SG and the sector which is not directly impacted. The core sector and loop which are directly impacted by the break will be termed the "affected" sector and loop. The remainder of the core and the remaining loops will be termed "unaffected."

This division of the core into two sectors, or parallel flow channels, for a CE plant is shown in Figure 5.2. [

The upper and lower plenums and other reactor pressure vessel components are divided similarly. To further refine the prediction of core thermal-hydraulic behavior, a [

].

The division of the core into two sectors for a three-loop Westinghouse plant is shown in Figure 5.3. [

]

5.4.3.3 Mixing Between Sectors

During an MSLB transient, mixing between the parallel affected and unaffected sectors within the reactor pressure vessel will occur in the lower plenum, the core, and the upper plenum—due to lateral momentum imbalances, turbulence or eddy mixing, and the relative angular positions of the cold legs to the hot legs. Some mixing will also occur in the downcomer. Mixing and/or crossflow will act to reduce the positive reactivity feedback effects—due to a reduced rate and magnitude of cooldown of the affected loop.

In the SPC methodology, [

]

5.4.3.4 Power Distribution, Reactivity Feedback, and Feedback Weighting

The SPC methodology [

]

One approach is to utilize a [

]

5.4.3.5 Upper Head Flashing

Flashing in the upper head is modeled by using [

]. The more stagnant the region is, the more flashing will occur—which will subsequently retard the pressure decay within the reactor coolant system.

5.4.3.6 Initial Power Level and Offsite Power Availability

The initial power level and availability of offsite power are two major factors in determining the most limiting MSLB transient.

The post-scrum phase of the MSLB event typically considers two initial power levels, HFP and HZP. The pre-scrum phase of the event is analyzed only at HFP conditions because the initial margin to the SAFDLs is the smallest.

Two offsite power availability assumptions are typically considered. These are offsite power available for operation of RCPs and safety injection pumps, and offsite power not available for operation of these pumps. In this latter case, the RCPs are assumed to be tripped at initiation of the MSLB, and a delay time to start diesel generators for operation of the SIS pumps is included in the analysis.

5.4.3.7 Safety Injection, Feedwater, and MSIVs

The SIS, feedwater system, and MSIVs have important impacts on the Post-Scrum MSLB analysis.

The SIS delivers boron to the core and may be one of the means for terminating the MSLB power excursion. The main factor of importance is the time delay from initiation of the break to the time when boron of adequate concentration to terminate the power excursion is delivered to the core. This time is determined by the concentration of the boron source, the flow delivery characteristics of the SIS versus reactor coolant system pressure, the number of SIS pumps available, the delay time required to bring the pumps to speed after receipt of the actuation signal, the SIS trip setpoint, the piping volume between the boron source and the reactor coolant system injection location, and the dilution that occurs between the source and the injection point.

The feedwater system consists of the MFW system utilized during normal operation and an AFW system of much reduced capacity for use when the main system is not available. For the post-scrum phase of the MSLB event, the higher the total feedwater flow is and the lower the inlet enthalpy is, the greater the cooldown and subsequent return to power will be. Upper bounds on the flow and lower bounds on the enthalpy of the main and AFW are used during the transient calculation.

The primary consideration for the MSIVs is the period of time the unaffected SGs are able to blow down before the MSIVs close. Closure will occur after a short time delay following a closure signal.

5.4.3.8 Containment Model

[

]

The Post-Scram MSLB analysis does not credit the containment high pressure trip, therefore a containment model is not necessary.

5.4.3.9 Input Parameter Biasing

Following is a description of the parameters to be biased with this methodology, including in which code it is to be biased. The biases discussed below are applicable to the pre-scrum and post-scrum phases of the MSLB event unless otherwise noted.

[

The methodology for determining the maximum credible accident (MCA) for a pressurized water reactor (PWR) is described in this section. The MCA is defined as the most severe accident that is physically possible and that can be analyzed using the methodology described in this section. The MCA is determined by considering all possible initiating events and their consequences, and selecting the most severe event. The MCA is then analyzed using the methodology described in this section to determine the maximum credible release of radioactivity from the reactor core.

The methodology for determining the MCA for a PWR is described in this section. The MCA is defined as the most severe accident that is physically possible and that can be analyzed using the methodology described in this section. The MCA is determined by considering all possible initiating events and their consequences, and selecting the most severe event. The MCA is then analyzed using the methodology described in this section to determine the maximum credible release of radioactivity from the reactor core.

The methodology for determining the MCA for a PWR is described in this section. The MCA is defined as the most severe accident that is physically possible and that can be analyzed using the methodology described in this section. The MCA is determined by considering all possible initiating events and their consequences, and selecting the most severe event. The MCA is then analyzed using the methodology described in this section to determine the maximum credible release of radioactivity from the reactor core.

The methodology for determining the MCA for a PWR is described in this section. The MCA is defined as the most severe accident that is physically possible and that can be analyzed using the methodology described in this section. The MCA is determined by considering all possible initiating events and their consequences, and selecting the most severe event. The MCA is then analyzed using the methodology described in this section to determine the maximum credible release of radioactivity from the reactor core.

The methodology for determining the MCA for a PWR is described in this section. The MCA is defined as the most severe accident that is physically possible and that can be analyzed using the methodology described in this section. The MCA is determined by considering all possible initiating events and their consequences, and selecting the most severe event. The MCA is then analyzed using the methodology described in this section to determine the maximum credible release of radioactivity from the reactor core.

]

5.4.4 Core Neutronics Model

5.4.4.1 Post-Scram MSLB

An NRC-approved neutronics code is used to calculate radial and axial power distributions and total core reactivity for a given core power level and moderator density distribution. Input to the neutronics code includes the core power level from S-RELAP5, the core coolant density distribution from XCOBRA-IIIC, and a reference set of nuclear cross sections appropriate for the core of interest, plus the conditions under which the cross sections were generated. For these imposed conditions, the code determines the distribution of power within the core, both axially and radially, [

] The code also determines the resultant core reactivity under the imposed core conditions.

The nodal moderator densities from XCOBRA-IIIC are transferred into the neutronics code, and iterative neutronics code/XCOBRA-IIIC calculations are performed until the power distribution converges.

5.4.4.2 Pre-Scram MSLB

For asymmetric cases, the neutronics code is used to calculate the case-specific radial power distribution. [

]

For symmetric cases, the thermal-hydraulic conditions and power distributions of the affected and unaffected sectors of the core are essentially identical. [

]

5.4.5 Core Thermal-Hydraulic Model

Input to the XCOBRA-IIIC core thermal-hydraulic analysis consists of assembly geometry and hydraulic descriptive information, including information regarding which assemblies are adjacent to each other. The S-RELAP5 calculated core outlet pressure, core inlet flow distribution, core inlet temperature distribution, and core-average LHGR, along with the neutronics code calculated axial and radial power distributions, must be input. [

]

5.4.6 Reactivity Comparison

5.4.6.1 Post-Scram MSLB

A three-channel S-RELAP5 core model can only accommodate relatively simple radial and axial power distributions, associated reactivity feedback, and feedback weighting models. This tends to result in simple and conservative representations of highly complex neutronics and thermal-hydraulic phenomena. The inherent conservatisms are demonstrated by comparing the reactivity change calculated with S-RELAP5 against that calculated with the neutronics code at points in time of particular interest. An important point of interest is the time at which MDNBR occurs.

The reactivity change calculated with the neutronics code is increased to account for an MTC bias adjustment and, for HFP cases, a scram curve adjustment. [

5.4.6.2 Pre-Scram MSLB

The Pre-Scram MSLB analysis does not require a reactivity comparison due to the calculations performed to find the most limiting combination of MSLB size and MTC. These calculations, in essence, cover a spectrum of reactivity insertions by varying the break size and MTC. Additionally, the neutronic response prior to scram is not as complex as that in the post-scram portion of the event.

5.4.7 MDNBR and FCM Analysis

The end result of an MSLB MDNBR and FCM analysis is to determine how many, if any, fuel rods penetrate the DNBR safety limit and/or the FCM limit. If the MDNBR is below the DNBR limit or if the peak LHGR is above the FCM LHGR limit, then the total number of fuel rods expected to fail is determined. The methods utilized as part of the MSLB methodology to determine the MDNBR and peak LHGR are discussed in the following sections.

5.4.7.1 XCOBRA-IIIC Subchannel DNBR Evaluation Method

[

]

5.4.7.2 Alternate DNBR Evaluation Method

[

]

5.4.7.3 Peak LHGR Evaluation Method

5.4.7.3.1 Post-Scram MSLB

The peak fuel rod LHGR which occurs after scram is calculated using the peak post-scram core power from S-RELAP5 and the corresponding power distribution from the neutronics code. [

]

5.4.7.3.2 Pre-Scram MSLB

The peak fuel rod LHGR which occurs prior to scram is calculated using the peak pre-scram core power from S-RELAP5. Asymmetric cases use the corresponding power distribution from the neutronics code while symmetric cases use a conservatively limiting axial power profile and radial power distribution. [

]

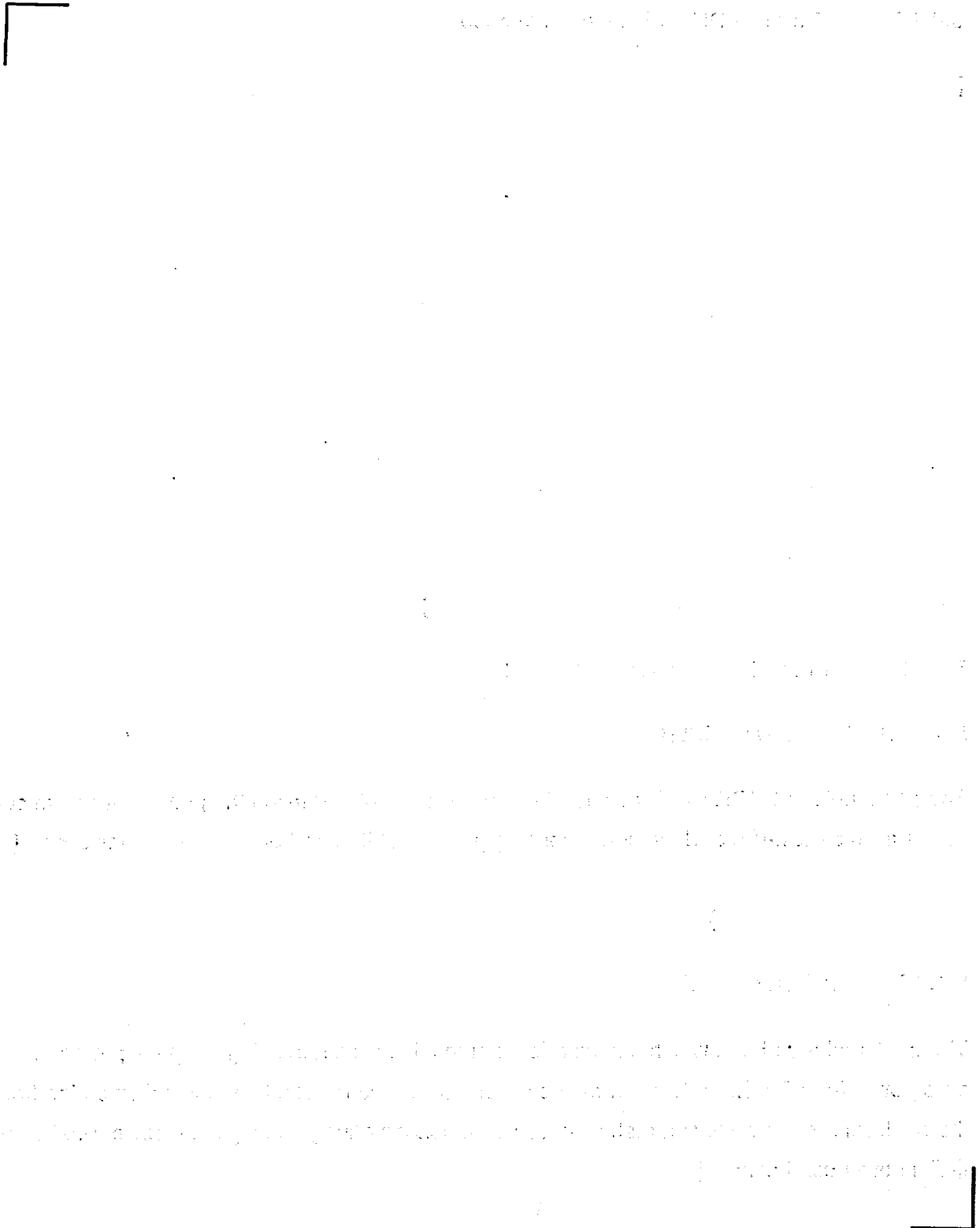


Figure 5.2 Core Model for CE Plant



Figure 5.3 Core Model for Three-Loop Westinghouse Plant



Figure 5.4 [] for Three-Loop Westinghouse Plant

5.5 *Steam Generator Tube Rupture (SGTR)*

This event is generally categorized as a Condition IV event. The acceptance criteria are given in Section 5.1. The system analysis provides the boundary conditions for use in the evaluation of radiological consequences. The system response is evaluated using the tools and methods applied for other non-LOCA events with appropriately bounding assumptions.

Event Description

The SGTR event is Event 15.6.3 of the SRP and is initiated by a break of a single steam generator tube. Coolant from the RCS begins to escape through the break, driven by the pressure differential between the RCS and the SG secondary side, increasing the inventory and pressure in the SGs.

As the break flow begins to de-pressurize the RCS, the charging pumps activate in order to make-up the lost inventory. If the RCS inventory and pressure are stabilized via the charging pumps, no reactor trip will occur. However, if the break flow exceeds the capacity of the pumps, the RCS pressure and inventory will continue to decrease resulting in a reactor trip on a low-RCS-pressure signal. Following the reactor trip, the turbine will trip and, in the case where offsite power is lost, the coolant pumps will coast down and make-up flow will terminate. If offsite power is available, a fast transfer to the offsite power will keep the pumps running and the make-up flow available.

The loss of offsite power results in the loss of condenser vacuum and the steam dump valves are closed to protect the condenser. The continued mass and energy transfer between the primary and secondary side results in a rapid increase in SG pressure and discharge to the atmosphere via the Main Steam Safety Valves (MSSVs) and Atmospheric Steam Dump Valves (ADVs).

As the RCS pressure continues to decrease, a low pressurizer pressure signal activates the SIS. The emergency diesels start and HPSI flow begins. For some plants, the HPSI pumps have a very high delivery head which may result in a rapid pressurization of the reactor coolant system. In this case, a high break flow rate is maintained leading to a more rapid filling of the SG. This may lead to liquid in the steamlines and MSSVs. Liquid in the steamlines may cause the MSSVs to fail open and potentially damage the steam piping.

The event can proceed in several directions from this point and is highly dependent on the emergency operating procedures (EOPs) for the plant. The ECCS tends to exacerbate the releases for this event by maintaining the pressure in the RCS and increasing the flow to the SGs. The HPSI and AFW flows may be secured, ADVs may be opened to de-pressurize the SGs and the RCS, and the pressure operated relief valves (PORVs) may be opened to bring the RCS pressure down and stop flow through the break. The operators will take a series of actions to regain control of the plant systems and to bring the RCS to a condition allowing for initiation of the residual heat removal (RHR) system. To regain control of the plant systems, the operators must first identify the event. The identification is based on a high secondary side activity in conjunction with a high water level reading for the affected steam generator.

The depressurization of the RCS does not generally present as great a challenge to fuel failure as the inadvertent opening of a PORV and the potential for fuel failure is quite low.

The key elements of this event are the primary-to-secondary pressure differential and the break flow path. The temperature of the RCS usually sets the pressure, which determines the flow. The temperature is established by the power in the primary and the secondary pressure. For plants with very high head HPSI pumps, the reactor coolant pressure can be dependent on the HPSI flow.

Events Analyzed

The event can be initiated from HZP or HFP conditions. Due to the lack of decay heat load for the HZP case, it may not be the limiting inventory release case. However, given the technical specification limits on activity, the HZP transient may lead to more limiting radiological consequences. Therefore, unless the HZP case can be dispositioned, it will be analyzed.

The loss of offsite power must be addressed due to the impact on condenser availability for the steam dump bypass system. The lack of such availability may lead to more limiting radiological consequences.

The potential for overflow of the secondary side exists. For some PWR designs, the make-up flow and HPSI flow are provided by the same pump. These designs have the highest potential for over-filling the secondary side and introducing liquid into the steamlines. The SGTR event analysis will address overflow for these designs which utilize very high head HPSI pumps.

Analysis Method

The system response is modeled using S-RELAP5, including cooldown to RHR operation. The phenomena that determine the release to the atmosphere and the challenge to fuel integrity are similar to those encountered in other non-LOCA events, with the exception of the break flow. The break flow is addressed using models similar to those used for small break LOCAs. The de-pressurization of the RCS is bounded by that experienced by Event 15.6.1. The SG pressurization transient is bounded by that modeled for Event 15.2.1. The SG level increase is bounded by Event 15.2.1 and by Event 15.1.2 (the Increase in Feedwater Flow).

The early portion of the transient (prior to operator action) is modeled using the ESFAS and RPS responses using a slightly modified S-RELAP5 model for Chapter 15 non-LOCA events. The modifications include the following:

- **Added SG Tube** – The normal non-LOCA model lumps all of the tubes in a SG together. The SGTR model has one SG tube modeled explicitly, with the remainder lumped. The rupture model is a double-ended guillotine break in this tube just above the tube sheet. Critical flow is modeled using the Moody model which provides a conservative model for choked flow and is used in SPC's LOCA and MSLB methodologies.
- **HPSI Flow** – HPSI models are added. The normal non-LOCA model does not include HPSI pumps. All pumps are assumed to be available and to operate at design capacity. This produces conservatively high flows.
- **Upper Head Flashing** - When a loss of offsite power is assumed, the cooldown of the reactor coolant system is based on natural circulation. If voiding occurs in any of the loops, it can affect the natural circulation flows. Voiding is strongly affected by the system pressure. Heat structures are added to model the metal masses in the upper head region of the reactor vessel. These modifications are based on the MSLB model and are made to increase the accuracy of the calculation of the pressure in the upper head. The boron injected with the HPSI flow is modeled for each volume. The pressure is also important for boron injection, since it determines the HPSI flow, which introduces borated water into the RCS.
- **Control System** - Since this event requires operator intervention, the S-RELAP5 input model for non-LOCA events is further modified to properly simulate operator actions consistent with the plant-specific EOPs. Generally, operation of the MSSVs, ADVs and PORVs are modeled to cool the plant down. Also, isolating the SGs and terminating HPSI flow is modeled, as appropriate.

Bounding Input

[

5.6 *CVCS Malfunction That Results In a Decrease In the Boron Concentration In the Reactor Coolant (Boron Dilution)*

The Boron Dilution event does not require an S-RELAP5 based system analysis. The methodology for performing Boron Dilution analyses is described in this section.

Identification of Causes and Event Description

One means of positive reactivity insertion to the core is the addition of unborated, primary grade coolant from the demineralized and reactor makeup coolant systems. This coolant is introduced to the RCS through the reactor charging/makeup portion of the CVCS.

The most limiting event resulting in an inadvertent boron dilution is typically a malfunction of the CVCS valve which causes pure coolant to be delivered to the RCS by all available charging/makeup pumps. The CVCS and makeup coolant systems are designed to limit, even under various postulated failure modes, the potential rate of dilution to values which will allow sufficient time for automatic or operator response to terminate the dilution. Typically, the sources of dilution may be terminated by closing isolation valves in the CVCS. The lost shutdown margin may be regained by the opening of isolation valves to the RWST, thus allowing the addition of highly borated coolant to the RCS.

The SPC Boron Dilution analysis will be performed consistent with the licensing bases as described in the FSAR for each plant. The acceptance criteria includes SRP requirements in Section 5.1 for a Condition II event. If operator action is required to terminate the transient, the minimum time intervals to respond are:

- 30 minutes (during refueling); and
- 15 minutes (for all other modes).

These times apply between either (a) the time when an alarm announces an unplanned moderator dilution, or (b) the initiation of the dilution, and the time of loss-of-shutdown margin.

The choice of (a) or (b) is determined from the plant licensing basis.

Analysis Method

To cover all modes of plant operation, boron dilution during modes 6 through 1 (Refueling, Cold Shutdown, Hot Shutdown, Hot Standby, Start-up, and Power operation) are considered. The purpose of the analysis is to demonstrate that sufficient time exists for termination by the operator before the shutdown margin is lost. Conservative values for parameters are used, i.e., high RCS critical boron concentration, minimum shutdown margin, minimum RCS volume, and maximum unborated water charging rate. These assumptions result in conservative determinations of the time available for operator or system response after initiation of a dilution transient.

There are two mixing models that can be used to represent mixing: dilution front and instantaneous mixing. For operating modes in which at least one reactor coolant pump is operating, the assumption of complete mixing of boron with water in the RCS is appropriate. For operation on the shutdown cooling system, flow rates may be insufficient to assure complete mixing of the reactor coolant system. If complete mixing cannot be assumed, then a dilution front approach is applied.

The instantaneous mixing model assumes complete and instantaneous mixing of boron within the applicable mixing volume in the RCS. The boron concentration vs. time, $C_{RCS}(t)$, and time to dilute the RCS boron concentration from the shutdown to critical states, $t_{Critical}$, are:

$$C_{RCS}(t) = C_{RCS}(0) * \exp\left(-\frac{W_{Charge}}{V_{RCS}} t\right)$$

$$t_{Critical} = \left(\frac{V_{RCS}}{W_{Charge}}\right) * \ln\left[\frac{C_{RCS}(0)}{C_{RCS}(Critical)}\right], \text{ minutes}$$

where:

- $C_{RCS}(0)$ = initial (shutdown) boron concentration, ppm
- $C_{RCS}(Critical)$ = critical boron concentration, ppm
- W_{Charge} = charging(dilution) flow rate (ft³/min),

$$V_{RCS} = \text{fluid volume of the RCS mixing volumes, ft}^3$$

In the dilution front model, the dilution is viewed as a series of 'dilution fronts' progressing through the reactor coolant system. A dilution front tracking model is used to calculate the RCS boron concentration vs. time and the time to reach criticality. The model is based on the following assumptions: (1) the charging flow mixes with the RCS flow and results in a reduced boron concentration at the mixing location, (2) the diluted mixture transit time to the bottom of the core is based on the flow volumes (between the mixing location and the bottom of the core) and the flow rates of both the charging and RCS flow, (3) if the diluted boron concentration for any front is higher than the critical concentration, the diluted mixture must sweep through the entire RCS (including the shutdown cooling system (SDCS) volumes) and pass by the dilution location another time. This dilution scenario continues until the RCS boron concentration is diluted below the critical concentration. The time-to-criticality is the number of complete RCS transit times required to achieve a boron concentration less than the critical value plus one transit time from the mixing location to the bottom of the core.

The general equations relating the Nth front boron concentration, C_N , and front transit time to reach the bottom of the core, T_N , are given by,

$$C_N = C_0 * MF * \left(\frac{W_{SDCS}}{W_{SDCS} + W_{Charge}} \right)^{(N-1)}$$

where $MF = \frac{W_{SDCS} * \text{Frac}}{(W_{SDCS} * \text{Frac}) + W_{Charge}}$,

and $T_N = \left(\frac{V_{RCS1} * \text{Frac}}{(W_{SDCS} * \text{Frac})} \right) + \left(\frac{V_{RCS}}{W_{SDC} + W_{Charge}} \right)^{N-1}$, minutes

where

W_{SDCS} = SDCS volumetric flow rate (the RCS loop volumetric flow) (ft³/min),

V_{RCS} = Applicable RCS mixing flow volume (ft³),

V_{RCS1} = RCS diluted mixture volume (volume between the mixing location and core inlet containing the diluted mixture),

Frac = fraction of the RCS coolant mixing with the charging flow between the mixing location and core inlet

Boron Dilution During Refueling (Mode 6)

An uncontrolled boron dilution transient during this mode of operation is typically prevented by administrative controls which isolate the RCS from the potential source of unborated water. If an analysis for Mode 6 is required, conditions similar to those for Mode 5, discussed below, are assumed.

Boron Dilution During Cold Shutdown (Mode 5)

The following conditions are typically assumed for inadvertent boron dilution while in this operation mode:

- a. Dilution flow is limited by the capacity of the charging/makeup pumps;
- b. For SDCS operation, a conservative RCS mixing volume consistent with the minimum active volume of the RCS is used and corresponds to the water level drained to mid-nozzle in the vessel while one train of SDCS is assumed to operate;
- c. For RCP operation, a minimum RCS mixing volume is used consistent with the active volume of the RCS minus the pressurizer volume;
- d. Control rod configuration consistent with shutdown margin requirements; and
- e. The shutdown margin is the value required by Technical Specifications for this mode.

Boron Dilution During Hot Shutdown (Mode 4)

The following conditions are assumed for an inadvertent boron dilution while in this mode:

- a. The dilution flow rate is limited by the capacity of the charging/makeup pumps;
- b. For RCP operation, a minimum RCS mixing volume is used consistent with the active volume of the RCS minus the pressurizer volume;
- c. For SDCS operation, a conservative RCS mixing volume while one train of SDCS is assumed to operate;
- d. Control rod configuration consistent with shutdown margin requirements; and
- e. The shutdown margin is the value required by Technical Specifications for this mode.

Boron Dilution During Hot Standby (Mode 3)

The following conditions are assumed for an inadvertent boron dilution while in this mode:

- a. The dilution flow is limited by the capacity of the charging/makeup pumps;

- b. For RCP operation, a minimum RCS volume is used consistent with the minimum active volume of the RCS minus the pressurizer volume. The RCS is filled and vented and at least one RCP is running;
- c. For SDCS operation, a conservative RCS mixing volume while one train of SDCS is assumed to operate;
- d. Control rod configuration consistent with shutdown margin requirements; and
- e. The shutdown margin is the value required by Technical Specifications for this mode

Boron Dilution During Startup (Mode 2)

During this mode of operation, the plant control systems are assumed in manual mode. The Technical Specifications typically require that all RCPs be operating. Other conditions assumed are:

- a. Dilution flow is limited by the capacity of the charging/makeup pumps;
- b. For RCP operation, a minimum conservative RCS mixing volume is used consistent with the active RCS volume, minus the pressurizer volume;
- c. Control rod configuration consistent with the shutdown margin requirements; and
- d. The shutdown margin required by the Technical Specifications is assumed.

This mode of operation is typically a transitory operational mode in which the operator intentionally dilutes and withdraws control rods to take the plant critical. During this mode, the plant is in manual control with the operator required to maintain a very high awareness of the plant status. For a normal approach to criticality, the operator may manually initiate a limited dilution and subsequently manually withdraw the control rods, a process that takes several hours. The plant Technical Specifications typically require that the operator determine the estimated critical position of the control rods prior to approaching criticality, thus assuring that the reactor does not go critical with the control rods below the insertion limits.

In the event of an unplanned dilution during power escalation while in the Startup mode, the plant status is such that minimal impact will result. The plant will slowly escalate in power and will activate a power related trip. There must be sufficient time to prevent return to criticality, as defined in the plant licensing basis.

Boron Dilution During Power Operation (Mode 1)

Since the slow power and temperature rise will cause a decrease in the DNBR, the event may result in a challenge to the SAFDLs. The boron dilution transient is to be bounded on the low reactivity insertion rate side by an Uncontrolled Rod Withdrawal at Power.

The erosion of shutdown margin in Mode 1 Boron Dilution is bounded by the Mode 2 analysis.

5.7 *Inadvertent Loading and Operation of a Fuel Assembly In an Improper Location (Misloaded Assembly)*

The misloaded assembly event is included here as part of the non-LOCA transient methodology. It does not require a thermal-hydraulic system analysis. The previously approved misloaded assembly methodology, Reference 19, is the basis for this methodology description.

Event Description

The misloaded assembly event is characterized by loading one or more fuel assemblies into improper locations and, where physically possible, with incorrect orientation. These fuel loading errors can result in changes in the core power distribution and increases in local power density (LPD) which may challenge the core safety limits.

To reduce the probability of core loading errors, each fuel assembly is marked with an identification number and is loaded in accordance with a specified core loading pattern. Following core loading, the identification number of each assembly loaded in the core is checked against the desired core loading pattern.

Additional safeguards against fuel loading errors include startup physics test measurements, excore instrumentation measurements, and incore instrumentation measurements. Although any of these measurements could detect power distribution anomalies, the incore instrumentation is used to perform an initial low-power measurement of the core power distribution specifically to ensure that the core is properly loaded.

A fuel loading error changes the core power distribution by an amount proportional to the change in reactivity of the misloaded assembly. Large deviations in the measured power distribution relative to the calculated power distribution are readily detectable at the initial low-

power measurement. However, small deviations between the measured and calculated power distributions may go undetected, resulting in full-power operation with the misloaded core. The most limiting misloaded configuration would be one that is undetectable and results in the highest core power peaking during the operating cycle.

The primary concerns with this event are the penetration of the DNB fuel design limit and violation of the FCM criterion.

Analysis Method

The standard SPC neutronics methodology is used to model several misloaded core scenarios. The three-dimensional steady-state core power distribution is calculated at the conditions of the initial low-power incore measurement for the correctly loaded core and for each misloaded core case. The power distribution from each misloaded case is used to represent measured data, and the power distribution for the correctly loaded core is used to represent calculated data. For each misloaded case analyzed, deviations between the measured and calculated data at incore detector locations and deviations between measured data in radially symmetric incore detector locations are evaluated. If the deviations exceed criteria used in plant procedures for detecting misloads, the misload is assumed to be detectable.

A spectrum of misloaded core cases is analyzed. Each misload scenario assumes that the core locations of two assemblies are swapped. These cases represent the misloading of assemblies into core locations which are designated to be occupied by exposed or fresh fuel with different reactivity characteristics.

Since the Technical Specification typically requires that the minimum fraction of incore detectors operable during the initial low-power incore measurement is 75 percent, each incore detector has at least a 75 percent probability of being operable during the measurement. Based on this probability, the detectors which are required to detect the misload are assumed to be operable.

For those cases which are undetectable at the initial low-power measurement, the cycle is depleted at nominal full-power conditions with the control rods withdrawn. The power distribution at each exposure may be used to detect the misloaded core consistent with plant procedures. The depletions provide calculated power peaking factors for those exposures at which the misload remains undetected. The resultant power peaking distributions are examined

to determine if the Technical Specification power peaking values are exceeded. If the power peaking values for the misloaded core are calculated to not exceed Technical Specification limits, no further evaluation is necessary, because the DNB fuel design limit and FCM criterion will not be exceeded.

If the event calculations indicate core power peaking limits would be exceeded, additional analyses become necessary. These analyses include applying the approved CHF correlation to obtain the MDNBR and calculating the steady-state peak LHGR to determine if the FCM limit is violated. Conservative values of local and assembly power distributions are input into the DNB and the FCM calculations if Technical Specification limits are violated. The DNBR and FCM calculations are performed at rated power conditions. If either DNBR or the FCM limit is penetrated, a fuel failure assessment is necessary to determine the radiological consequences of the event. The radiological consequences must be less than 10 percent of 10 CFR 100 limits.

5.8 Control Rod Ejection

Control Rod Ejection is designated event number 15.4.8 in the SRP. The event is postulated to be caused by mechanical failure of a control rod drive mechanism pressure housing resulting in rapid ejection of the control rod and drive shaft. The Control Rod Ejection event is characterized by positive reactivity insertion in conjunction with an increase in radial power peaking. The event is mitigated by Doppler reactivity feedback from increased fuel temperature. The transient is terminated by either the high flux trip on Westinghouse type PWRs or by the variable high power (VHP) trip on CE PWRs. The event is a very fast reactivity transient. The scram has no effect on the initial peak rise in power. The scram timing does however affect the fuel temperatures and the rod heat fluxes.

Guidance for analysis of this event is provided in Regulatory Guide 1.77 (Reference 20). The acceptance criteria for the Control Rod Ejection event are:

1. The radial average pellet enthalpy at the hot spot must be less than 280 cal/g.
2. The maximum reactor pressure during any portion of the transient must be less than the value that will cause stresses to exceed emergency condition stress limits as defined in Section III of the ASME Boiler and Pressure Vessel Code.
3. Fuel failure from DNB or FCM will be limited to keep off-site dose consequences well within the guidelines of 10 CFR Part 100, namely 25 percent of 10 CFR 100 limits.

Reference 21 describes the approved methodology for evaluating criterion 1. The overall system response and fuel centerline temperature for the Control Rod Ejection event is calculated with S-RELAP5. XCOBRA-IIIC is used to obtain the predicted MDNBR (Reference 6). If FCM and/or DNB are predicted, the percentage of fuel failures is computed as input for a radiological assessment.

Four cases are considered: HFP and HZP, each evaluated for BOC and EOC conditions. Key parameters biased to ensure a bounding calculation of the impact of control rod ejection are:

[
•
]]

5.9 Radiological Consequences of the Failure of Small Lines Carrying Primary Coolant Outside Containment

This event is initiated by an outside-containment rupture of a small line connected to the RCS. The flow of reactor coolant out the rupture releases activity. The event is a Condition III event, and the acceptance criteria are presented in Section 5.1. This event does not require a system model such as S-RELAP5 to evaluate the radiological consequences. SPC will evaluate the event using the following calculational process:

- Identify the small lines postulated to fail. These lines are separated into two categories: those with isolation valves inside and outside containment and those with only isolation valves outside containment. With a single failure of an isolation valve, the former will blow down to the environment until the other isolation valve is closed. With the latter, the line will blow down until the reactor coolant system is depressurized.
- Choked flow at the break, based on the reactor coolant pressure, is assumed for all cases.
- The flashing fraction downstream of the break is used to model the amount of activity becoming airborne.

A separate radiological analysis would be performed.

6.0 Sample SRP Transients

A selected set of sample SRP (Reference 2) non-LOCA transients has been analyzed to demonstrate the adequacy of the non-LOCA transient methodology. The analyses have been performed for a CE 2x4 plant.

The nodalizations for the reactor vessel, reactor coolant system piping, and SG secondary side are shown in Figure 6.1 to Figure 6.3 and the nominal initial conditions for the sample problems are given in Table 6.1. The reactor coolant system piping includes two SGs and the four pumps in four cold legs. Pressurizer and HPSI systems are also included.

The MSLB transient requires modified nodalizations for the vessel and SG secondary side. These are shown in Figure 6.4 and Figure 6.5. The reactor vessel nodalization features a sectored core, containing an affected sector and an unaffected sector. Within the affected sector is a stuck rod region. The secondary side of the SG is a simplified model, featuring a steam-only junction, consistent with the methodology in Section 5.4.

Seven transients were analyzed for a CE 2x4 PWR plant. These seven transients were:

- Pre-Scram MSLB (SRP 15.1.5)
- Post-Scram MSLB (SRP 15.1.5)
- LOEL/TT (SRP 15.2.1 and 15.2.2)
- LONF (SRP 15.2.7)
- LOCF (SRP 15.3.1)
- UCBW at Power (SRP 15.4.2)
- SGTR (SRP 15.6.3)

These seven transients were chosen to exercise both the primary and secondary systems in the plant input model. The results presented in the following sections demonstrate the adequacy of the developed methodology. Note, this sample problem is new and is not the same as the sample problem presented in Reference 3.

Table 6.1 Sample Problem Initial Conditions

<u>System Parameter</u>	<u>HFP Value</u>
Core Power (MW)	2700
Primary Pressure (psia)	2250 ^a
Pressurizer Level (% of span)	65.6
Cold Leg Temperature (°F)	548
Primary Flow Rate per Loop (lb _m /s)	21,320
Secondary Pressure (psia)	868
Total SG Mass (lb _m) per SG	130,000
Steam Flow (lb _m /s) per SG	1646
MFV Temperature (°F)	435

^a In SGTR, the pressure was 2300 psia, consistent with the methodology.



Figure 6.1 Sample Problem Vessel Nodalization



**Figure 6.2 Sample Problem Reactor Coolant System
Piping Nodalization**



Figure 6.3 Sample Problem SG and Secondary Nodalization



Figure 6.4 Sample Problem Vessel Nodalization for MSLB

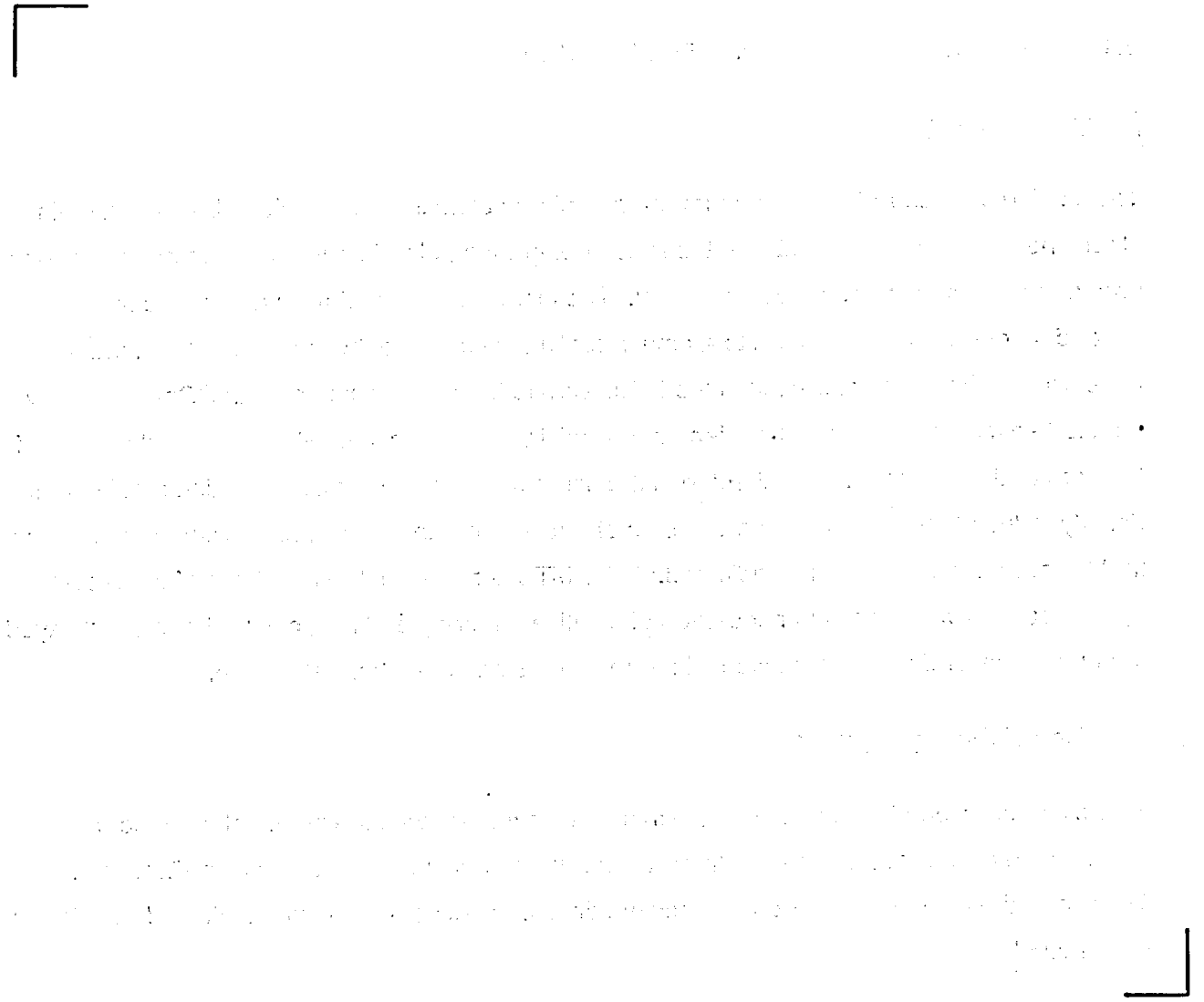


Figure 6.5 Sample Problem Steam Generator and Secondary Nodalization for MSLB

6.1 *Pre-Scram Main Steamline Break (MSLB)*

Event Description

The limiting pre-scrum MSLB event for the sample problem is initiated with a break in a main steamline outside containment with the reactor operating at HFP conditions. Coincident with the break, the turbine control valves open fully. The increased steam flow and consequent secondary depressurization lead to a power-cooling mismatch between the heat generated in the core and that being extracted in the SGs. Due to the break location, both SGs are equally affected so that the cooldown transient is essentially symmetric, i.e., all cold legs, all regions of the core and both hot legs are affected in the same manner. Power decalibration results from density-induced changes in the downcomer shadowing of the power-range excore detectors so that lower than actual power is indicated. If the MTC is negative, the cooldown of the reactor system coolant would cause an insertion of positive reactivity and this, coupled with the delayed trip due to power decalibration, would lead to an erosion of the thermal margin.

Definition of Events Analyzed

This event is predominantly an increase in steam flow event with the potential for a more pronounced power level increase. At full power, the margin to the SAFDLs is the smallest. Therefore, the event initiated from full power conditions will bound the event initiated from lower power levels.

[

]

Analysis Results

The MDNBR for this event occurred for a symmetric steamline break outside the containment with an area of 4.0 ft² and a -16 pcm/°F MTC. For this break location, both SGs were affected so that the cooldown was maximized. [

]

The response of key system variables is given in Figure 6.6 to Figure 6.15. For comparison purposes, the predictions of ANF-RELAP are included with the S-RELAP5 results. The sequence of events is given in Table 6.2. [

] and resulted in an XCOBRA-IIIC

calculated MDNBR of 1.27 with an applicable safety limit of 1.164. The peak fuel centerline temperature calculated with S-RELAP5 was 4002°F, and the applicable fuel melting temperature is 4967°F.

The S-RELAP5 and ANF-RELAP calculations for this event are nearly identical up until the time of scram. However, a small difference exists in the time at which the reactor trip signal is generated and the RPS setpoint that generates this signal is different for the two codes. S-RELAP5 calculates that the reactor will trip on high indicated thermal power at 19.9 seconds, while ANF-RELAP predicts the trip to occur on low SG pressure about 0.38 seconds earlier. This small difference in trip time makes an insignificant difference in the parameters that affect the MDNBR. Specifically, no observable differences exist in the core inlet flow rate or inlet temperature, and the peak rod heat flux calculated by S-RELAP5 is 133.4 percent of rated compared to 133.2 percent for ANF-RELAP.

Although the effect of this difference in scram time is negligible, it is still important to understand the underlying cause of the difference in predicted behavior. With ANF-RELAP the break flow is calculated to be about 2 percent higher than that of S-RELAP5 (see Figure 6.6). Therefore, SG inventories and pressures decline at a slightly faster rate and the SG low pressure setpoint is reached before the indicated thermal power setpoint. In the MSLB event, a steam-only constraint is placed on the flow leaving the SGs. The break flow, however, is a high quality two-phase mixture due to a small amount of condensation in the steamline, as frictional losses cause the pressure to decrease between the SGs and the break location. Consequently, the

magnitude of the break flow would be affected by code modifications that affect the upstream pressure and quality. Specifically, modifications to the interfacial drag package and the improved formulation of the energy equation (see Section 3.3) would account for this small (~2 percent) difference in critical flow rate.

Conclusion

The results of the analysis demonstrate that S-RELAP5 provides a satisfactory representation of the event. Furthermore, despite minor differences in the predicted value of the break flow, the S-RELAP5 results were in close agreement with the ANF-RELAP results. Specifically, the reactor trip signal times differed by only 0.38 seconds and the peak core power was the same, 137.6 percent of rated power.

Also, the predicted MDNBR is greater than the applicable safety limit and the peak fuel centerline temperature is well below the fuel melting point. These results indicate that no fuel failures due to either DNB or to FCM would occur and, therefore, the event acceptance criteria are met.

Table 6.2 Pre-Scram MSLB Event Summary

Event	Time (s)
4.0 ft ² Break in Steamline	0.0
Turbine Control Valves Open Fully	0.0
VHP Trip Setpoint Reached (Nuclear)	18.8
Reactor Trip Signal Generated	19.2
RCPs Trip (Loss of Offsite Power)	19.2
Peak Core Power	19.3
Scram CEA Insertion Begins	19.9
Peak Fuel Centerline Temperature	20.5
MDNBR	21.3

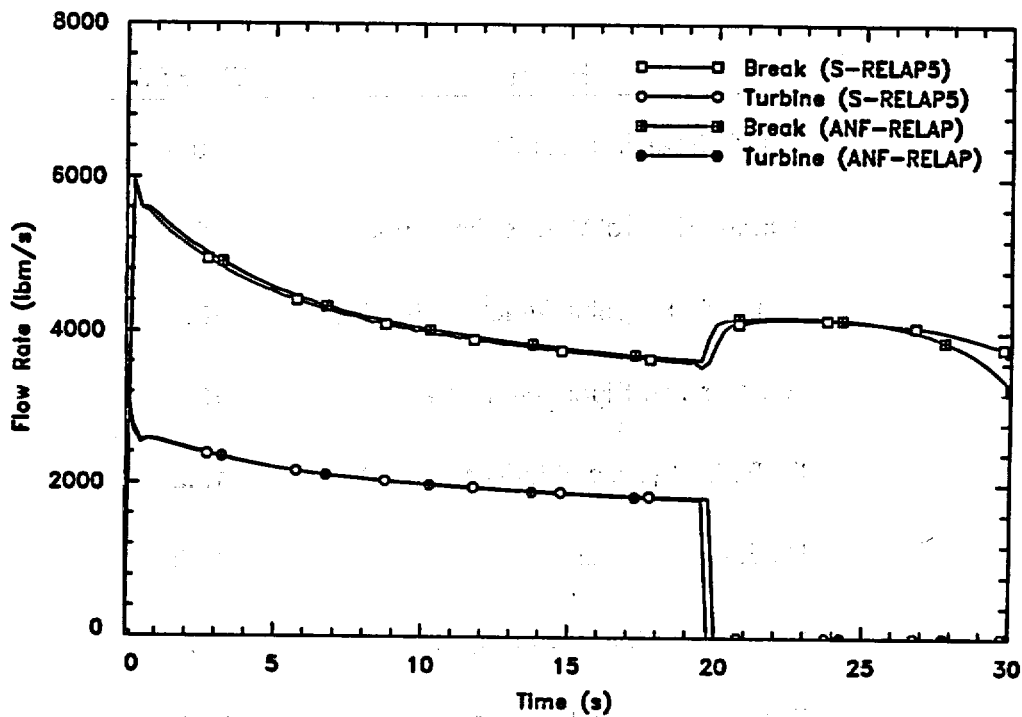


Figure 6.6 Pre-Scram MSLB Break and Turbine Steam Flow Rates

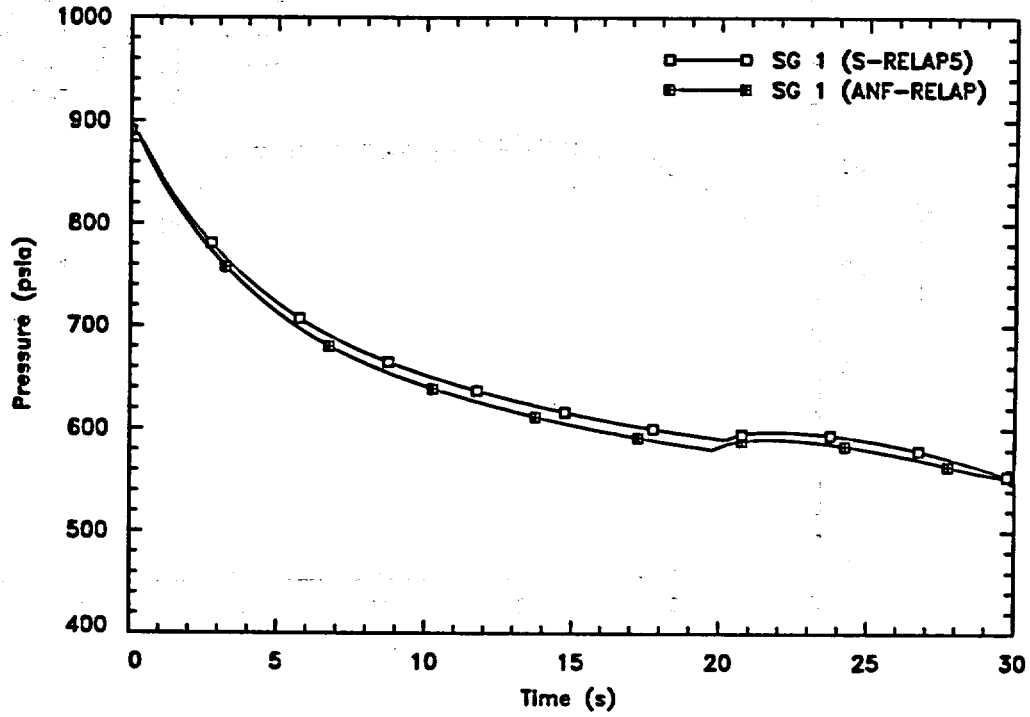


Figure 6.7 Pre-Scram MSLB Steam Generator Pressures

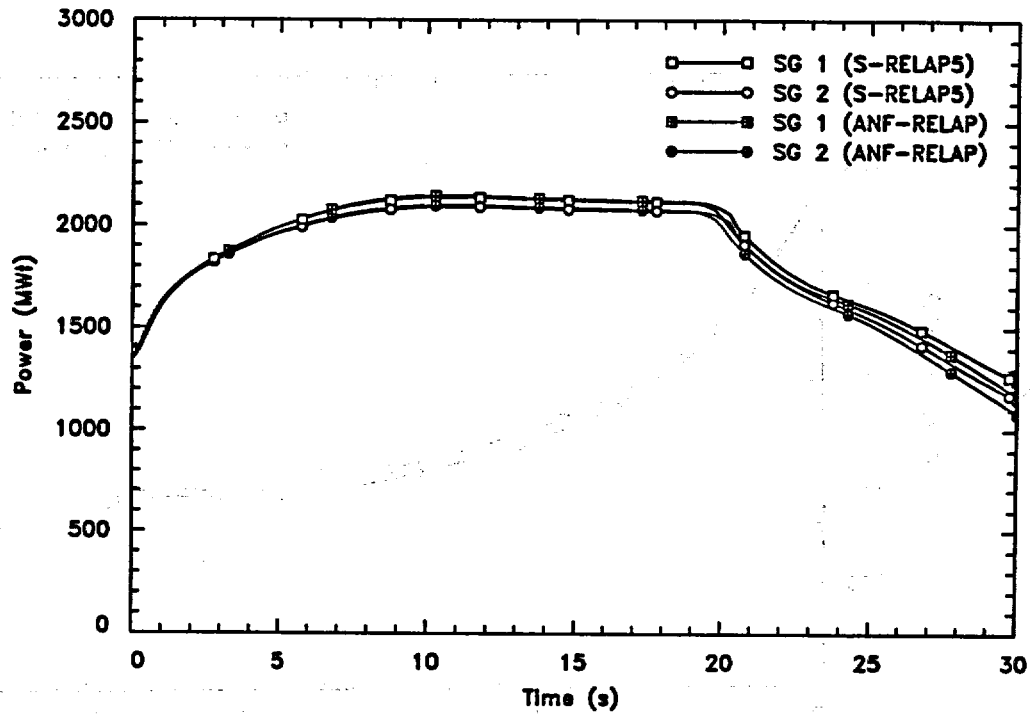


Figure 6.8 Pre-Scram MSLB Steam Generator Heat Transfer Rates

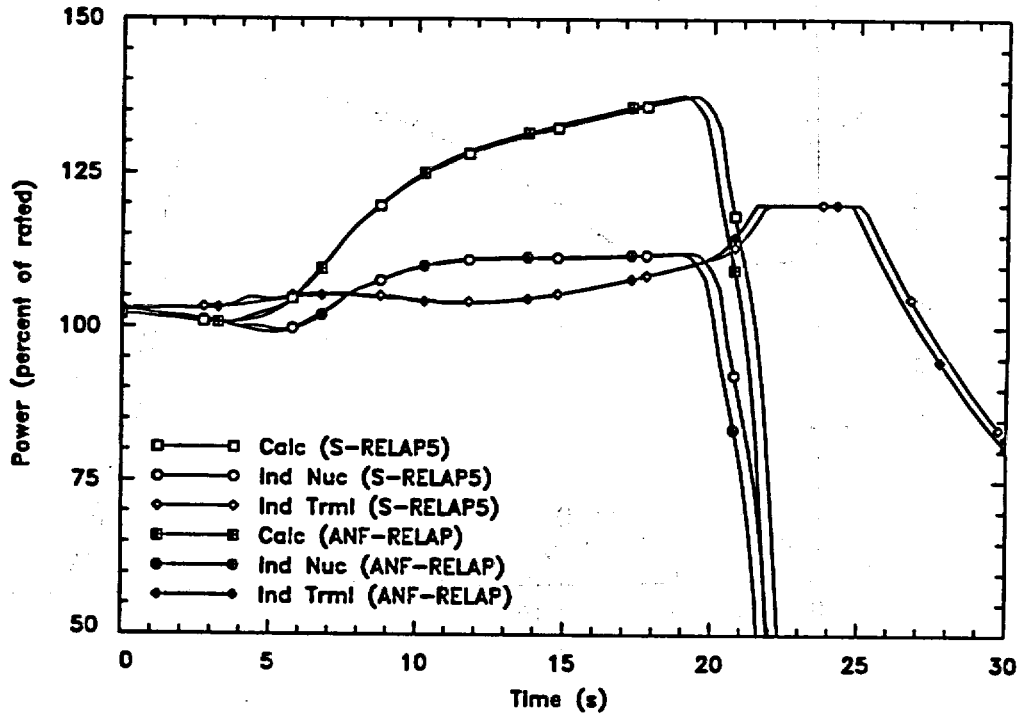


Figure 6.9 Pre-Scram MSLB Calculated Reactor, Indicated Nuclear, and Indicated Thermal Core Powers

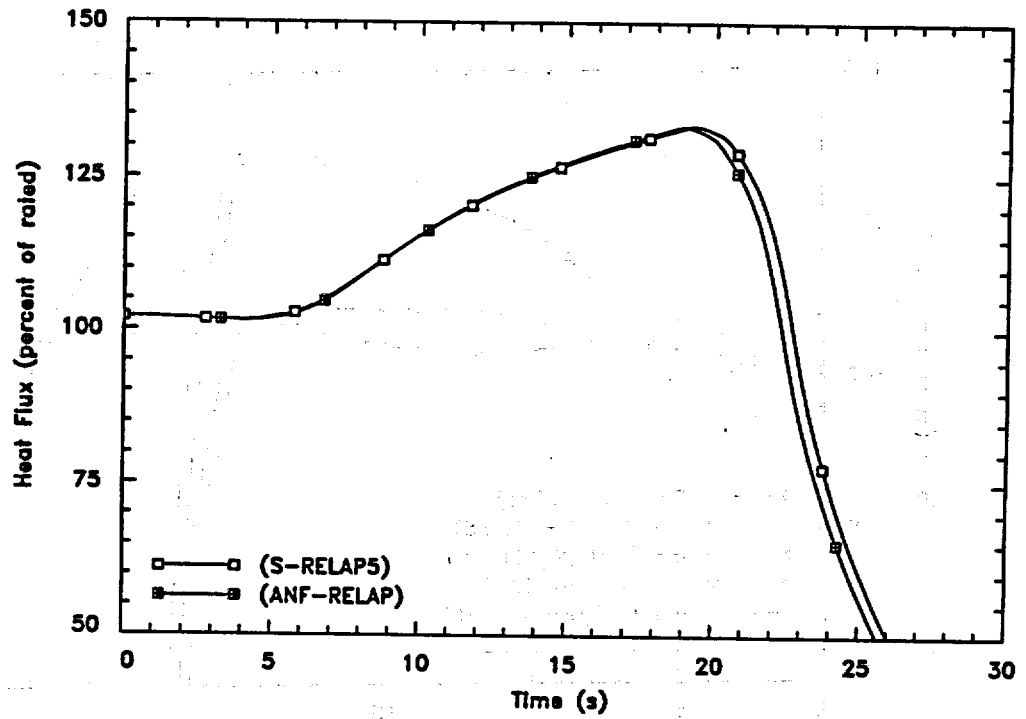


Figure 6.10 Pre-Scram MSLB Average Fuel Rod Heat Flux

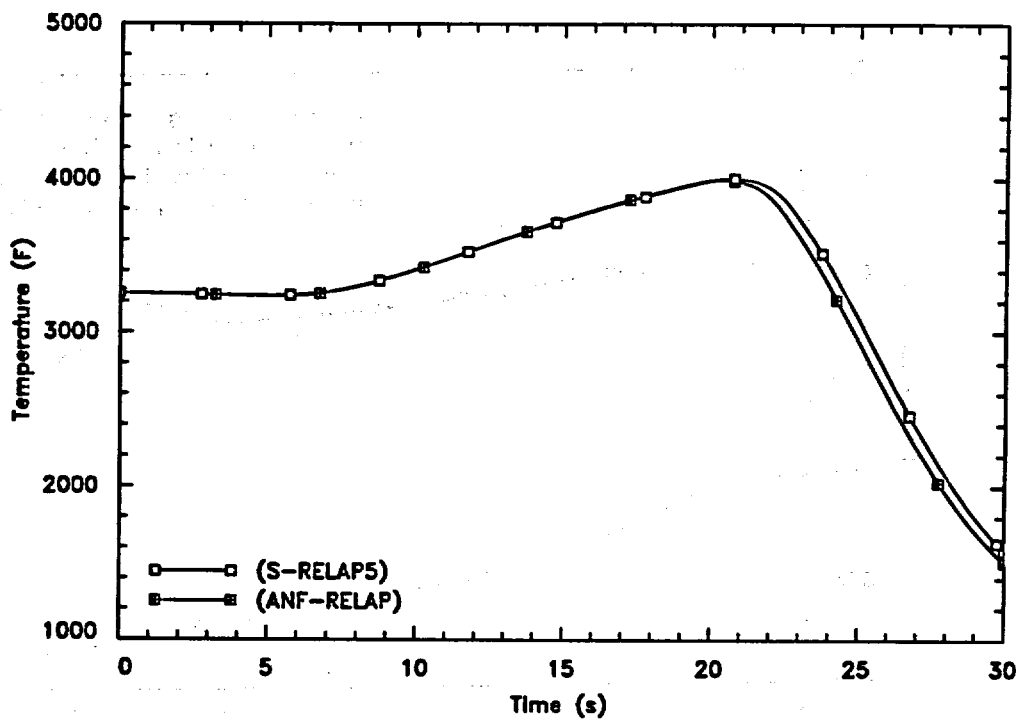


Figure 6.11 Pre-Scram MSLB Peak Fuel Centerline Temperature

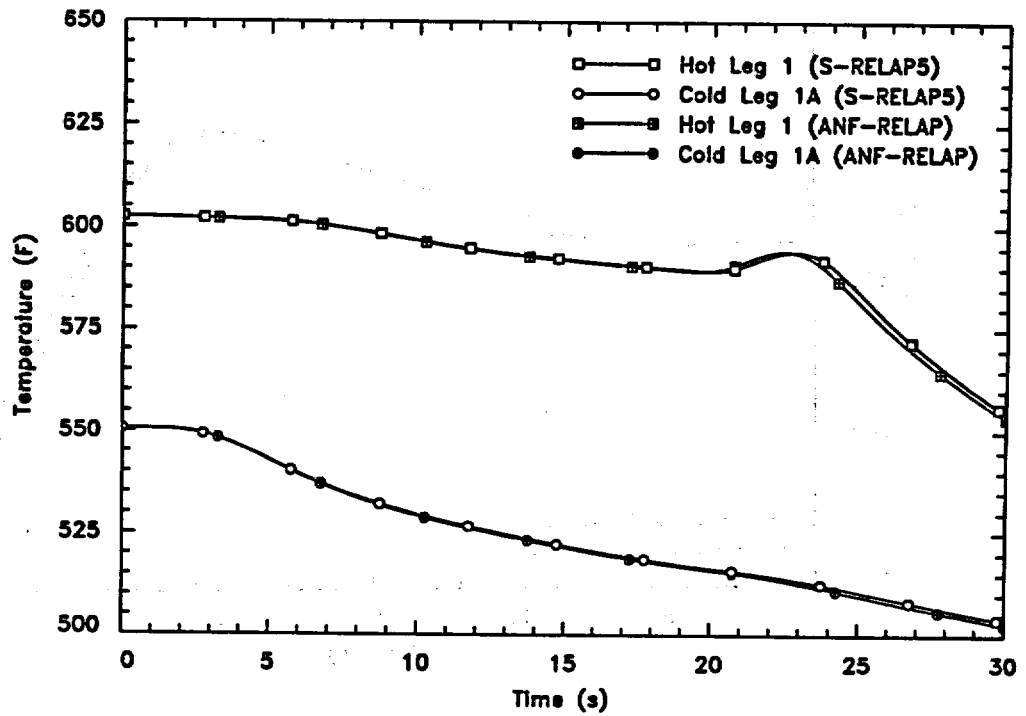


Figure 6.12 Pre-Scram MSLB RCS Hot Leg and Cold Leg Temperatures

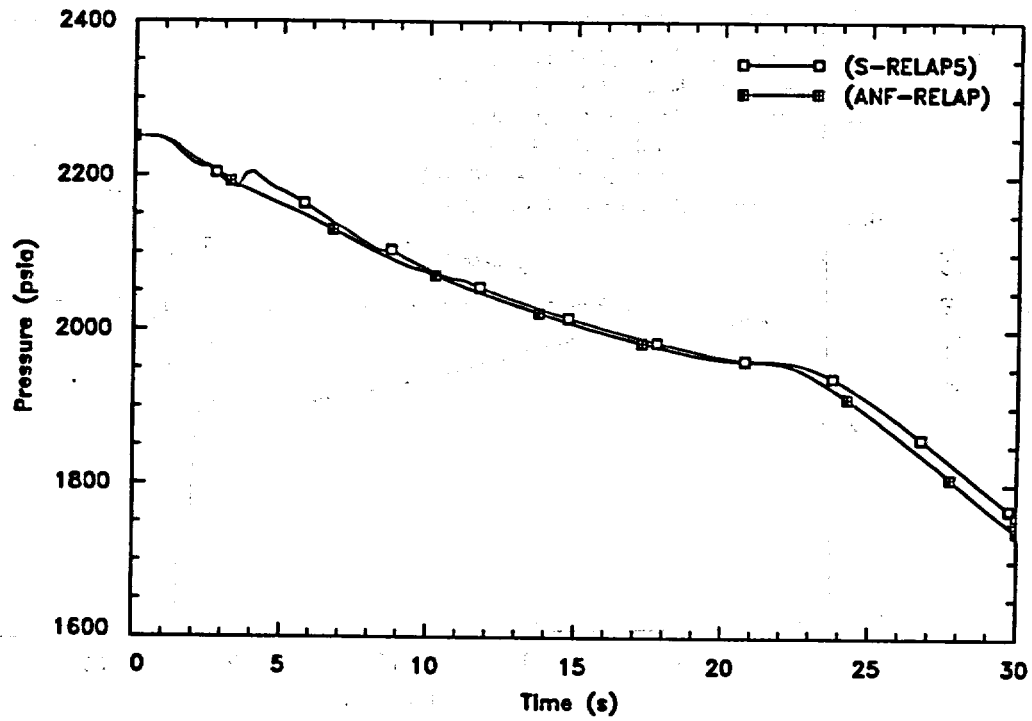


Figure 6.13 Pre-Scram MSLB Pressurizer Pressure

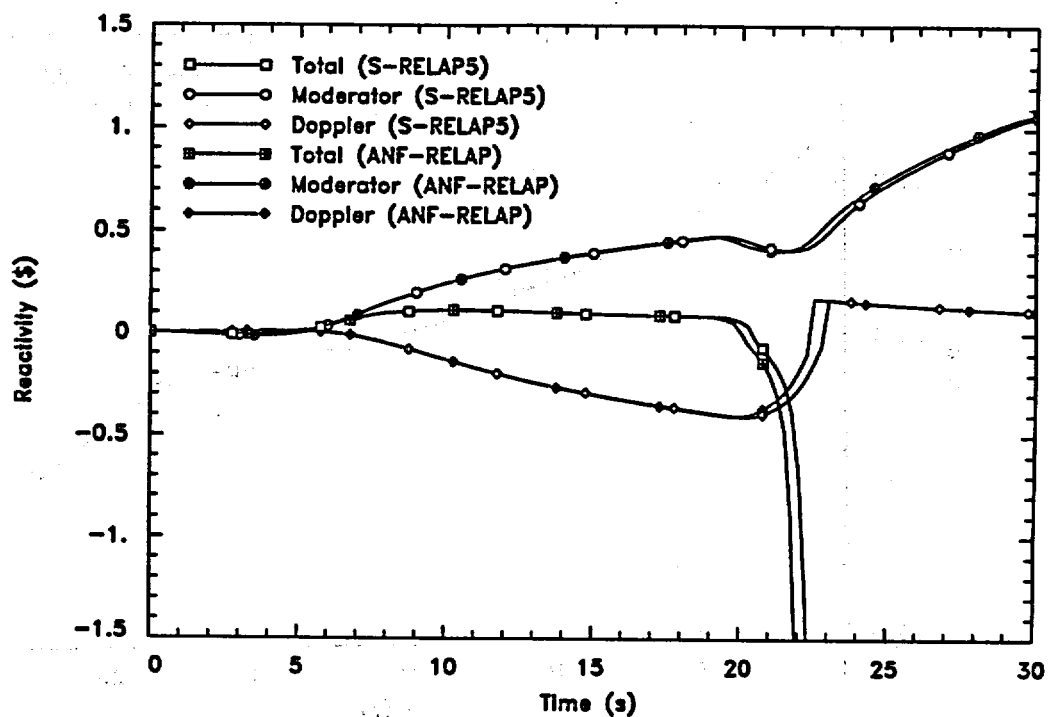


Figure 6.14 Pre-Scram MSLB Reactivity Components

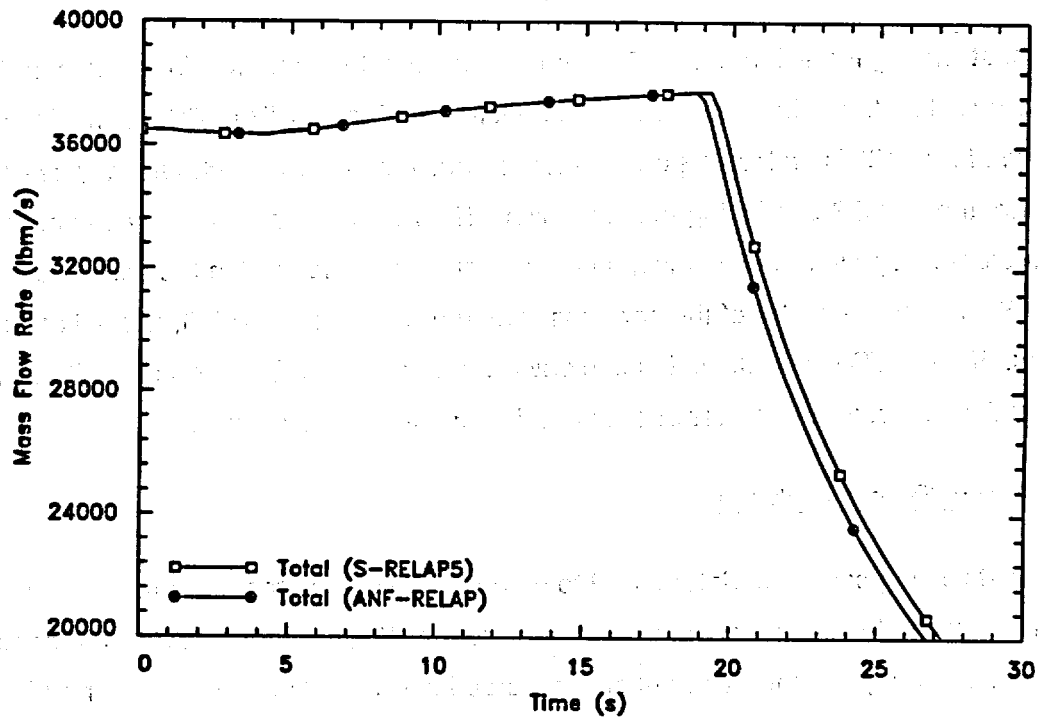


Figure 6.15 Pre-Scram MSLB Core Inlet Flow Rate

6.2 *Post-Scram Main Steamline Break (MSLB)*

Event Description

The most limiting Post-Scram MSLB event for the sample problem is initiated by a double-ended guillotine break in a main steamline upstream of the MSIV at EOC conditions. After closure of the MSIVs on low SG pressure, the transient becomes substantially asymmetric, with only the affected SG continuing to blow down. The release of high-energy steam through the break creates a power-cooling mismatch between heat generated in the core and that removed in the SGs. For the sector of the core associated with the affected SG, a rapid cooldown results. If the MTC is negative, this cooldown would cause an insertion of positive reactivity with a potential for a return to power and an erosion of the thermal margin.

Definition of Events Analyzed

The most limiting case was determined to be an inside-containment break initiated at HFP conditions with offsite power available to operate the RCPs. All four RCPs were assumed to be operational throughout the transient so that forced flow conditions are maintained in the RCS. EOC conditions were selected to maximize the magnitude of the negative MTC, thereby maximizing the positive reactivity insertion. Following reactor scram on low SG pressure, all control element assemblies (CEAs) were assumed to be inserted except for the most reactive CEA which is assumed to be stuck in the withdrawn position. Additional conservatism is obtained by locating the stuck CEA in the core sector being cooled with inlet water from the affected loop.

[

]

In accordance with the worst-single-active-failure analysis requirement, it was postulated that one of the two HPSI pumps required to be in service fails. However, note that this transient

simulation is completed before the SI lines fill with borated water and begin delivery to the RCS cold legs.

Analysis Results

Table 6.3 presents the sequence of events and the responses of key system variables are given in Figure 6.16 through Figure 6.26. To provide a direct comparison with S-RELAP5, the ANF-RELAP results are included in these figures.

Initially, the release of high-energy steam through the break causes an increase in the primary-to-secondary heat transfer rate for both SGs. Upon MSIV closure (on low SG Pressure ESFAS signal), the cooldown of the loop with the unaffected SG ends, but the cooldown of the affected loop continues until the AFW is terminated and the SG dries out.

Shortly after the transient is initiated, the reactor is scrammed (on a Low SG Pressure RPS signal). However, as the cooldown progresses, the shutdown worth is eroded by moderator and Doppler feedback (accentuated by the EOC conditions) until a return to power occurs. The increase in core power above the decay heat level is eventually terminated by negative Doppler and moderator feedback after the AFW flow is shut off by operator action. The core power peaks at 8.8 percent of the rated power, with most of the power produced in the stuck-CEA region. The resulting MDNBR is 3.21 and the peak LHGR is 17.54 kW/ft.

Only small differences between the S-RELAP5 and ANF-RELAP results are observable for this event. The key parameter is the degree to which the plant experiences a post-scram return to power due to the reactivity insertion associated with the cool down. S-RELAP5 calculated a very modest return to power of only 8.8 percent of rated, and the ANF-RELAP results were within 0.1 percent of this value. Still, there were some minor differences in the predicted plant behavior as discussed below.

Early in the transient, see Figure 6.26, the return to power begins a little sooner in the ANF-RELAP calculation due to a slightly more rapid cool down for the affected sector (see Figure 6.21). This initial difference in the core inlet temperature for the affected sector is a result of the slightly more rapid SG blowdown (see Figure 6.17) associated with the difference in the calculated critical flow noted above for the MSLB pre-scram event.

Later in the transient, for the unaffected SG, a noticeable difference in pressure occurs (see Figure 6.17) with S-RELAP5 predicting a higher value than ANF-RELAP. Similarly, there is a small difference in the core inlet temperature for the unaffected sector and the S-RELAP5 value for the primary pressure (see Figure 6.22) is slightly higher as well. For this part of the transient, the heat removal rate to the unaffected SG is minimal (see Figure 6.18) with just enough heat transfer to cause its pressure to slowly approach equilibrium with the primary. The increase in the primary pressure for the S-RELAP5 calculation relative to that of ANF-RELAP is small and appears to be due to increased RCP heat generation which in turn is a result of the increased wall drag for the SG tubes due to the improved formulation for the single-phase friction factor.

The most obvious difference between the two calculations is the difference in HPSI flow rate as shown in Figure 6.24. For this event, the RCS pressure is very close to the HPSI pump shut off head, so that the maximum calculated HPSI flow is only about 25 percent of the full minimum degraded flow for one HPSI pump. Consequently, small differences in the calculated RCS pressure are reflected as relatively large changes in the HPSI flow rate. However, the difference in the calculated values for HPSI flow rate is only a small fraction (~ 2-4 percent) of the rated HPSI flow and is a negligible fraction of the core flow since the RCPs were not tripped. As was the case with the pressure in the unaffected SG, the difference in HPSI flow is caused by the small difference in primary pressure.

These observable differences in the predicted behavior for this event are attributable to two improvements made to the S-RELAP5 code, the more exact formulation for wall drag and the improved energy equation due to its effect upon the critical flow. However, none of these differences had a significant effect upon the predicted peak power since the values calculated by the two codes agreed to within 0.1% of rated power.

Conclusion

This analysis demonstrates that S-RELAP5 provides a satisfactory representation of the event. Also, the predicted MDNBR is much greater than the applicable safety limit, and the peak LHGR is well below the FCM threshold. These results indicate that no fuel failures due to either DNB or FCM would occur and, therefore, the event acceptance criteria are met.

The S-RELAP5 calculated results are in close agreement with those of ANF-RELAP except for the HPSI flow rate (Figure 6.24). The observed difference in HPSI flow rate was discussed above and has no significant effect for this event.

Table 6.3 Post-Scram MSLB Event Summary

Event	Time (s)
Double-Ended Guillotine Break in Main Steamline Upstream of MSIV	0.0
Turbine Valve is Assumed to Open Fully	0.0
Low SG Pressure and MSIS Setpoints Reached	7.4
Reactor Trip	8.3
Scram CEA Insertion Begins and Turbine Trips	9.1
MSIVs Fully Closed	14.3
Low Pressurizer Pressure Signal Initiates HPSI Pump Startup	26.4
MFW Valves Closed	67.4
RCS Pressure Reaches HPSI Pump Shutoff Head and Borate Water Begins Filling SI Lines	124.6
AFW Starts and is all Directed to Affected SG	170.0
Core Returns to Critical Condition	229.0
AFW Terminated (Operator Action)	600.0
Peak Post-Scram Power Reached	602.0

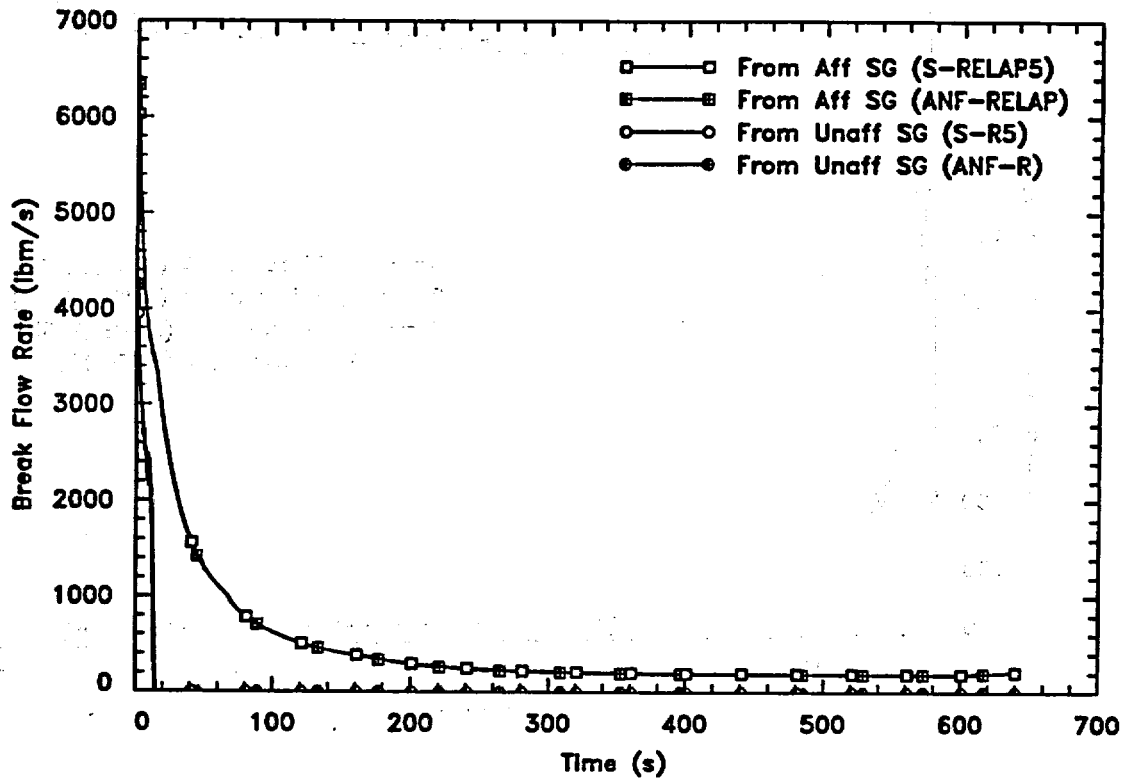


Figure 6.16 Post-Scram MSLB Break Flow Rates

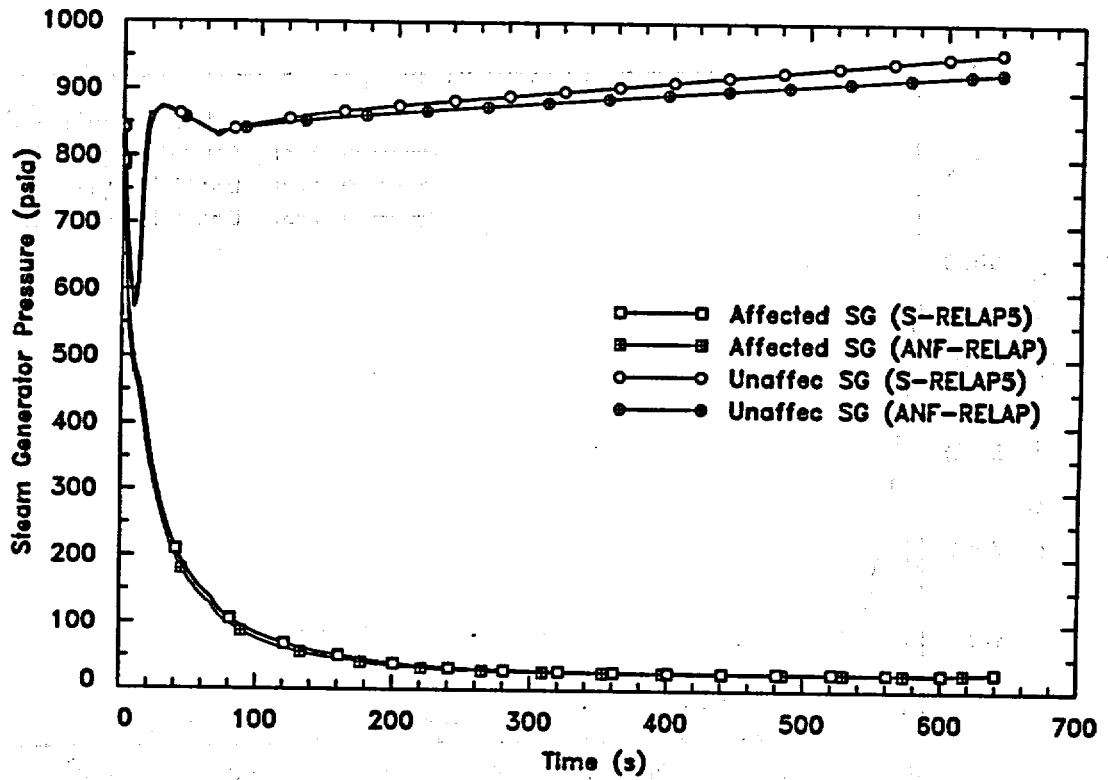


Figure 6.17 Post-Scram MSLB Steam Generator Pressures

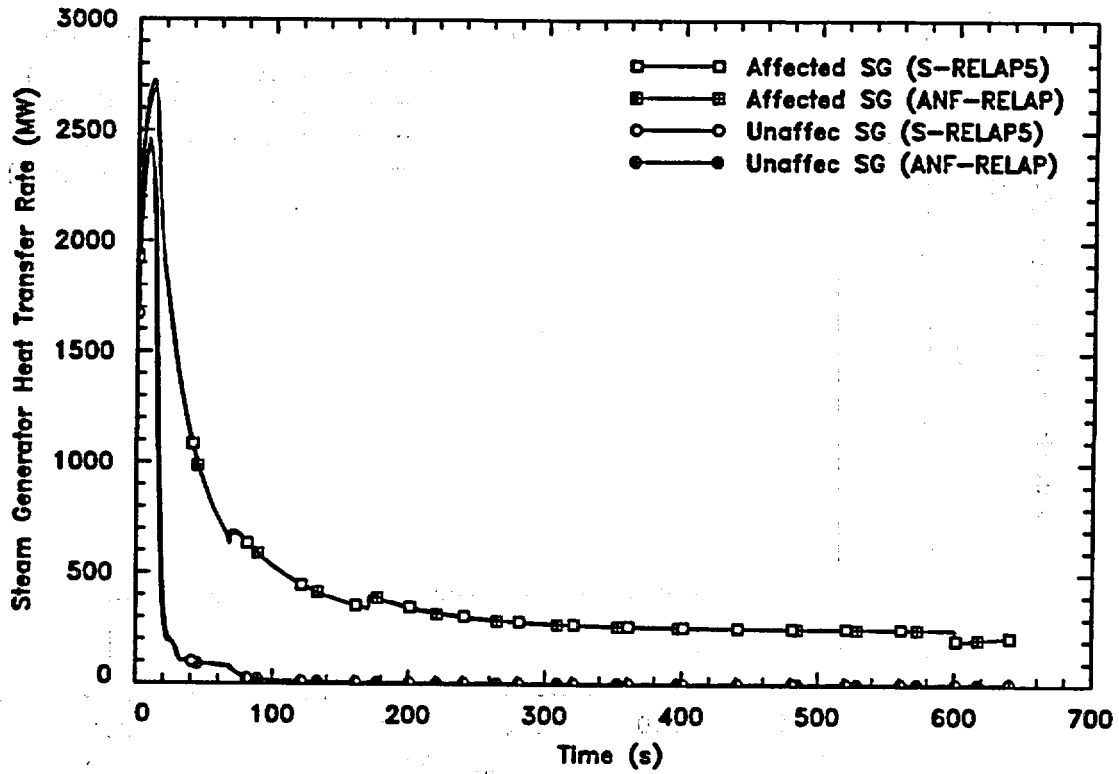


Figure 6.18 Post-Scram MSLB Steam Generator Heat Transfer Rates

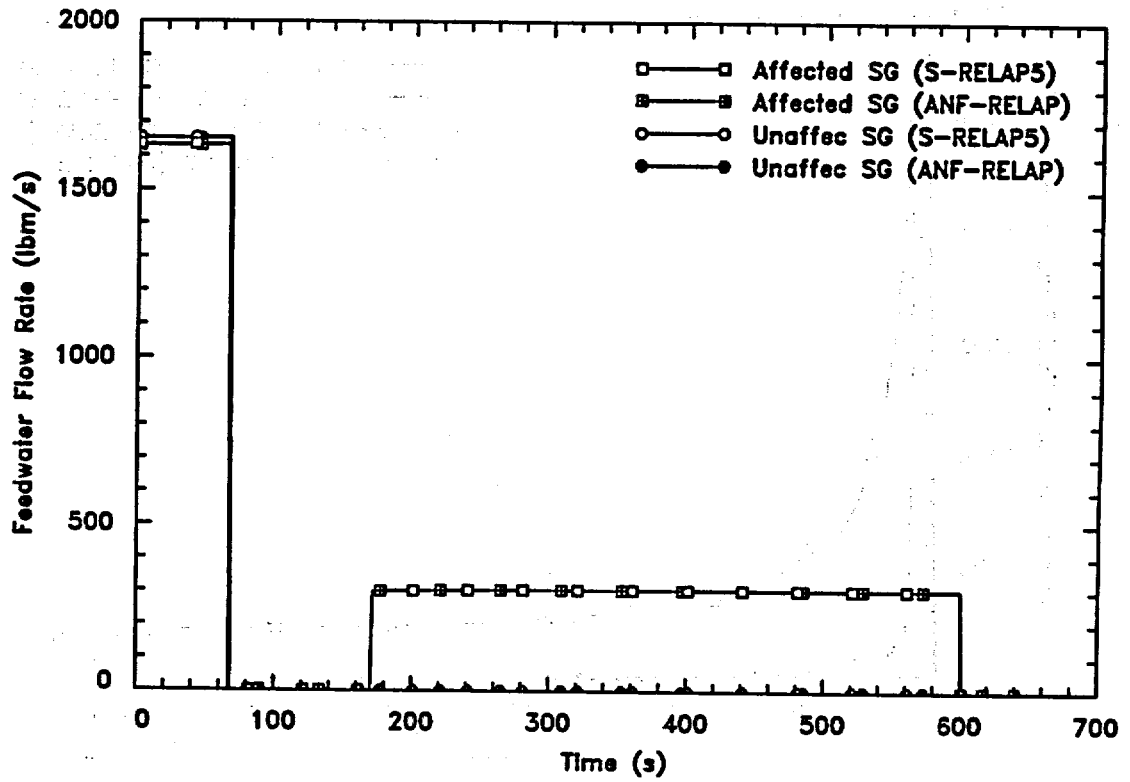


Figure 6.19 Post-Scram MSLB Feedwater Flow Rates

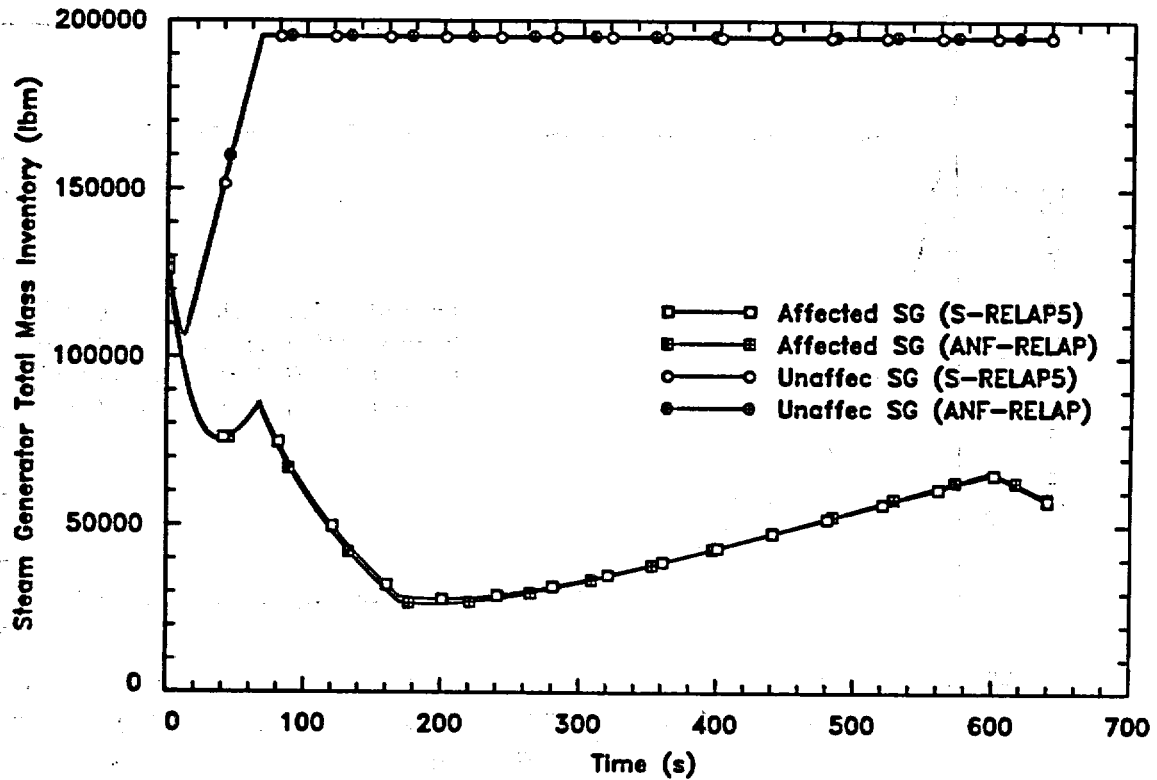


Figure 6.20 Post-Scram MSLB Steam Generator Total Mass Inventories

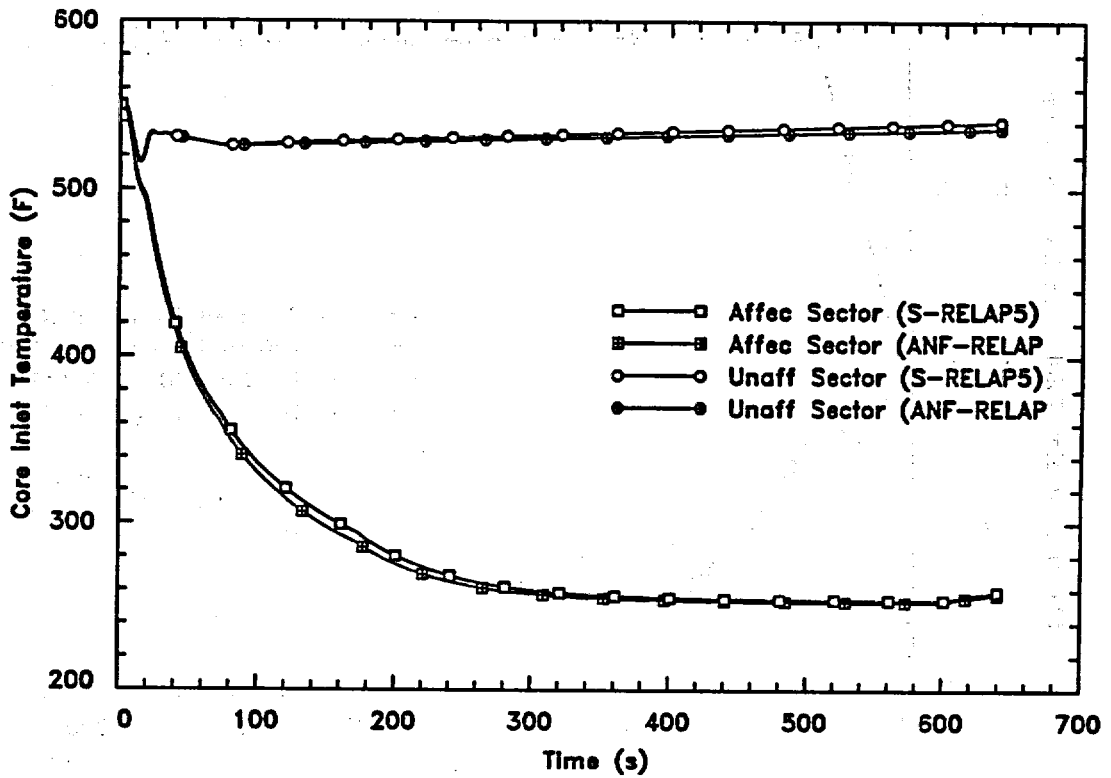


Figure 6.21 Post-Scram MSLB Core Inlet Temperatures

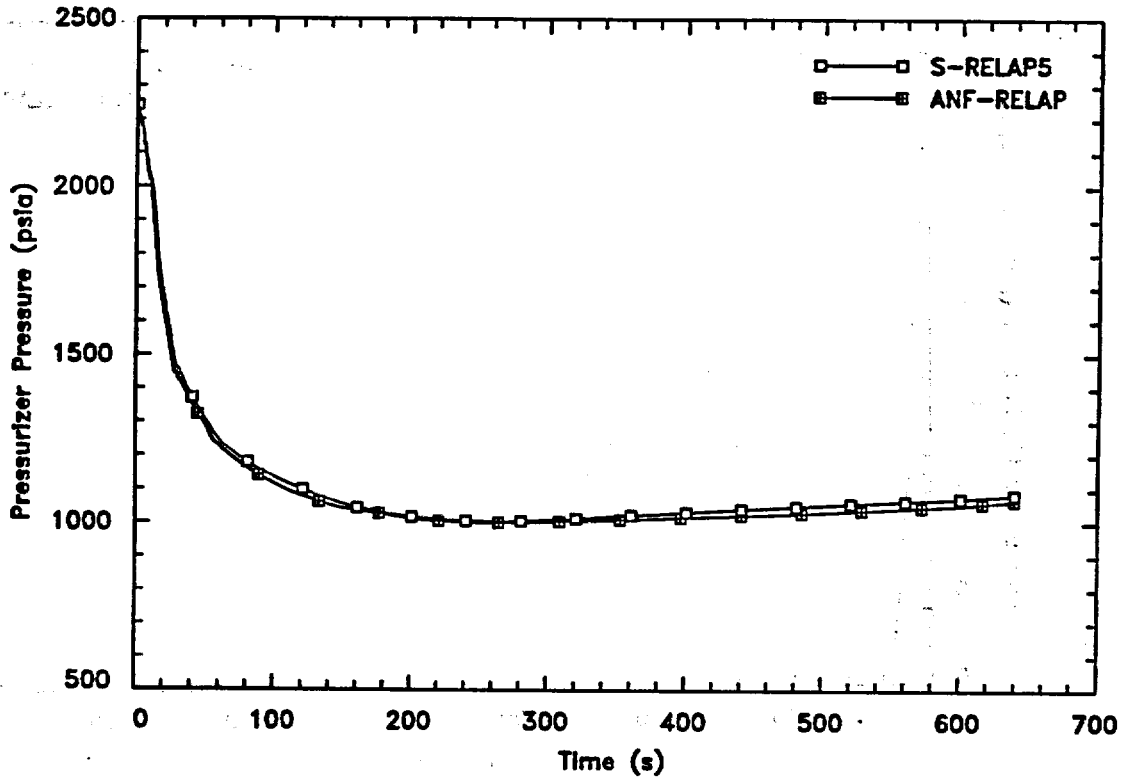


Figure 6.22 Post-Scram MSLB Pressurizer Pressure

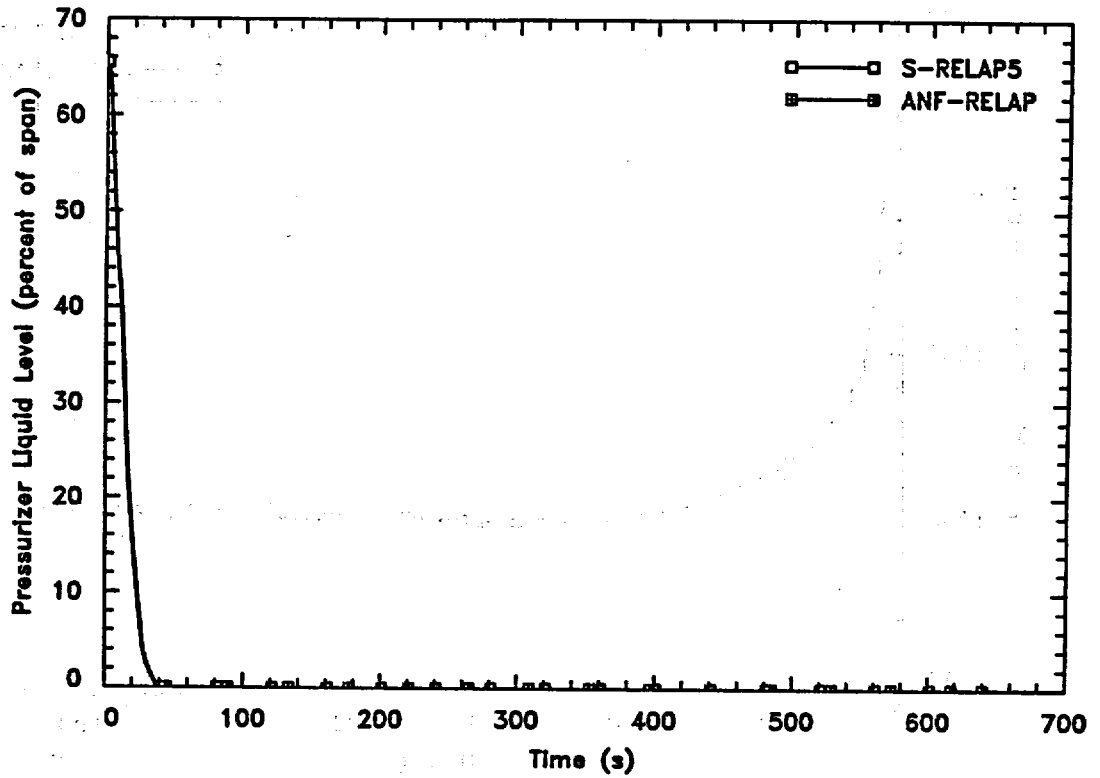


Figure 6.23 Post-Scram MSLB Pressurizer Liquid Level

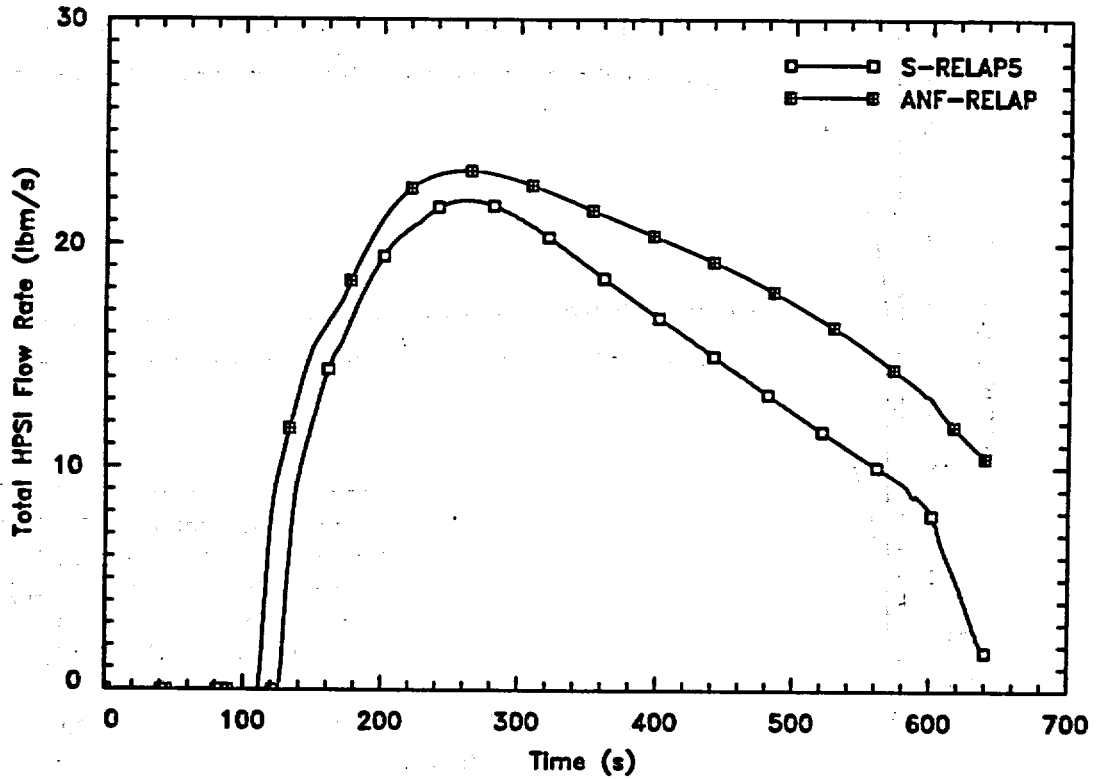


Figure 6.24 Post-Scram MSLB Total HPSI Flow Rate

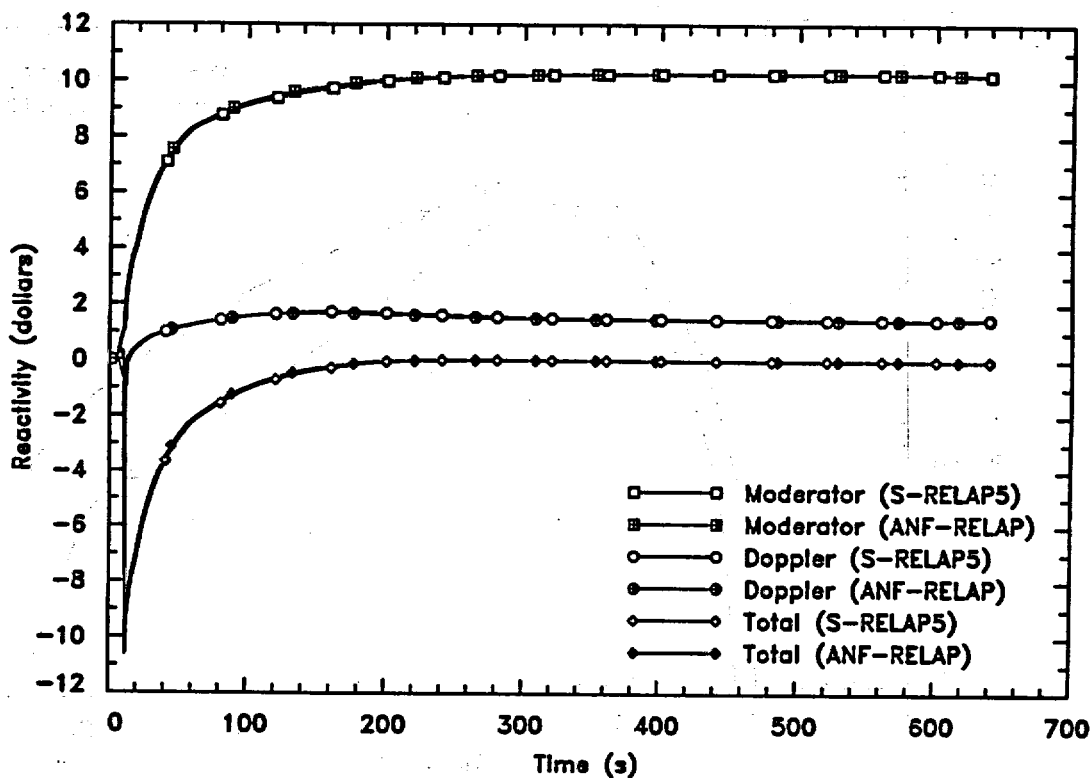


Figure 6.25 Post-Scram MSLB Reactivity

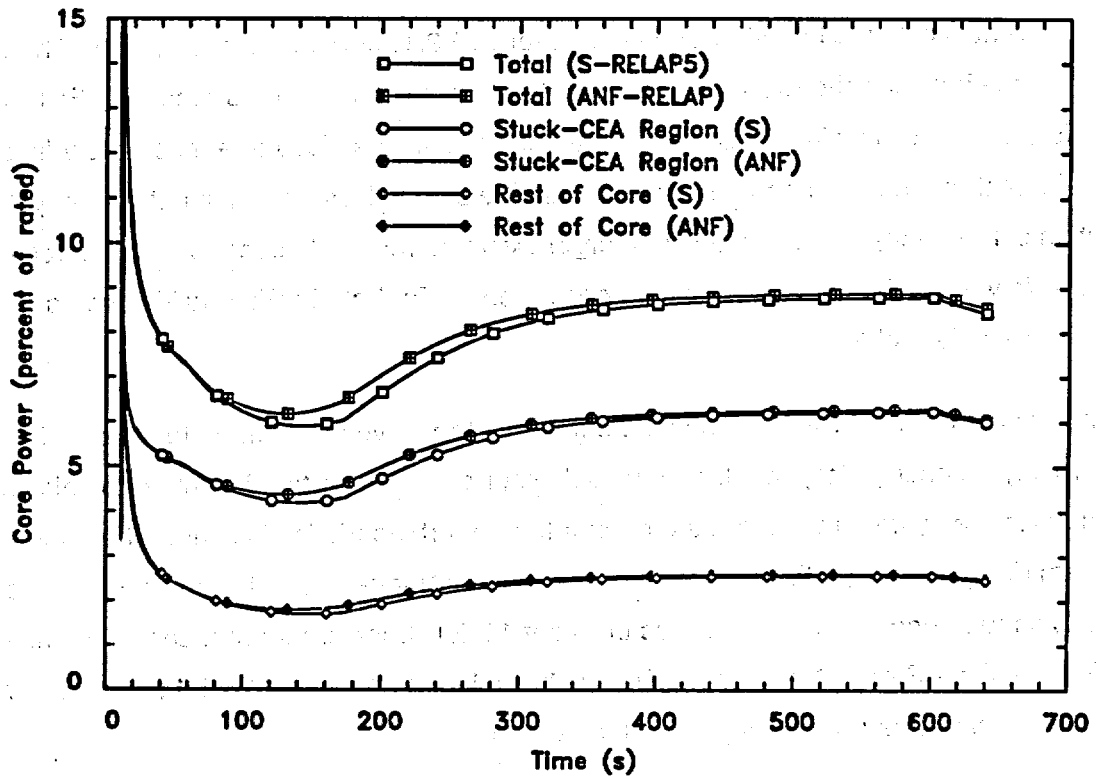


Figure 6.26 Post-Scram MSLB Core Power

6.3 *Loss of External Load (LOEL)*

Event Description

This event is initiated by either an LOEL (Event 15.2.1) or a TT (Event 15.2.2). The major difference between the two events is the rate at which steam flow is reduced. Following a LOEL, a runback is initiated and the turbine throttle valves close at a moderately fast rate, but not instantaneously. In a turbine trip, the turbine stop valves close almost instantly (typically within 0.1 second). When sufficient margin exists, a transient scenario is constructed so that the safety analysis results bound the consequences for both LOEL and TT events as illustrated in this sample problem.

Upon either of these two conditions, the turbine stop valve is assumed to rapidly close (0.1 s). Normally an anticipatory reactor trip would occur on a turbine trip; however, to calculate a conservative system response, the reactor trip on turbine trip is disabled. The atmospheric steam dump valves (ADVs) are also assumed to be unavailable. These assumptions allow the analysis to bound the consequences of Event 15.2.1 (Loss of External Load), Event 15.2.2 (Turbine Trip - Steam Atmospheric Dump Unavailable) and Event 15.2.4 (Closure of both MSIVs - valve closure time is greater than 0.1 s).

The LOEL/TT event challenges the acceptance criteria for both primary and secondary system overpressure and DNBR. The event results in an increase in the reactor coolant system temperatures due to an increase in the secondary side temperature. As the reactor coolant system temperatures increase, the reactor coolant throughout the RCS expands causing an increase in the pressurizer pressure. The reactor coolant system is protected against overpressurization by the pressurizer safety and relief valves. Pressure relief on the secondary side is afforded by the steamline safety and relief valves. Actuation of the primary and secondary system safety valves limits the magnitude of the reactor coolant system temperature and pressure increase.

With a positive MTC, increasing reactor coolant system temperatures result in an increase in core power. The increasing primary side temperature and power reduces the margin-to-thermal limits and challenges the DNBR acceptance criterion.

Definition of Events Analyzed

The objectives in analyzing this event are to demonstrate that: 1) the reactor coolant pressure relief capacity is sufficient to limit the pressure to less than 110 percent of the design pressure, 2) the secondary side pressure relief capacity is capable of limiting the pressure to less than 110 percent of the design pressure, and 3) the MDNBR remains above the safety limit. To conservatively bias the calculation, no credit is taken for direct reactor trip on turbine trip, for the turbine bypass system, or for the steam dump system. For each of the above three objectives, a separate analysis would be conducted with the plant parameters biased so as to maximize the challenge for the particular criterion being examined.

In this sample problem, the analysis is biased to challenge the RCS design pressure limit. [

] This procedure provides for a conservative estimate of the peak RCS pressure during the transient.

Analysis Results

This maximum RCS pressurization case initiates with a ramp closure of the turbine valve in 0.1 seconds. The pressurization of the secondary side results in decreased primary-to-secondary heat transfer, and a rise in reactor coolant system temperatures. An insurge into the pressurizer occurs, compressing the steam space and pressurizing the reactor coolant system. The reactor trips on high pressure. The capacity of the pressurizer safety valves is sufficient to contain the maximum RCS pressure (bottom of the vessel) to a maximum value of 2692 psia.

The sequence of events is given in Table 6.4 for this maximum RCS pressure case. The responses of key system variables are given in Figure 6.27 to Figure 6.33. For code-to-code comparisons, ANF-RELAP results are included in the figures.

The S-RELAP5 calculated results are in excellent agreement with those of ANF-RELAP. In particular, the peak RCS pressure was the key parameter and differed by only 0.8 psia for the two codes. This small difference is insignificant compared to the margin remaining to the RCS

pressurization acceptance criterion (about 57 psia). Until the time that the peak primary pressure occurs, the results of the two calculations are virtually indistinguishable. After this time, a minor difference in the calculated SG flow rates is observed due to a difference in the MSSV re-seating behavior.

This difference is not the result of any difference in the valve models between the two codes but rather is the product of the way the control variable logic (user input) has been set up. The safety relief valves are modeled using a motor valve with trips specified for valve opening and closing. If one of these trips is true, then the valve opens (or closes) at a specified rate, however, if neither of these trips is true the valve position remains unchanged. Consequently, insignificant differences in the computed variables that govern the trips can lead to noticeable differences in the position of a partially open valve.

Conclusion

The S-RELAP5 results are in excellent agreement with the ANF-RELAP results and reasonably represent the plant transient. The difference in the peak pressure calculated with the two codes is only 0.8 psi. The maximum predicted RCS pressure (2692 psia) remains below 110 percent of the design pressure (2748 psia). Therefore, the RCS pressurization criterion for the LOEL and TT events is met.

Table 6.4 LOEL/TT Event Summary

RCS Overpressurization Case Event Summary

Event	Time (s)
Turbine Trip	0.00
Turbine Stop Valve Fully Closed	0.1
MSSVs Open	4.0
Reactor Trip Setpoint Reached on High Pressurizer Pressure	5.3
Scram Rod Insertion Begins (Instrumentation and Holding Coil Delays)	6.9
Peak Core Power	6.9
Pressurizer Safety Valves Open	7.4
Peak RCS Pressure (Bottom of Vessel)	8.3
Pressurizer Safety Valves Close	10.9

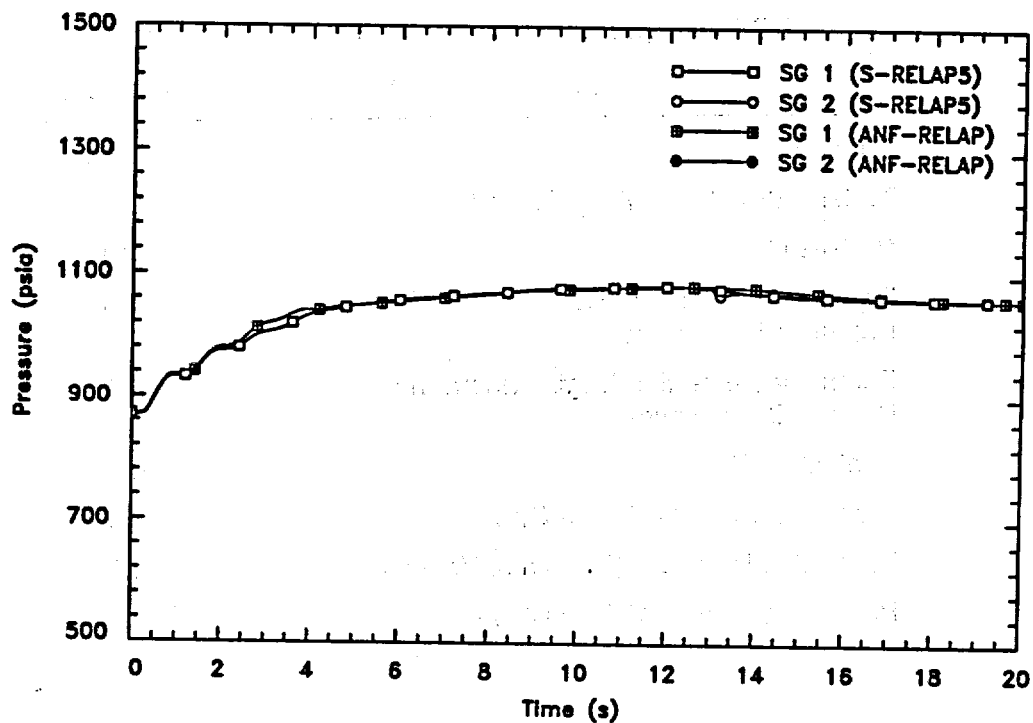


Figure 6.27 LOEL/TT Steam Generator Pressures

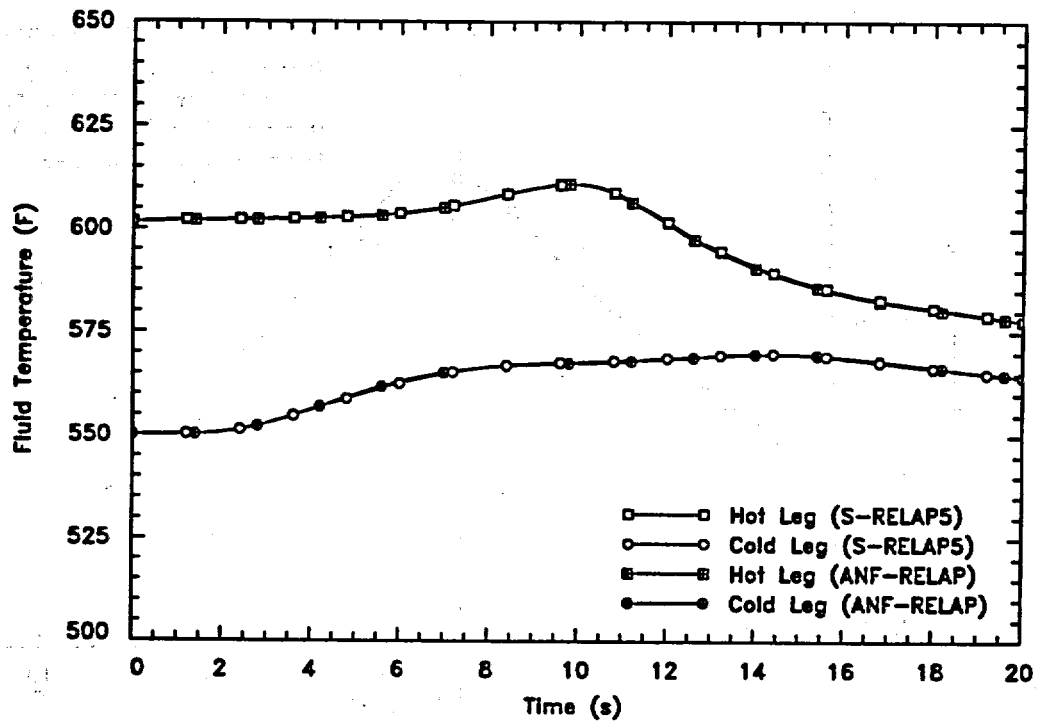


Figure 6.28 LOEL/TT RCS Temperatures

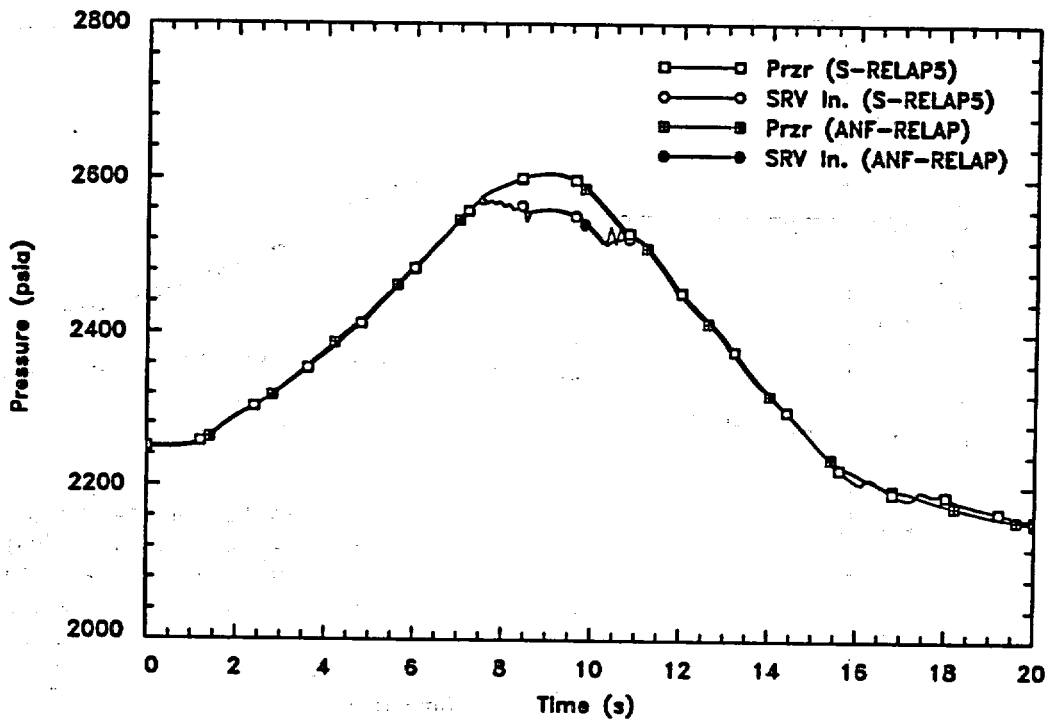


Figure 6.29 LOEL/TT Pressurizer and SRV Inlet Pressures

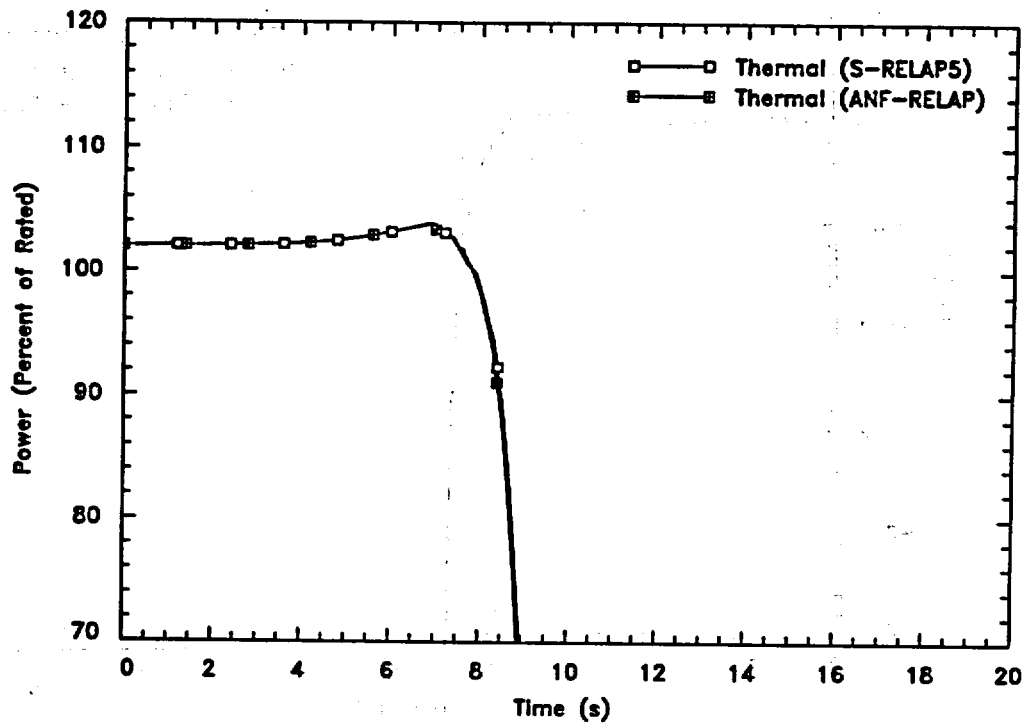


Figure 6.30 LOEL/TT Reactor Power

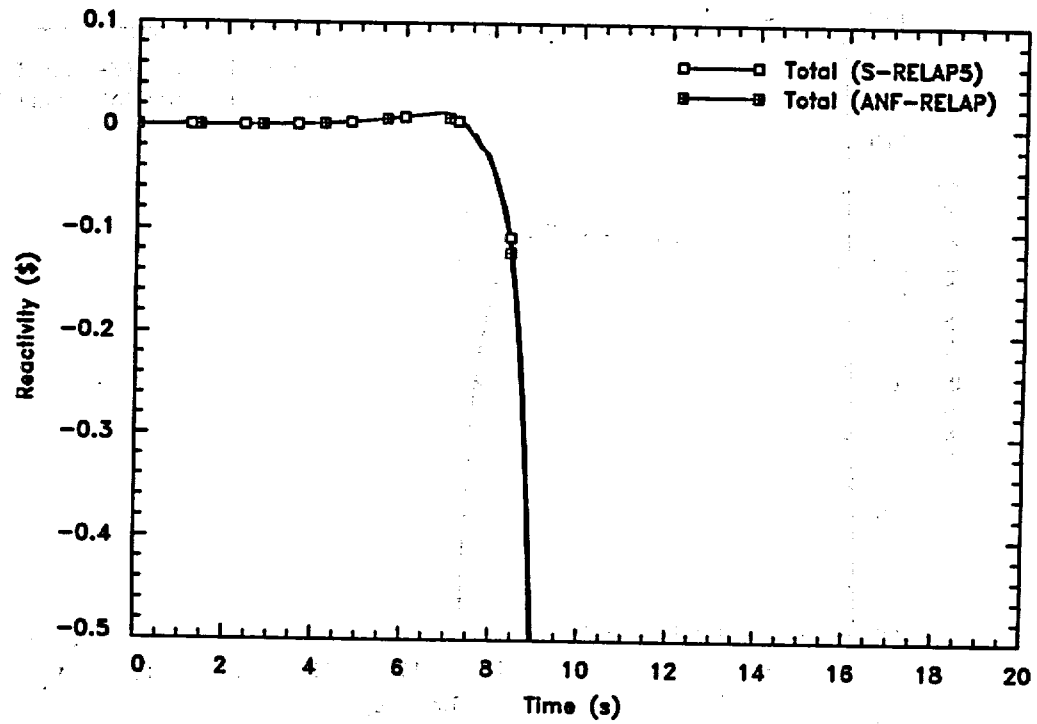


Figure 6.31 LOEL/TT Total Reactivity

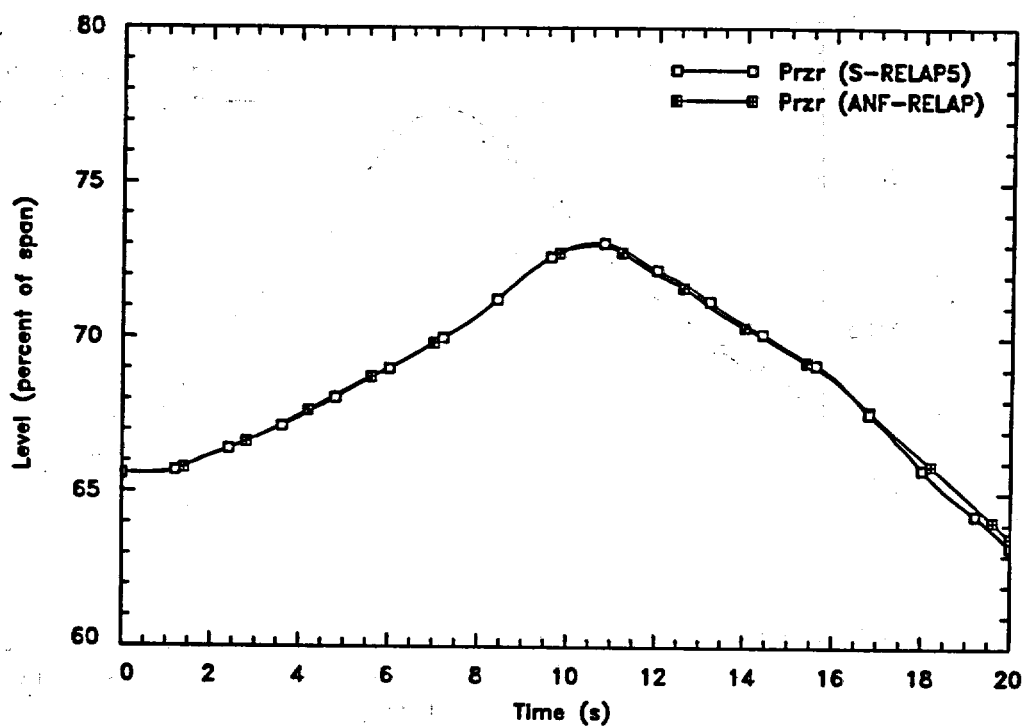


Figure 6.32 LOEL/TT Pressurizer Level

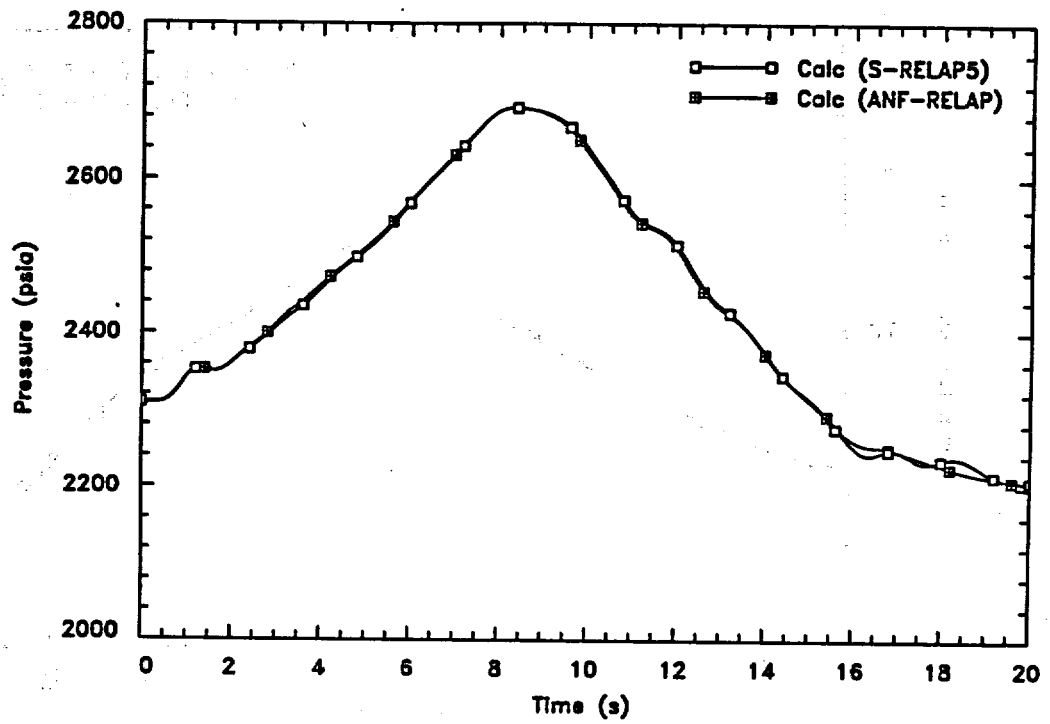


Figure 6.33 LOEL/TT Pressure at Bottom of Reactor Vessel

6.4 Loss of Normal Feedwater (LONF) Flow

Event Description

A LONF Flow transient is initiated by the termination of the MFW flow due to failures in the MFW or condensate systems. (The termination of MFW flow that results from a loss of power is considered in the Loss of Nonemergency AC Power event.) The termination of MFW flow while the plant continues to operate at power will eventually result in reactor scram on low SG level (or TM/LP or OTAT^a) with long-term cooling subsequently provided by the AFW system.

This event is evaluated to confirm that the low SG level reactor trip setpoint, the low-low SG level^b AFW actuation setpoint, and the AFW flow capacity are adequate to provide for long-term decay heat removal. This event is also evaluated to confirm that the plant design and operating conditions preclude pressurizer overfill.

The loss of normal feedwater flow while the plant continues to operate at power causes the primary-to-secondary heat transfer rate to decrease. The resulting heatup of the reactor coolant causes a pressurizer surge due to the fluid expansion. Reactor coolant pressure increases and the pressurizer sprays actuate, leading to further filling of the pressurizer. SG liquid levels, which have been steadily dropping since the termination of the MFW flow, soon reach the low SG level reactor trip setpoint. This initiates a reactor scram which ends the short-term heatup phase of the event. The reactor trip and subsequent cooling of the reactor coolant act to reduce the fluid expansion and prevent pressurizer overfill.

The automatic turbine trip at reactor scram and the continuing primary-to-secondary transfer of the decaying core power and the RCP heat (for cases with offsite power available) cause SG pressures to rapidly increase. When SG pressures become high enough, the steam dump system and the ADVs (or, if they are not available, the MSSVs) serve to limit the increase in SG pressure.

SG levels continue to drop and soon reach the low-low SG level AFW actuation setpoint. When the delivery of AFW begins, the rate of level decrease in the fed SGs slows. If AFW flow is

^a The OTAT trip applies to Westinghouse designed PWRs.

^b For this sample problem, the difference between these two setpoints is only 2.5% of the instrument span and the time difference is negligible.

sufficient to prevent dryout in the SGs then, as the decay heat rate diminishes, liquid levels in the SGs stabilize and begin to rise. Reactor coolant temperatures also stabilize and begin to decrease, marking the end of the challenge to the event acceptance criteria.

Definition of Events Analyzed

The objective of this analysis is to demonstrate the adequacy of the SG level setpoints and the AFW capacity to avoid the expulsion of liquid from the PORVs and pressurizer safety valves and assure long-term cooling capability to a safe shutdown condition.

There are four potential acceptance criteria that could apply: 1) the DNB SAFDL, 2) the FCM SAFDL, 3) the pressure limit, and 4) the plant condition restriction (event must not generate a more serious plant condition without other faults occurring independently). For the short-term heatup phase, the MDNBR is bounded by the LOCF event, and for the long-term heat-up phase, the DNB SAFDL is not challenged, provided that the SGs retain liquid inventory (or the reactor coolant subcooling margin satisfies the plant-specific criterion). The FCM criteria is bounded by other Condition II events and is not credibly challenged by this event.

The peak primary and secondary pressures for this event are less than those of the LOEL/TT events provided that the pressurizer retains a steam "bubble" for pressure control, that is, the pressurizer does not overflow. Finally, the plant condition restriction is satisfied if the pressurizer does not become so full that liquid is expelled through the PORVs (the pressurizer level remains below the PORV inlet piping penetrations). In summary, the acceptance criteria for this event reduce to the requirements that: 1) the pressurizer level must remain below the PORV inlet piping penetrations, and 2) the fed SGs must not dry out (or the reactor coolant subcooling margin must satisfy the plant-specific criterion).

Consequently, the plant state and RPS setpoints are conservatively biased to maximize the potential for pressurizer overflow and SG dryout. Thus, a number of event specific analysis conservatisms are applied in addition to the more general ones that are routinely applied. [

1

Analysis Results

The event is initiated by tripping both MFW pumps for the two SGs. The liquid levels of both SGs drop rapidly and at 27.45 seconds, a low SG level signal trips the reactor. The sequence of events for the transient is presented in Table 6.5 and the transient responses of key parameters are presented in Figure 6.34 through Figure 6.39. For code-to-code comparisons, ANF-RELAP results are included in the figures.

There is a large margin to pressurizer overflow. Both codes predicted the maximum pressurizer level to be at 70.6 percent of the span and the top of the span is approximately 3.5 feet below the PORV inlet piping penetrations. Similarly, both codes predicted that the AFW flow capacity was sufficient to arrest the SG level decrease and prevent dryout so that long-term cooling was assured. However, the minimum calculated SG inventory was somewhat different, with S-RELAP5 giving a value of 20.1 percent (relative to initial inventory) while ANF-RELAP gave a value of 27.4 percent. While there are minor differences in some of the other variables (e.g., RCS fluid temperatures), the SG inventory is the one significant difference and is addressed here.

The difference in minimum predicted SG inventory is about 7.3 percent of the initial inventory as shown in Figure 6.39. S-RELAP5 calculates a larger reduction in SG inventory primarily because of a delay in the reactor trip of almost 5 seconds. During this 5 second period, the S-RELAP5 calculation continues at full power with the consequent boil-off of SG inventory as all of the reactor heat is absorbed by the latent heat of the SG residual mass. This calculated scram delay accounts for about 90 percent of the difference in minimum SG inventory with the remaining 10 percent due to the difference in RCP energy deposition as discussed above.

In both the S-RELAP5 and ANF-RELAP calculations, the reactor tripped on low SG level. The reason that the S-RELAP5 trip occurred later in time is due to the initial distribution of liquid within the SG secondary side which in turn is a result of differences in the interfacial drag package between the two codes. At the initial steady-state conditions, the SG inventory for both calculations is the same. However, for S-RELAP5, more water is present in the boiler so downcomer loss coefficients were adjusted to reduce the recirculation ratio allowing the initial mass to be matched.

Conclusion

The S-RELAP5 calculated results are shown to be in general agreement with the ANF-RELAP calculated results and reasonably represent the plant transient, with a negligible difference in the maximum pressurizer level and approximately a 7 percent difference in SG minimum inventory. This difference in SG inventory is the result of S-RELAP5 predicting the scram time approximately 5 seconds later than ANF-RELAP. For both codes, the reactor trip occurred on low SG level, however, differences between the codes' interfacial drag packages led to a difference in the predicted water holdup and in trip timing.

The capacity of the AFW system was shown to be more than adequate to allow a safe and orderly plant shutdown and to prevent SG dryout. Since SG dryout does not take place, the LONF event does not result in the violation of SAFDLs.

Table 6.5 LONF Event With Offsite Power Available Event Summary

Event	Time (s)
MFW Valve Closes	0.0
Pressurizer Spray On	18.0
Low SG Level Reached	26.55
Reactor Trip on Low SG Level Signal	27.45
Turbine Trip	28.2
Control Rods Begin to Fall	28.2
MSSVs Open	30.0
Pressurizer Backup Heaters On	30.1
Maximum Pressurizer Level	31.0
Pressurizer Proportional Heaters On	43.0
AFW Flow Starts	197.0
Maximum Pressurizer Pressure	1100
Pressurizer PORVs Open	1100
Pressurizer Backup Heaters Off	1220
Pressurizer Proportional Heaters Off	1230
Pressurizer PORVs Close	1250
Minimum Inventory – SG 1	1890
Minimum Inventory – SG 2	1900

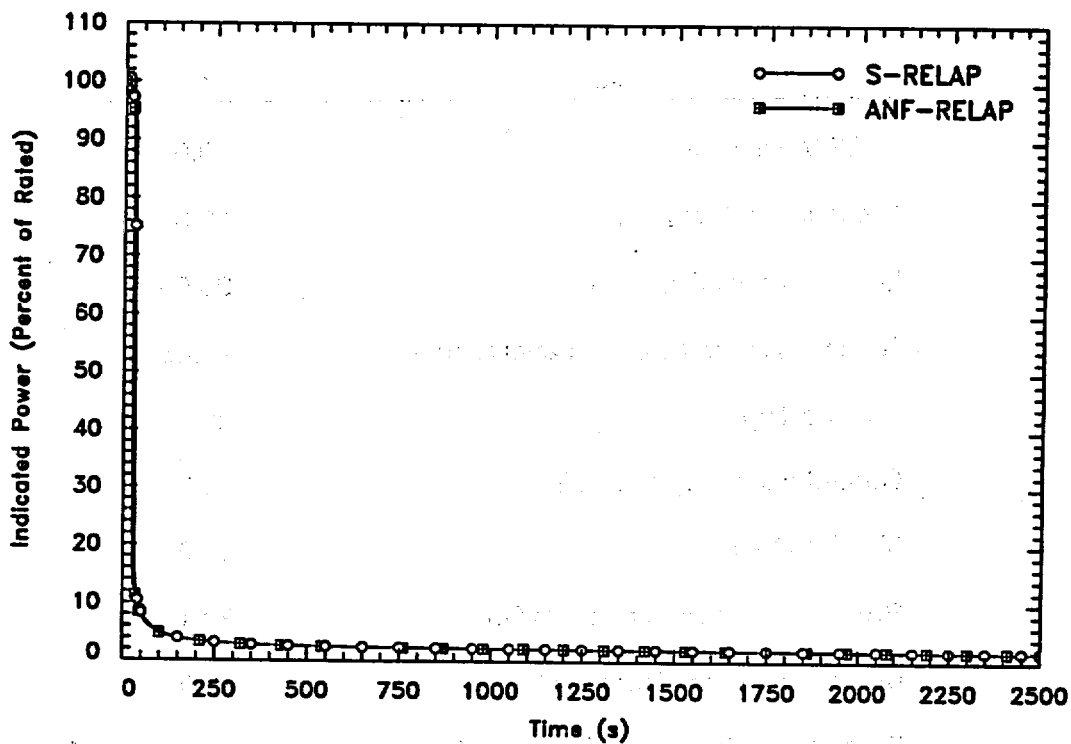


Figure 6.34 LONF (With Offsite Power) Reactor Power Level

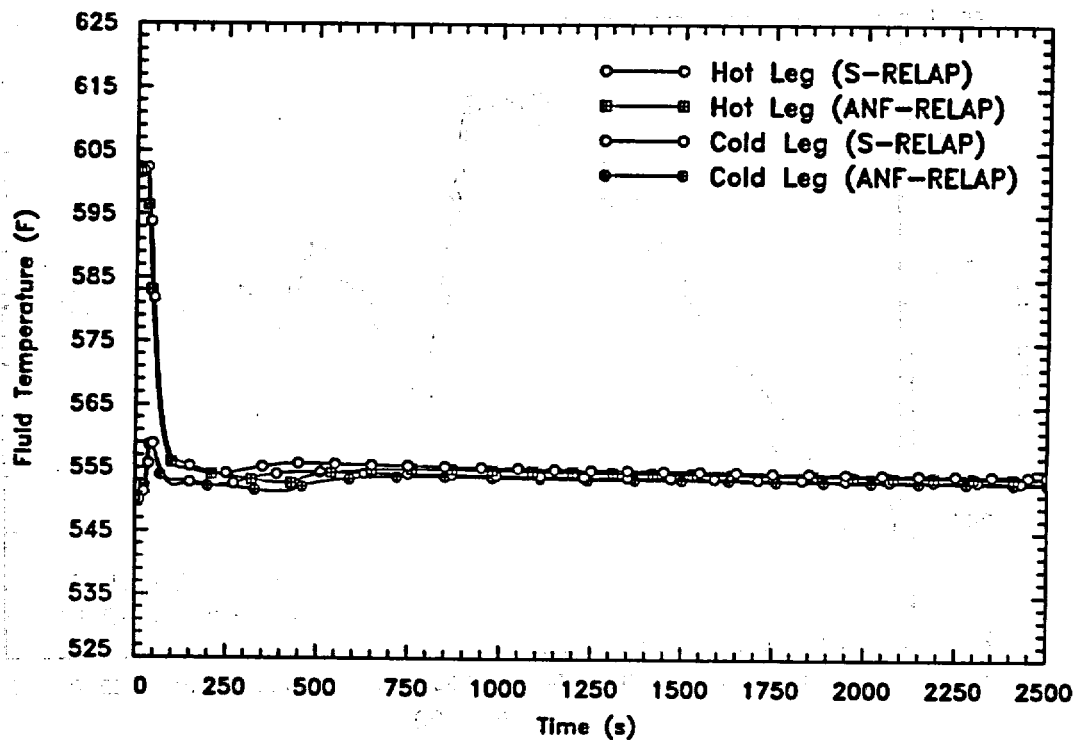


Figure 6.35 LONF (With Offsite Power) RCS Temperatures

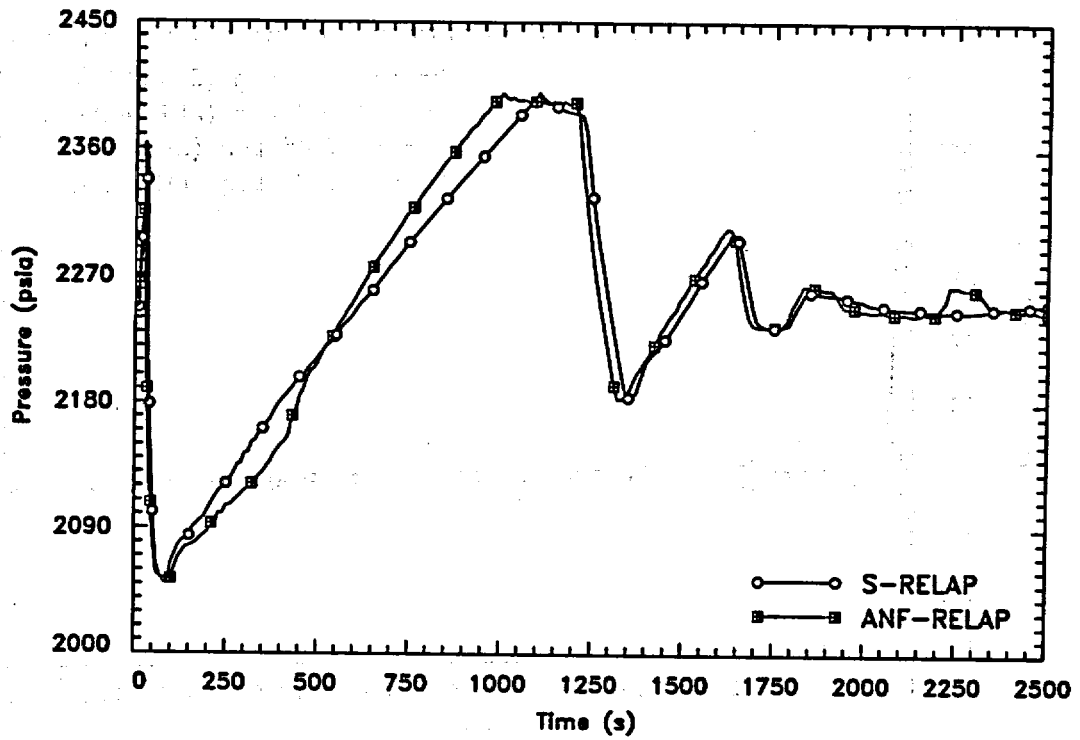


Figure 6.36 LONF (With Offsite Power) Pressurizer Pressure

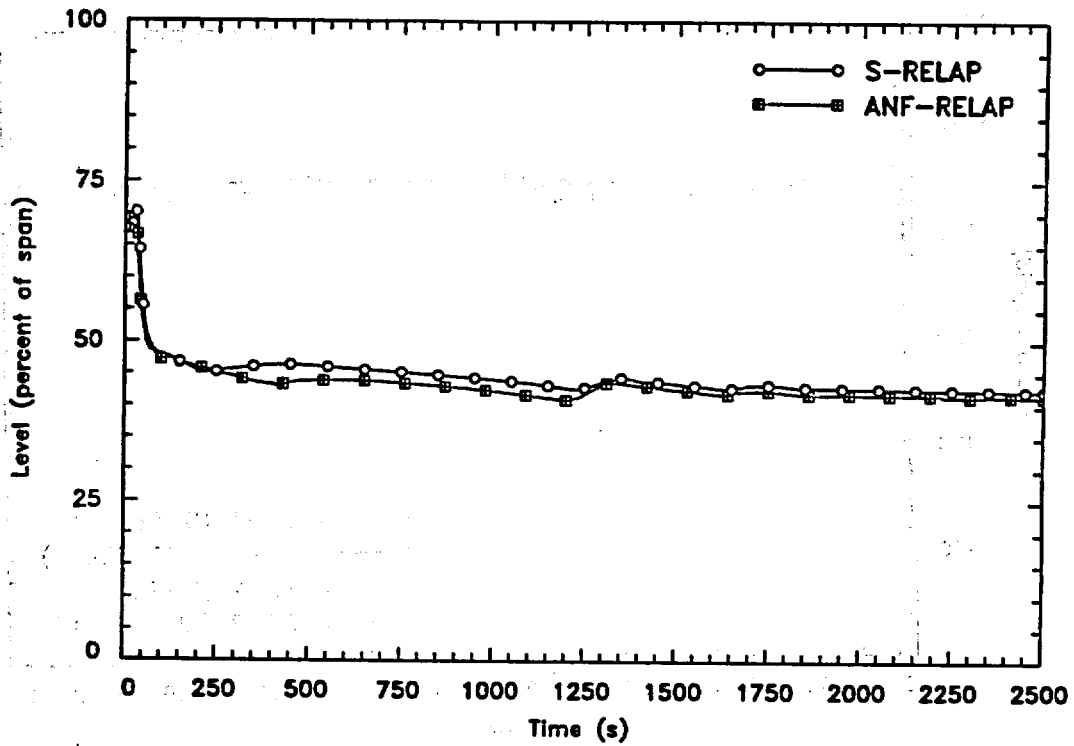


Figure 6.37 LONF (With Offsite Power) Pressurizer Liquid Level

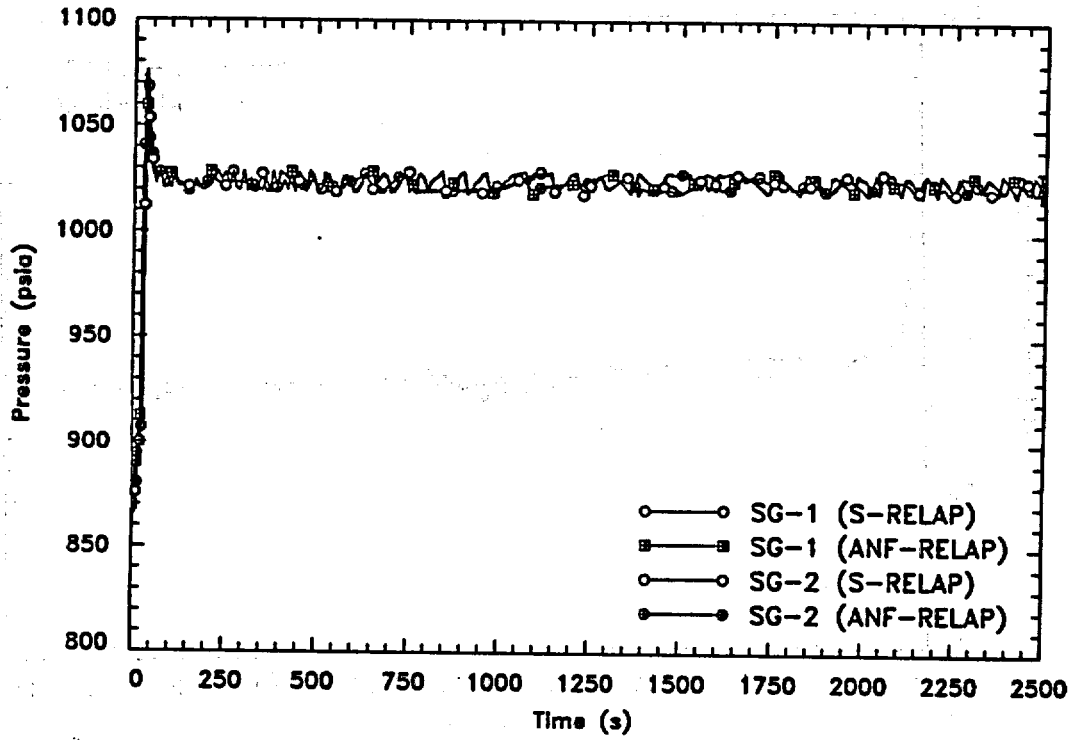


Figure 6.38 LONF (With Offsite Power) Steam Generator Pressure

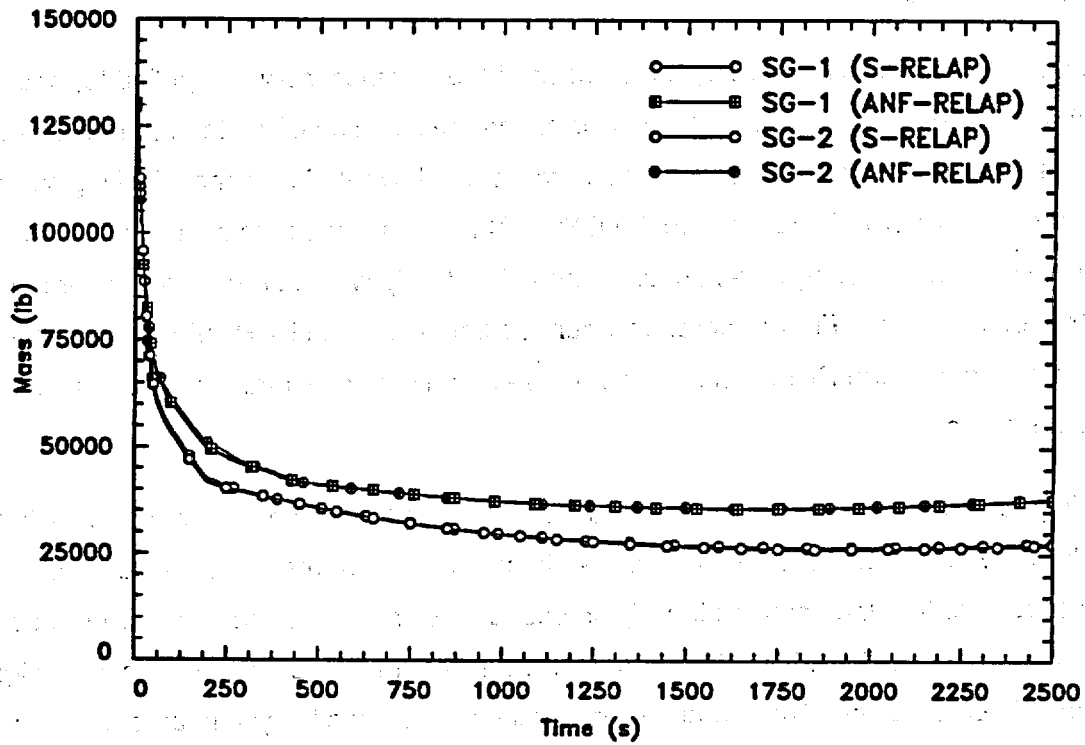


Figure 6.39 LONF (With Offsite Power) Steam Generator Inventory

6.5 Loss of Forced Reactor Coolant Flow (LOCF)

Event Description

The LOCF transient is initiated by a disruption of the electrical power supplied to, or a mechanical failure, in an RCP. These failures may result in a complete or partial loss of forced coolant flow. The complete LOCF with scram on low flow rate is the most limiting transient, from the perspective of challenge to the DNB SAFDL. This scenario occurs when an under-frequency or under-voltage event causes the RCPs to trip without removing power from the control rod restraints. Furthermore, between the time when the RCPs trip and the time when their breakers trip, the RCPs act as generators and an electrical braking occurs, accelerating the coastdown.

The impact of losing one or more RCPs is a decrease in the active coolant flow rate in the reactor core and, consequently, an increase in core temperatures. The reactor trips on low flow. Prior to reactor trip, the combination of decreased flow and increased temperature poses a challenge to the DNB SAFDL. The FCM SAFDL is not challenged since there is no significant increase in core power. This event also produces an increase in system pressure due to increased temperatures and reduced heat transfer to the secondary side of the SGs, but it does not create a credible challenge to system pressure limits.

This event is terminated by reactor scram on the RCS low flow trip, and the purpose for analyzing this event is to verify that the RPS can respond fast enough to prevent violation of the DNB SAFDL.

Definition of Events Analyzed

The partial loss of coolant flow event is a less severe transient than the complete loss of coolant flow event. This sample problem simulates a complete loss of coolant flow event.

The issue being evaluated is the challenge to the DNB SAFDL. Therefore the plant state and trip points are biased so as to maximize this challenge. This event is analyzed from full power initial conditions and the core thermal margins are minimized. [

Analysis Results

The overall response of the primary and secondary systems for this event is calculated by S-RELAP5. The MDNBR for this event is calculated using the thermal-hydraulic conditions from S-RELAP5 as input to XCOBRA-IIIC.

The transient is initiated by tripping all four RCPs. As the pumps coast down, the core flow is reduced causing a reactor scram on low flow. The flow decrease causes reactor coolant temperatures to increase with a subsequent power rise due to moderator reactivity feedback. The primary challenge to DNB is from the decreasing flow rate and resulting increase in coolant temperatures. Using XCOBRA-IIIC, the MDNBR is calculated to be 1.58.

The sequence of events is given in Table 6.6. The responses of key system variables for this event are given in Figure 6.40 to Figure 6.45. For code-to-code comparisons, the ANF-RELAP predictions are included on the figures.

The key parameter is the MDNBR and both codes predicted the MDNBR to be well above the applicable DNB SAFDL of 1.164. The predicted response for most of the key system variables is nearly identical. However, the MDNBR calculated by XCOBRA-IIIC using S-RELAP5 results was about 2.5 percent higher than that using the ANF-RELAP results.

The cause of this difference in the predicted MDNBR is the calculated behavior of the flow coast down. As shown in Figure 6.45, the RCS flow rate calculated by S-RELAP5 degrades somewhat more slowly than that of ANF-RELAP. At the time of MDNBR, about 3.1 seconds for both codes, the RCS flow rate is about 3 percent higher for the S-RELAP5 calculation. The root cause for this difference in transient response is the increased wall drag inside the SG tubes for S-RELAP5 due to the improvement to the single-phase wall drag model. Specifically,

due to the increased pressure drop for the RCS (about 10 percent higher), the initial pump speed in S-RELAP5 is higher than the pump speed for ANF-RELAP and the ensuing flow coast down is slightly slower for S-RELAP5.

Conclusion

The results of the analysis demonstrate that S-RELAP5 provides a satisfactory representation of the event. Furthermore, the S-RELAP5 results are in close agreement with the ANF-RELAP results, because most of the predicted responses for key system variables are virtually indistinguishable. The largest predicted variation is in the XCOBRA-IIIC MDNBR based on S-RELAP5 and ANF-RELAP results and has a magnitude of 3.0 percent; the DNB margin is about 36 percent above the applicable limit of 1.164.

Since the predicted MDNBR is greater than the applicable safety limit, this result indicates that no fuel failures due to DNB would occur. Therefore, the event acceptance criteria are met.

Table 6.6 LOCF Event Summary

Event	Time (s)
RCPs Trip	0.0
RCP Breakers Trip	0.5
Flow Reaches Low Flow Trip Setpoint	0.8
Peak Power Occurs	2.5
Reactor Scram (Begin Rod Insertion)	2.6
Turbine Isolates (Stop Valve Closed)	2.6
Pressurizer Spray Actuates	3.1
MDNBR	3.1
Peak Pressurizer Pressure	5.8

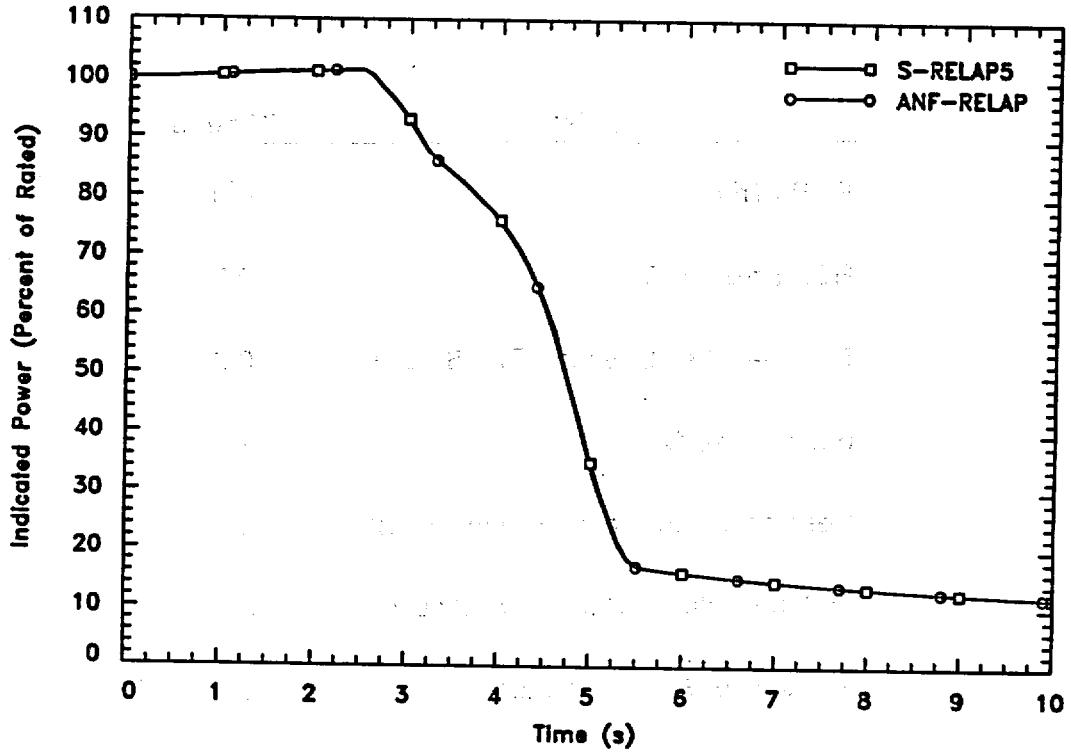


Figure 6.40 LOCF Reactor Power Level

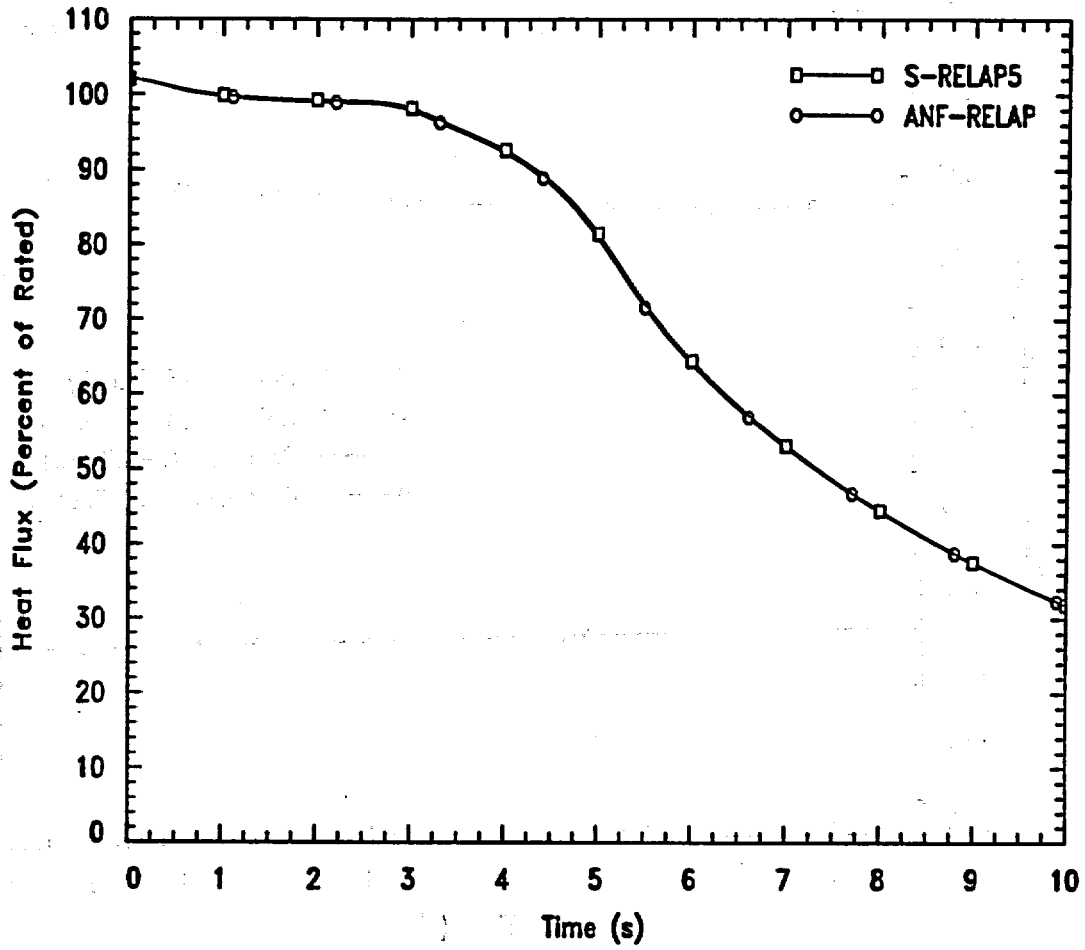


Figure 6.41 LOCF Core Average Heat Flux

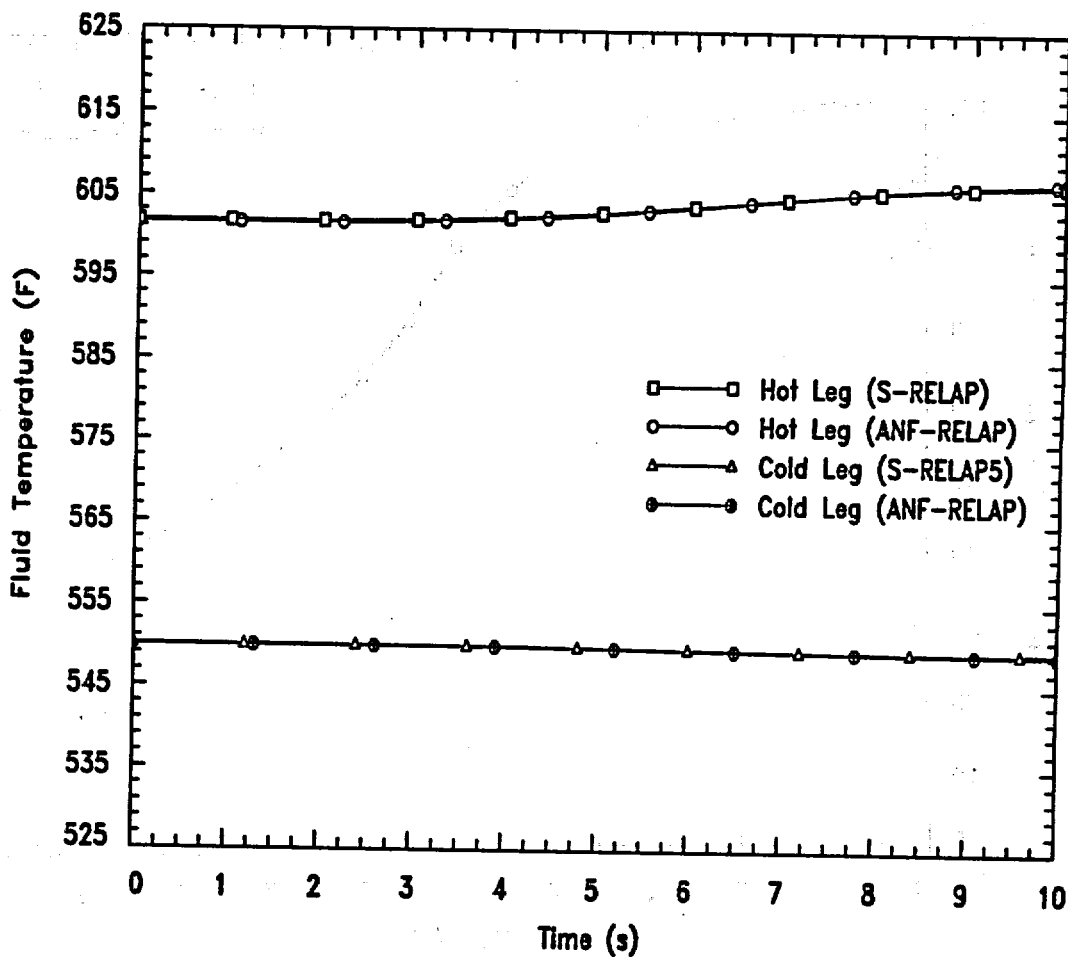


Figure 6.42 LOCF RCS Temperatures

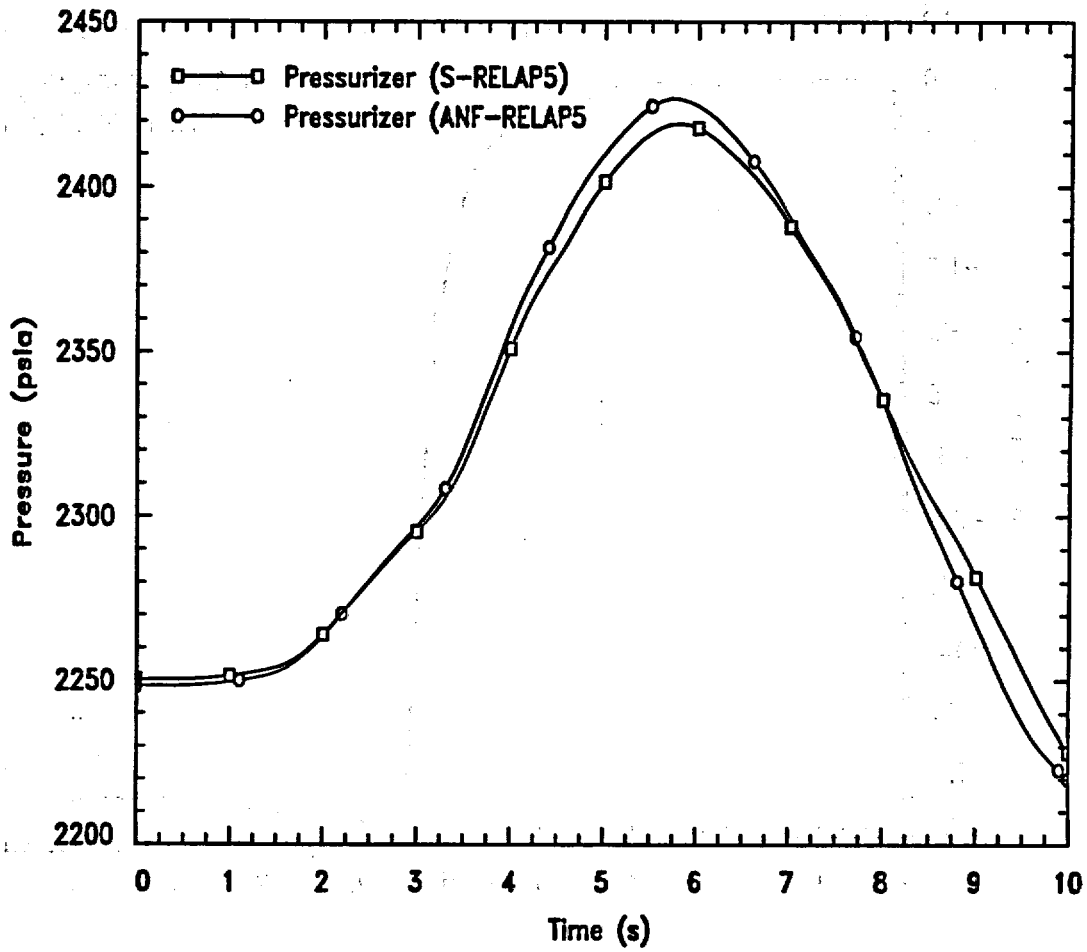


Figure 6.43 LOCF Pressurizer Pressure

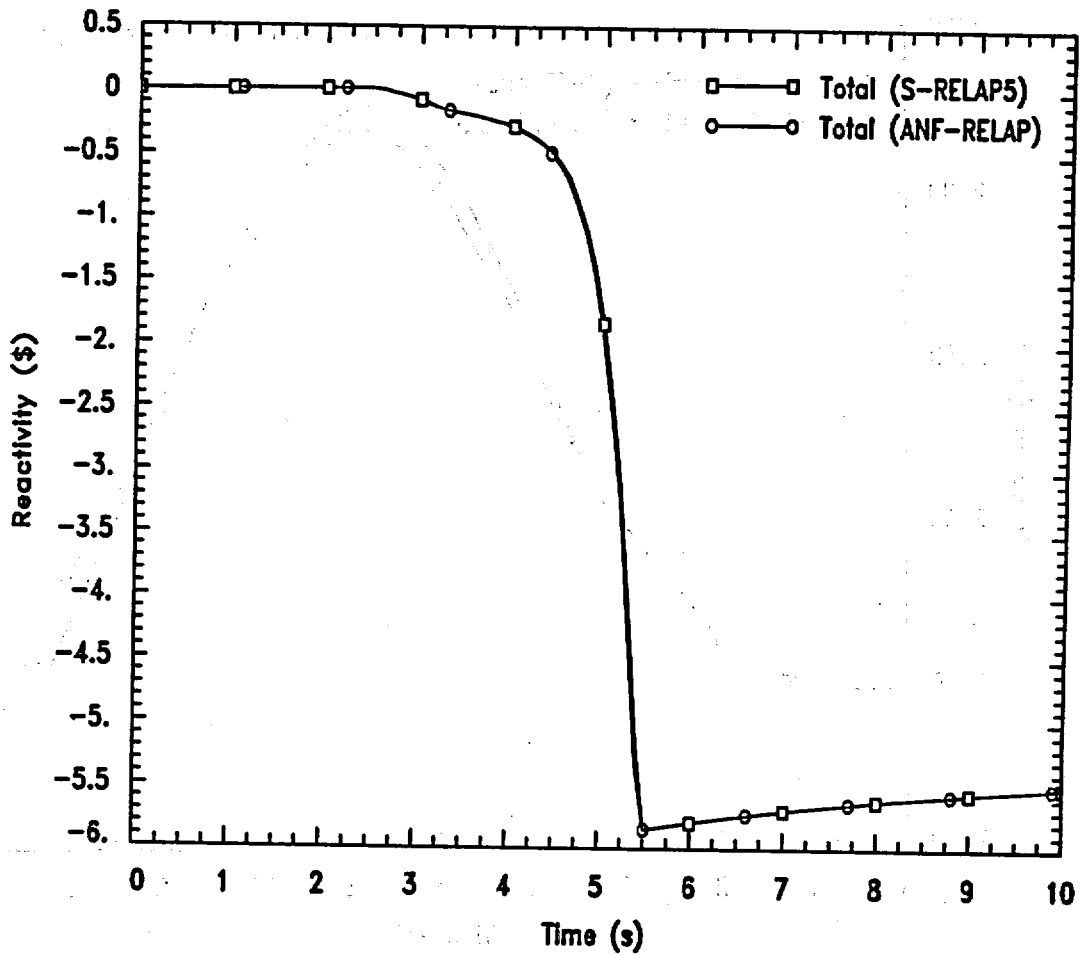


Figure 6.44 LOCF Reactivity

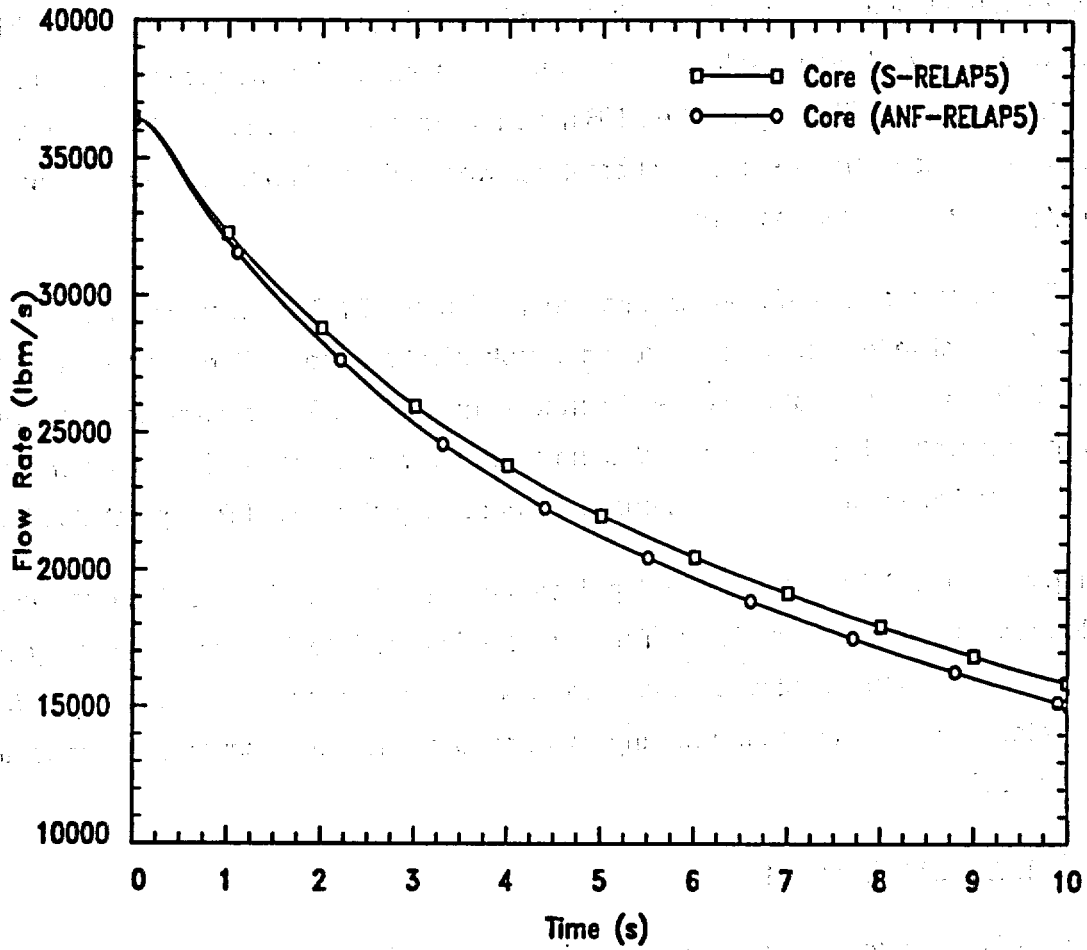


Figure 6.45 LOCF Reactor Coolant Flow Rate

6.6 *Uncontrolled Control Rod Bank Withdrawal (UCBW) at Power*

Event Description

This event is initiated during power operation (mode 1) by an uncontrolled withdrawal of a control rod bank due either to a failure in the rod control system or to operator error. The positive reactivity addition results in a power transient, increasing the core heat flux and creating a challenge to the DNB margin. The DNB margin is further reduced by an increase in the reactor system temperature resulting from the power-cooling mismatch, due to the increased energy generation rate in the core.

The RPS is designed to terminate this transient before the DNB limits are reached. The principal protective trips in this case for the sample plant are the VHP trip and the TM/LP trip. The TM/LP trip is specifically designed to protect against DNB for slow transients where the coolant temperature is able to respond to the reactor power changes. One of the primary objectives of this event analysis is to check the adequacy of the TM/LP setpoint algorithm.

The trip margin to DNB for the TM/LP trip decreases as the reactivity insertion rate increases due to thermal inertia and trip delay. This decrease in DNBR continues with reactivity insertion rate increases until the point where the neutron power challenges the VHP trip. MDNBR is typically found close to where the two trips act simultaneously and occurs just after control rod insertion begins.

Definition of Events Analyzed

This analysis evaluates the consequences of an uncontrolled control rod bank withdrawal from full power conditions. (CEA bank withdrawals at lower power levels, with correspondingly lower VHP reactor trip setpoints, offer less challenge to the DNB acceptance criterion and, therefore, have not been evaluated in this analysis.) A matrix of cases considering a range of reactivity insertion rates, from very slow (e.g., gradual boron dilution) to the maximum possible CEA bank withdrawal rate at maximum worth for two banks moving in normal sequence and overlap, and at BOC and EOC was calculated. Only the most limiting DNBR case is described here. The limiting DNBR case occurred for a slow CEA bank withdrawal rate (3.30×10^{-4} $\$/s$) at BOC conditions.

[

]

Analysis Results

The overall response of the primary and secondary systems for this event is calculated by S-RELAP5. The MDNBR for this event is calculated using the thermal-hydraulic conditions from the S-RELAP5 calculation as input to XCOBRA-IIIC.

The DNB-limiting uncontrolled control bank withdrawal transient was analyzed for full power conditions (102 percent of rated) with BOC kinetics and with an insertion rate of 3.30×10^{-4} $\$/s$. The MDNBR was calculated to be 1.50. The scram occurred on a VHP trip near the point where the two trips would have acted simultaneously (the TM/LP trip signal would have been received 0.5 seconds after the time of the VHP signal).

An event summary is presented in Table 6.7. The transient responses for key parameters are presented in Figure 6.46 through Figure 6.52. For code-to-code comparisons, the ANF-RELAP predictions are included on the figures.

The focus of this reactivity insertion event is the challenge to the DNB SAFDL resulting from the power increase. The MDNBR calculated for the DNB-limiting transient was 1.50 which is well above the applicable limit of 1.164. The predicted response of the key system parameters that govern DNBR (e.g., see Figure 6.49 for the RCS fluid temperatures) was essentially identical for the two codes up until the time of the reactor trip.

The only significant difference is in the behavior of the pressurizer pressure, see Figure 6.50, after the PORVs open. The sensitivity of the control logic that governs the opening/closing of the motor valve used to model the PORVs, as noted in the LOEL sample problem, and small differences in the calculation, cause the differences in the predictions of the two codes to be magnified. However, the effect on the MDNBR is minimal.

Conclusion

The S-RELAP5 results are nearly identical to those of ANF-RELAP and reasonably represent the plant transient response. The MDNBR was calculated to be 1.50 and the applicable safety limit is 1.164. This indicates that no fuel failures due to DNB would occur and, therefore, that the acceptance criteria are met.

Table 6.7 DNB-Limiting UCBW at Power Event Summary

Event	Time (s)
Slow CEA Bank Withdrawal Begins	0.0
Pressurizer Spray On	47.0
Pressurizer PORVs Open	151.0
SG 1 MSSVs Open	202.0
SG 2 MSSVs Open	204.0
Indicated Power Reaches VHP Setpoint	208.7
Pressurizer Pressure Reaches TM/LP Setpoint	208.7
Peak Core Power Occurs	209.0
VHP Signal Initiates Reactor Trip	209.1
Scram CEA Insertion Begins, and Turbine Trips	209.9
MDNBR Occurs	210.0
Pressurizer PORVs Close	214.0

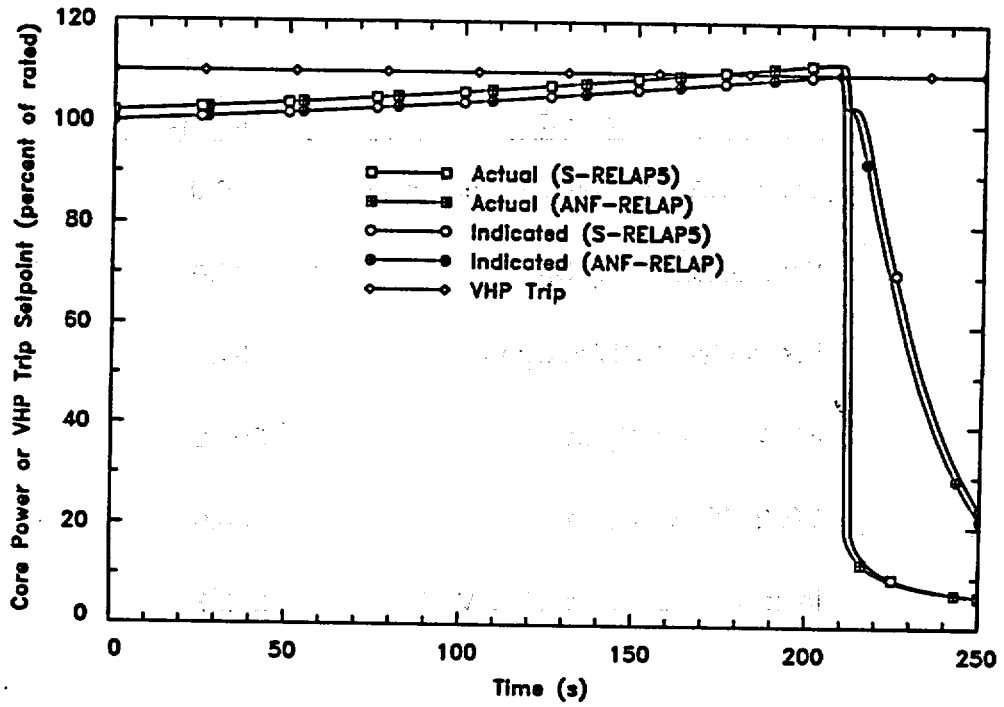


Figure 6.46 DNB-Limiting UCBW Core Power and VHP Trip Setpoint

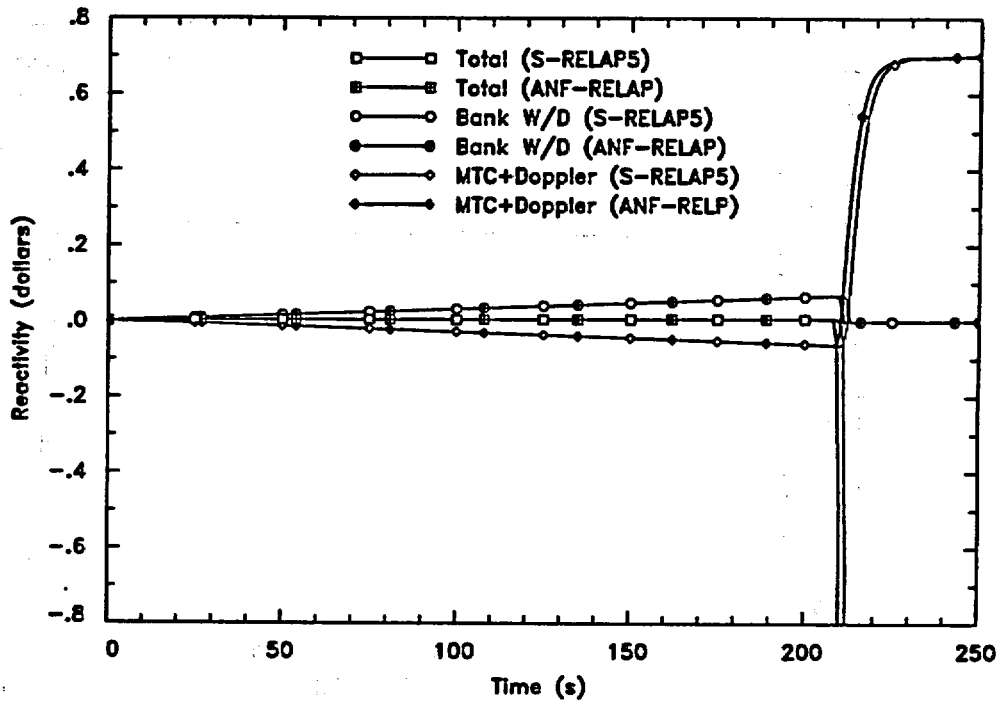


Figure 6.47 DNB-Limiting UCBW Reactivity

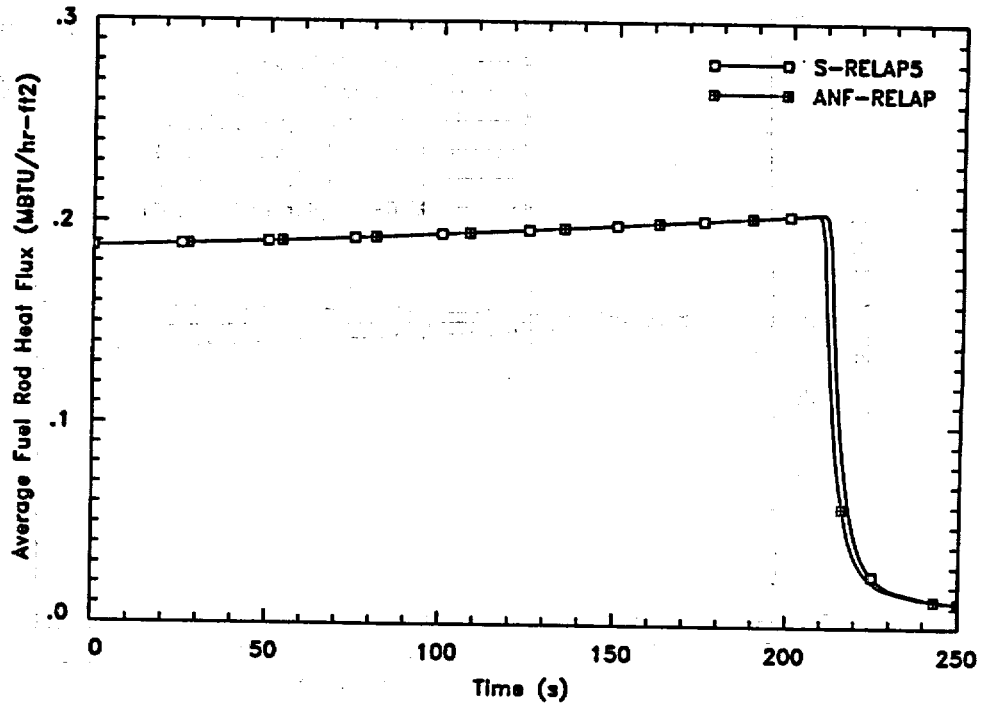


Figure 6.48 DNB-Limiting UCBW Average Fuel Rod Heat Flux

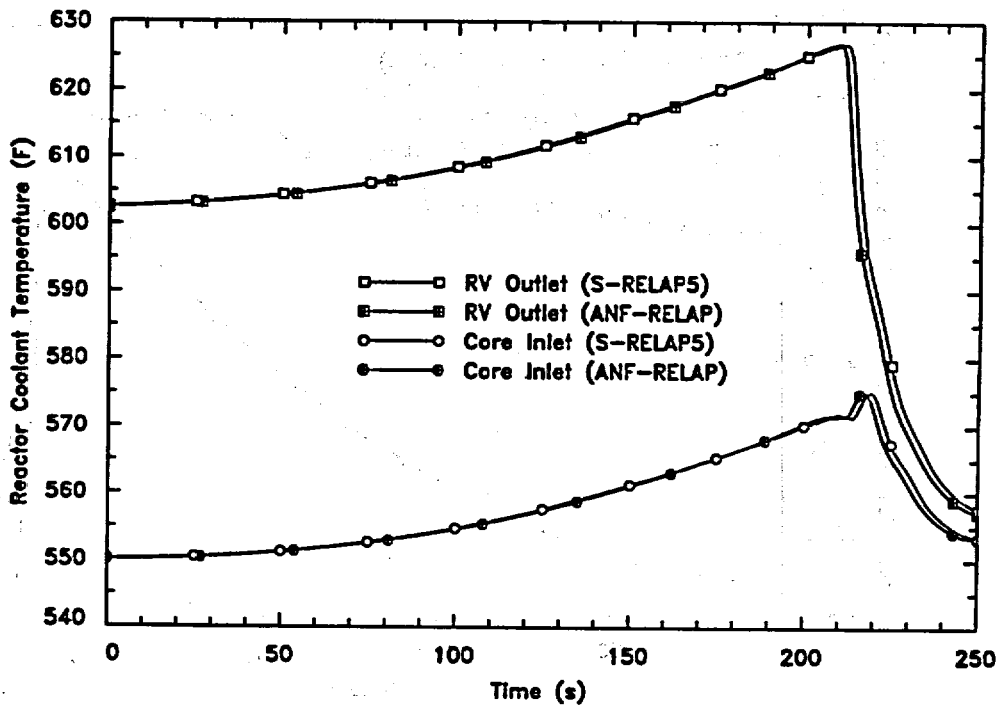


Figure 6.49 DNB-Limiting UCBW RCS Temperatures

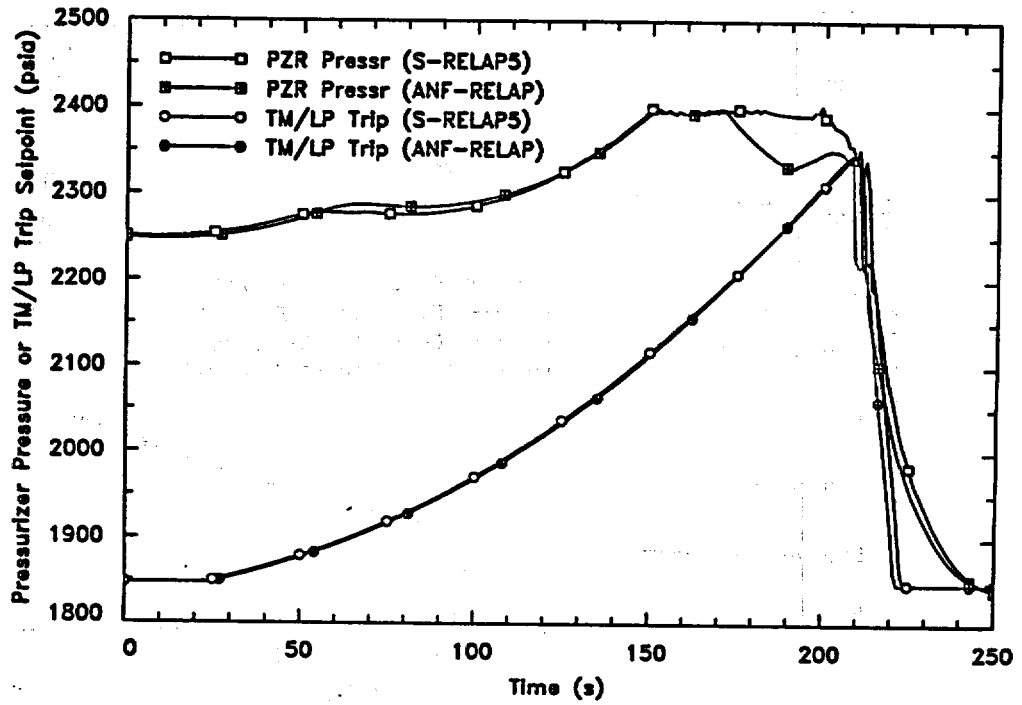


Figure 6.50 DNB-Limiting UCBW Pressurizer Pressure and TM/LP Trip Setpoint

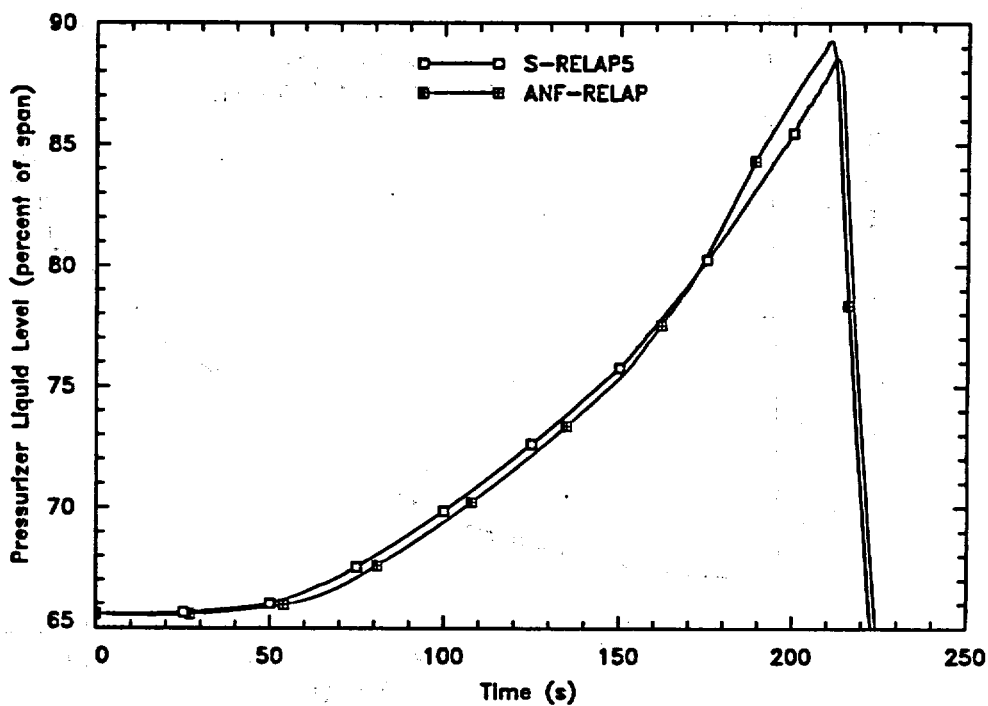


Figure 6.51 DNB-Limiting UCBW Pressurizer Liquid Level

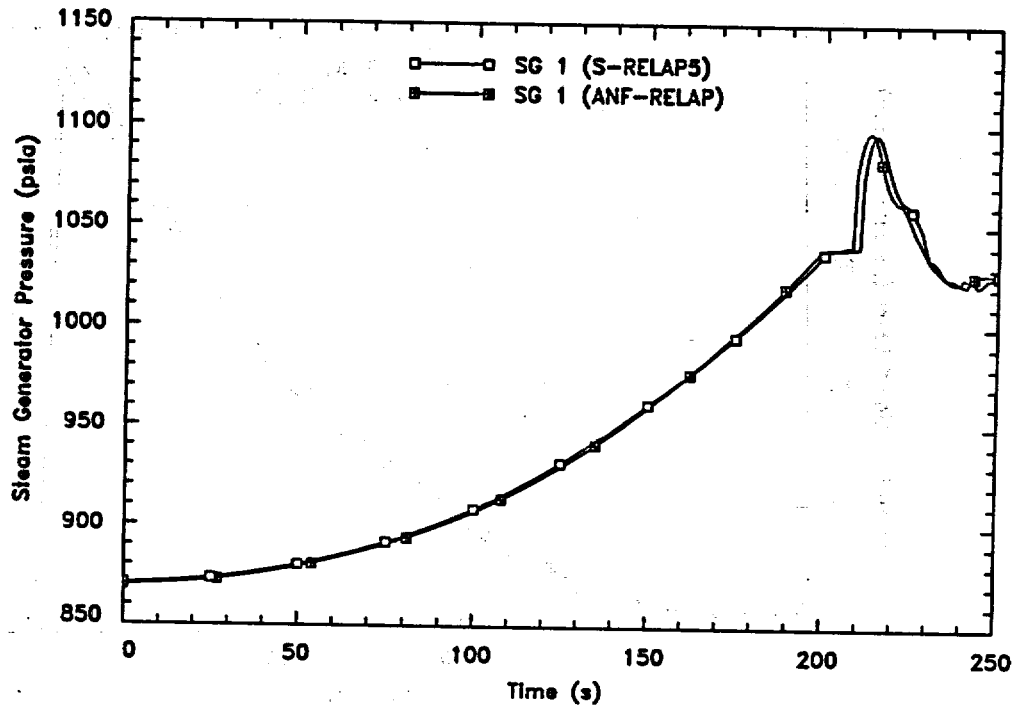


Figure 6.52 DNB-Limiting UCBW Steam Generator Pressure

6.7 *Steam Generator Tube Rupture (SGTR)*

Event Description

The SGTR event is initiated by a break of a single steam generator U-tube. RCS inventory begins to flow into the SG secondary side due the pressure differential. The break flow exceeds the make-up capacity of the charging pump causing the pressurizer pressure and level to decrease, leading to a reactor trip on the low pressure setting of the TMLP trip. The trip of the reactor is followed by a turbine/generator trip so that the secondary side pressurizes and inventory from the RCS and the SG is released by the MSSVs. HPSI flow is initiated by the low-pressurizer-pressure signal. The reactor coolant pressure falls to saturation and a quasi-static relief of decay heat by steam through the MSSVs occurs until the operators intervene.

In this sample calculation, operator actions (including a 30 minute delay for operator identification of event) were assumed for a typical CE 2x4 plant. These actions included isolating the AFW system and closing the MSIV of the ruptured SG. Then, the operators used the ADVs and pressurizer PORVs to reduce the RCS pressure. Finally, the PORVs were cycled to regain control of the plant.

Events Analyzed

The initiator for this event is a double-ended break of a single steam generator U-tube in the downstream side just above the tube sheet. The event analyzed is initiated at HFP without offsite power available. This leads to a loss of power to the bus upon turbine trip. The initial plant state is also biased, based on technical specification limits and instrumentation uncertainties, to maximize the releases. The event summary, Table 6.8, describes the operator actions assumed.

For the purposes of this analysis, the SGTR event is considered terminated at 8000 seconds with the plant fully under operator control.

Analysis Results

Figure 6.53 through Figure 6.65 present the S-RELAP5 predicted response for key plant parameters. For code-to-code comparison, the ANF-RELAP predictions are also included on these figures. The sequence of events for the SGTR event is given in Table 6.8.

The key parameters affecting the radiological release are the cycling of the MSSVs and ADV for the affected steam generator. Upon turbine trip, the turbine admission valves are closed and the steam dump system is unavailable due to the loss of condenser vacuum. The result is a rapid increase in SG pressures up to the MSSV setpoints. The MSSVs cycle, releasing heat and inventory to the atmosphere. After 1800 seconds, the operator is assumed to take action to isolate the affected steam generator and begin a cooldown of the RCS. This cooldown includes opening the ruptured SG ADV in an effort to limit further actuation of its MSSVs.

For the SGTR event, the results of the system thermal-hydraulic code are used as boundary conditions for an analysis of the radiological consequences. The purpose of this analysis is to compare the predicted response of S-RELAP5 to that of ANF-RELAP for the parameters that are input to the radiological release model. Specifically, the parameters of interest are the total break flow and steam release for the ruptured SG. The total steam release from the ruptured steam generator is predicted to be 101,000 lb_m and the integrated break flow (for the entire 8000 seconds transient) is 168,000 lb_m. For these parameters, the agreement between S-RELAP5 and ANF-RELAP is excellent. The integrated break flow is within 1.5 percent and the total steam release from the ruptured SG (ADV and MSSVs) is within 0.5 percent.

There are a number of small differences in the calculated values of the other system variables (e.g., the RCS temperatures) that did not have a significant impact on the course of the transient. The largest difference shows up in the predictions for the inventory for the unaffected SG, see Figure 6.59. For the unaffected SG, the total steam release for the ADVs and MSSVs is about 2.7 percent greater for ANF-RELAP. This magnitude is within the difference expected in the calculated critical flow, as described in Section 3.3.

Conclusion

The results demonstrate that S-RELAP5 provides a satisfactory representation of the SGTR event. Furthermore, the S-RELAP5 results were generally in close agreement with the

ANF-RELAP results for the response of key system variables. In particular, the predicted total steam release from the affected steam generator was within one percent for the two codes.

Table 6.8 SGTR Event Summary

Event	Time (s)
Double-Ended Rupture of SG Tube	0.0
Reactor Trips on TMLP Signal	673.8
Turbine Trips, Loss of Offsite Power, RCP Coastdown, and MFW Trips	674.5
Low Pressurizer Pressure Trip of SIS	689.2
HPSI Flow Begins	719.2
AFW Flow Begins (Low SG Level Trip)	1031.6
Operator Action to Isolate AFW and MSIV to Ruptured SG	1800
Operator Opens ADVs on Both SGs	1800
Operator Isolates Ruptured SG ADV	3000
Operator Opens Pressurizer PORV	5000
Operator Closes Pressurizer PORV	5035
Operator Terminates HPSI and Charging Flow	6000
Operator Re-opens Pressurizer PORV	6000
Operator Closes Pressurizer PORV	6035
Operator has Full Control of Plant	8000

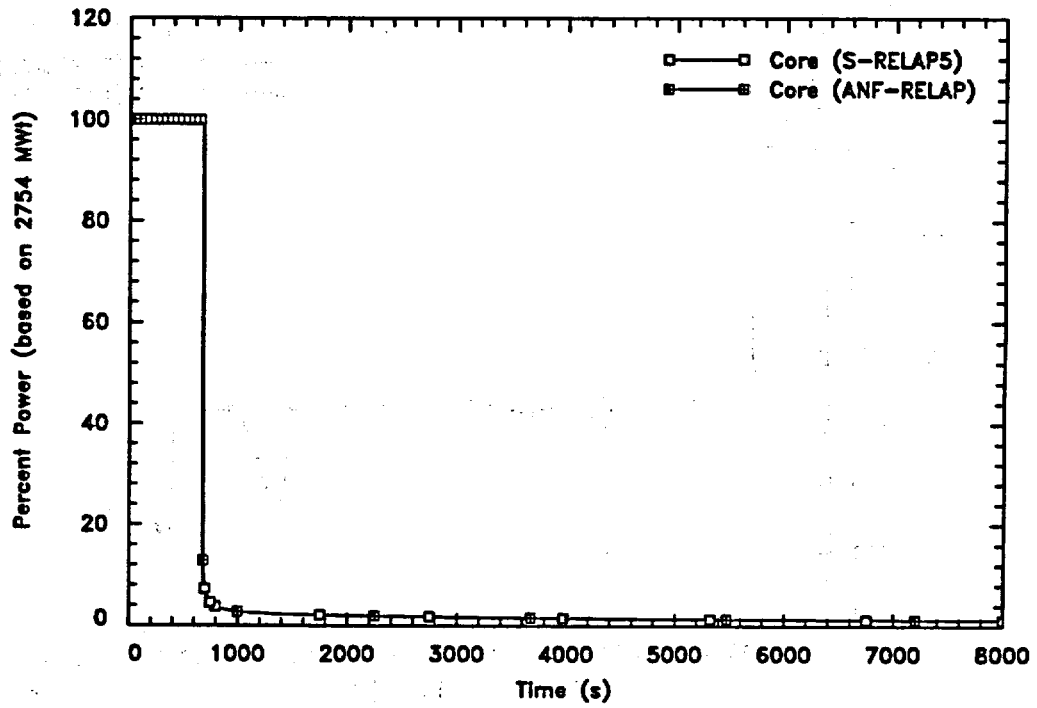


Figure 6.53 SGTR Reactor Power

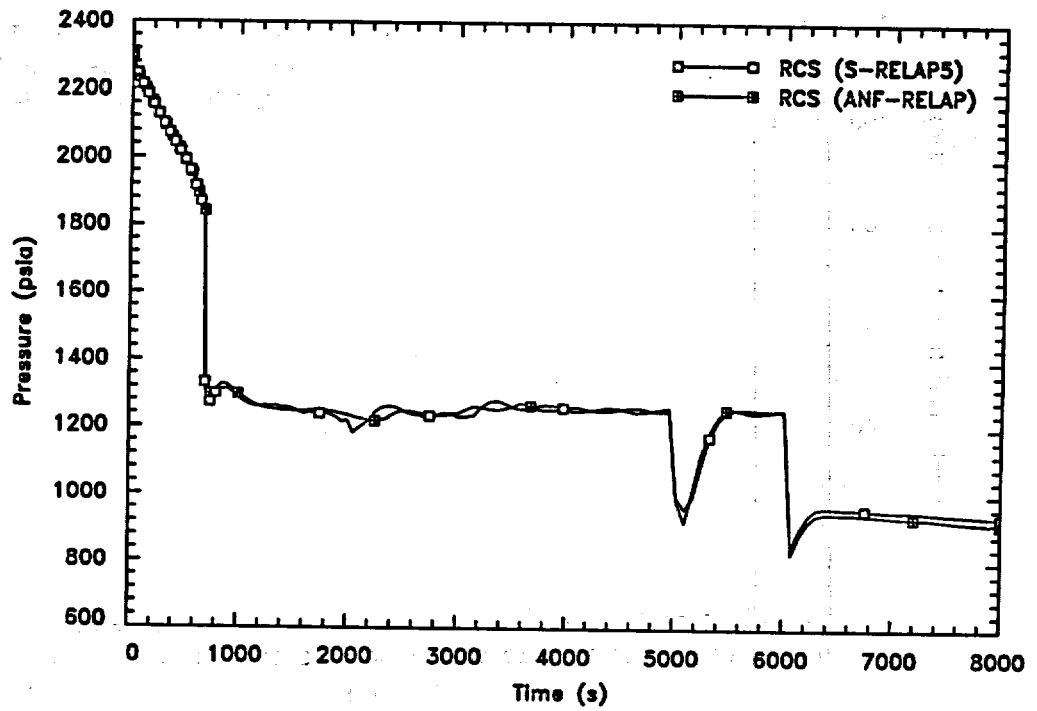


Figure 6.54 SGTR Pressurizer Pressure

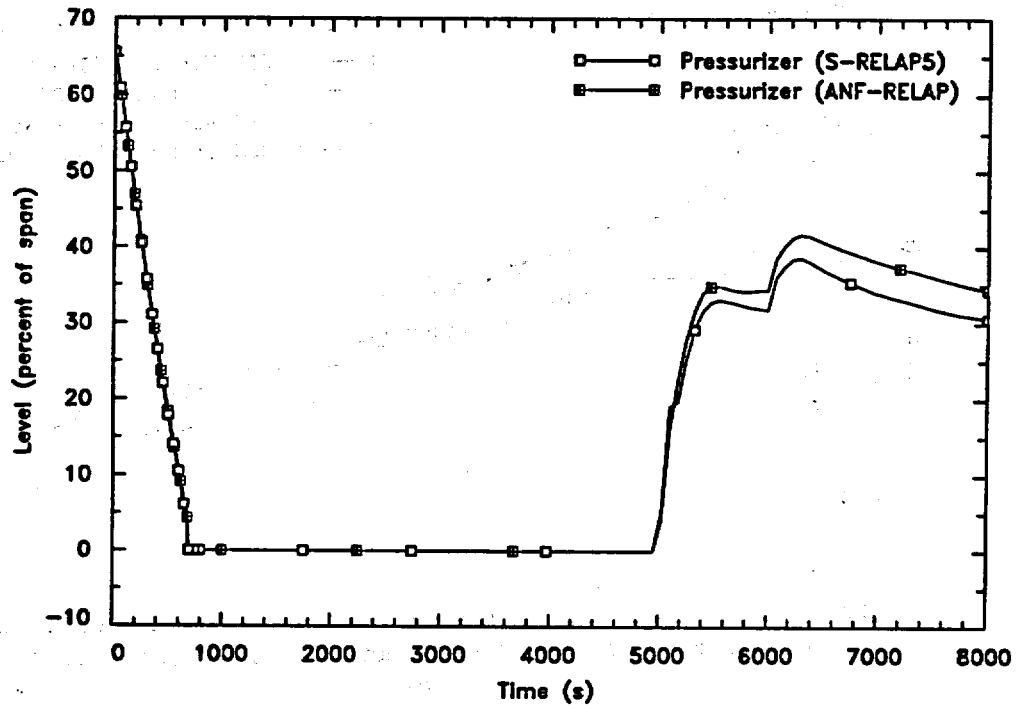


Figure 6.55 SGTR Pressurizer Liquid Level

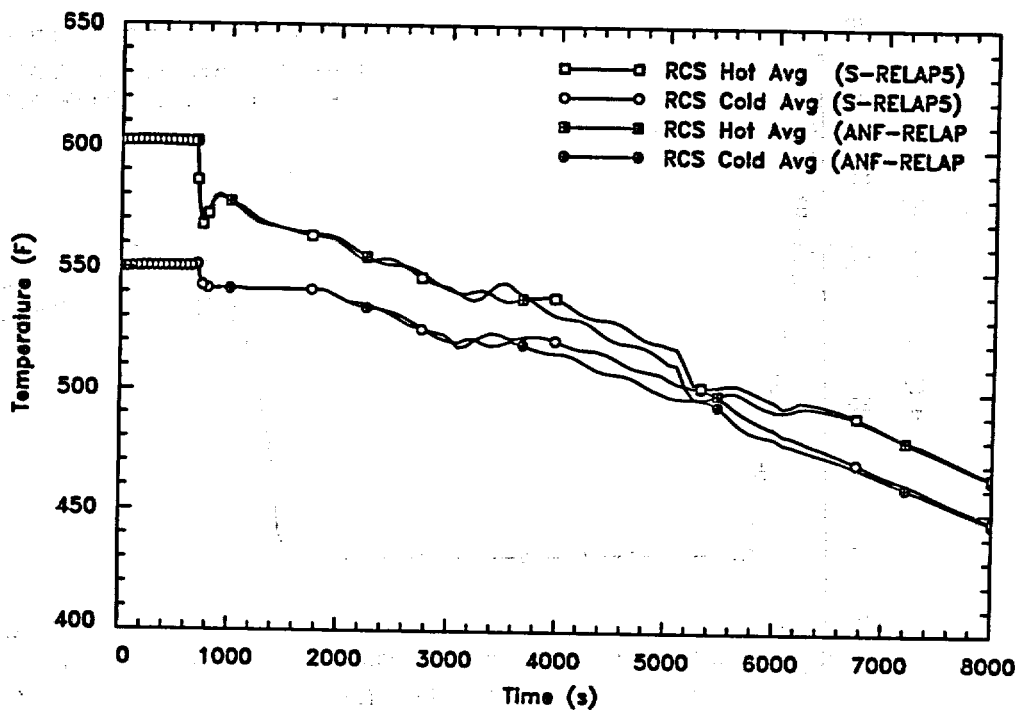


Figure 6.56 SGTR RCS Temperatures

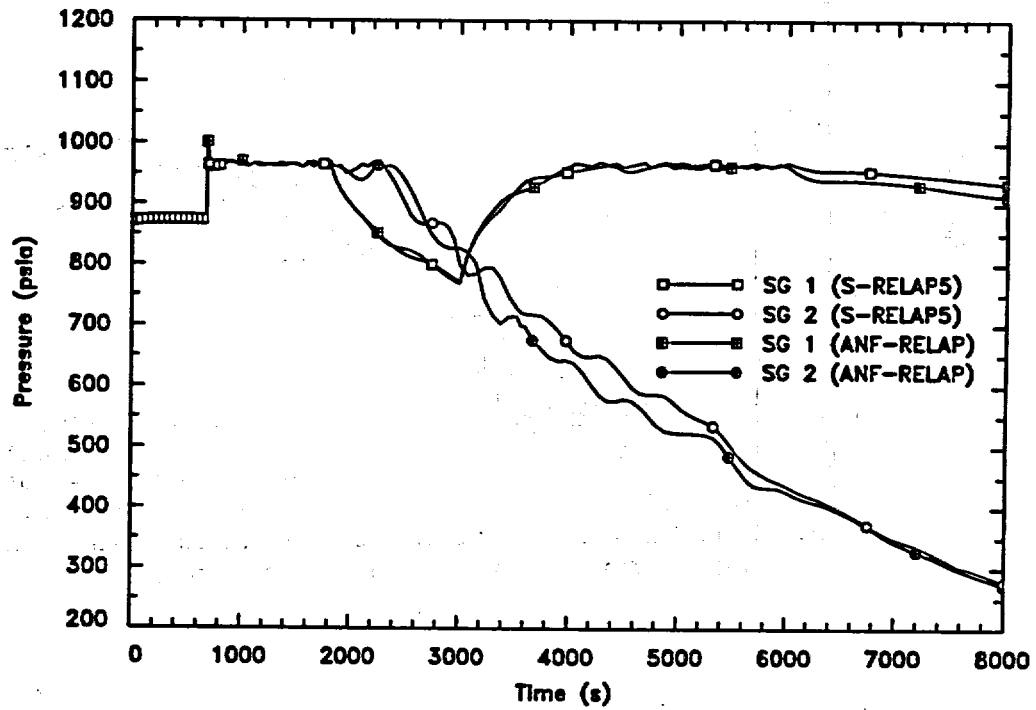


Figure 6.57 SGTR Steam Generator Pressures

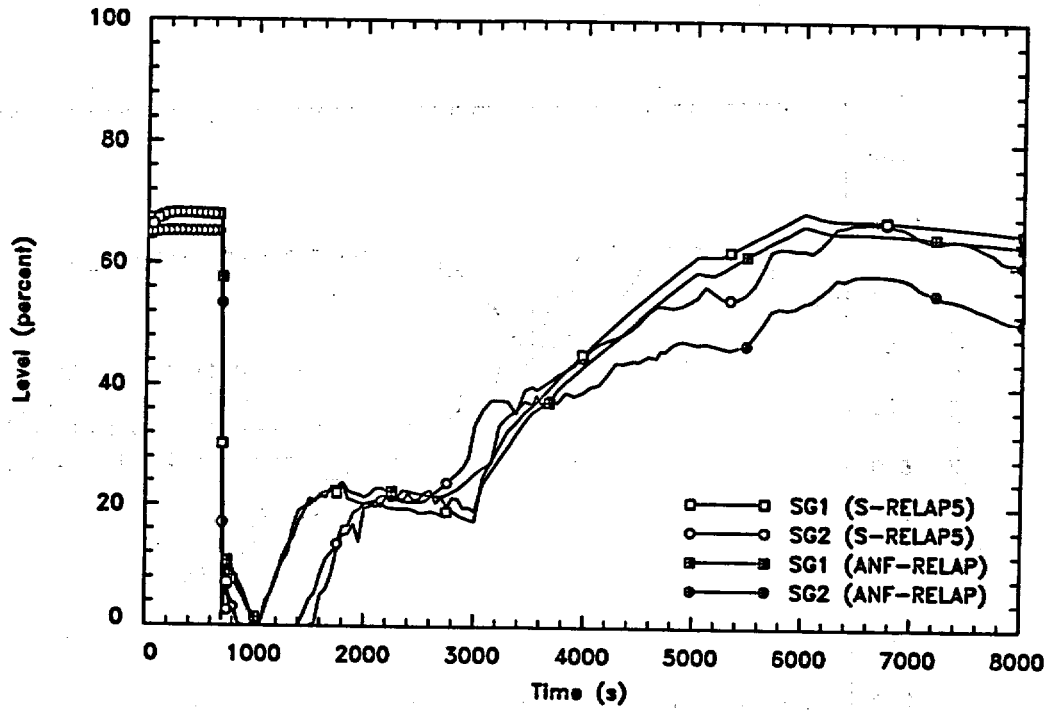


Figure 6.58 SGTR Steam Generator Levels

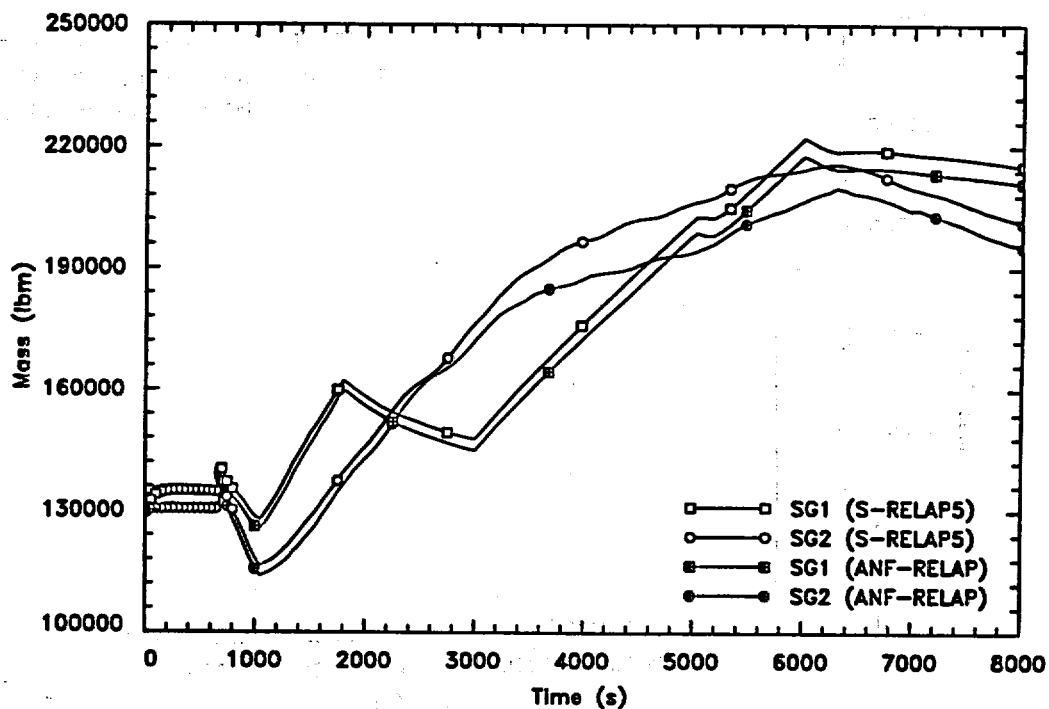


Figure 6.59 SGTR Steam Generator Mass

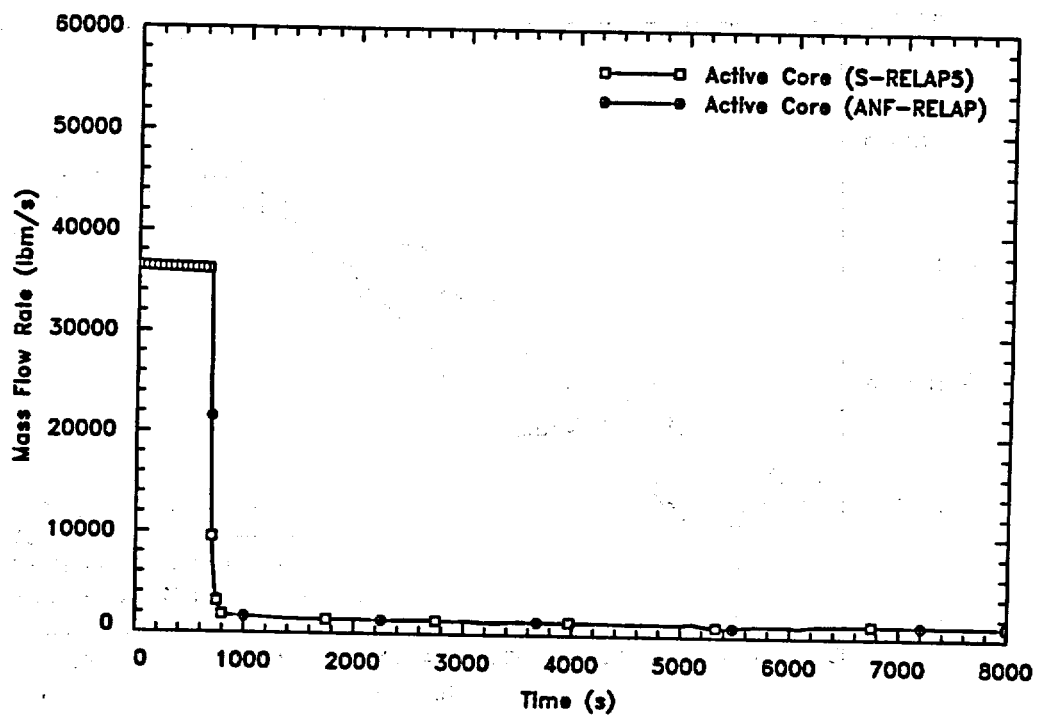


Figure 6.60 SGTR Active Core Mass Flow Rate

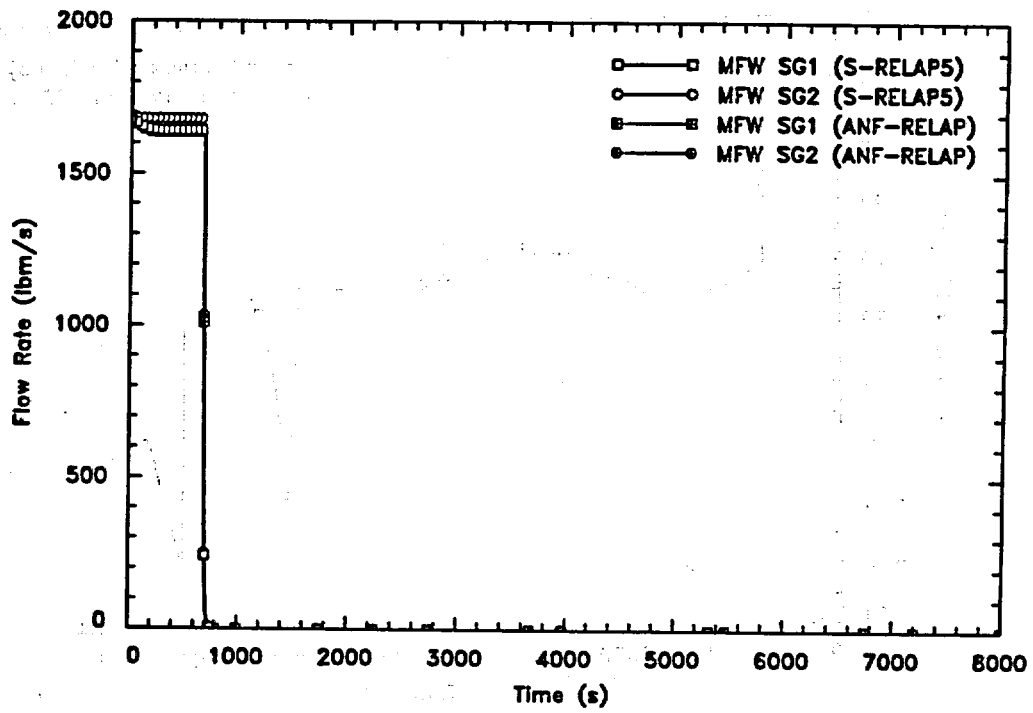


Figure 6.61 SGTR MFW Flow Rates

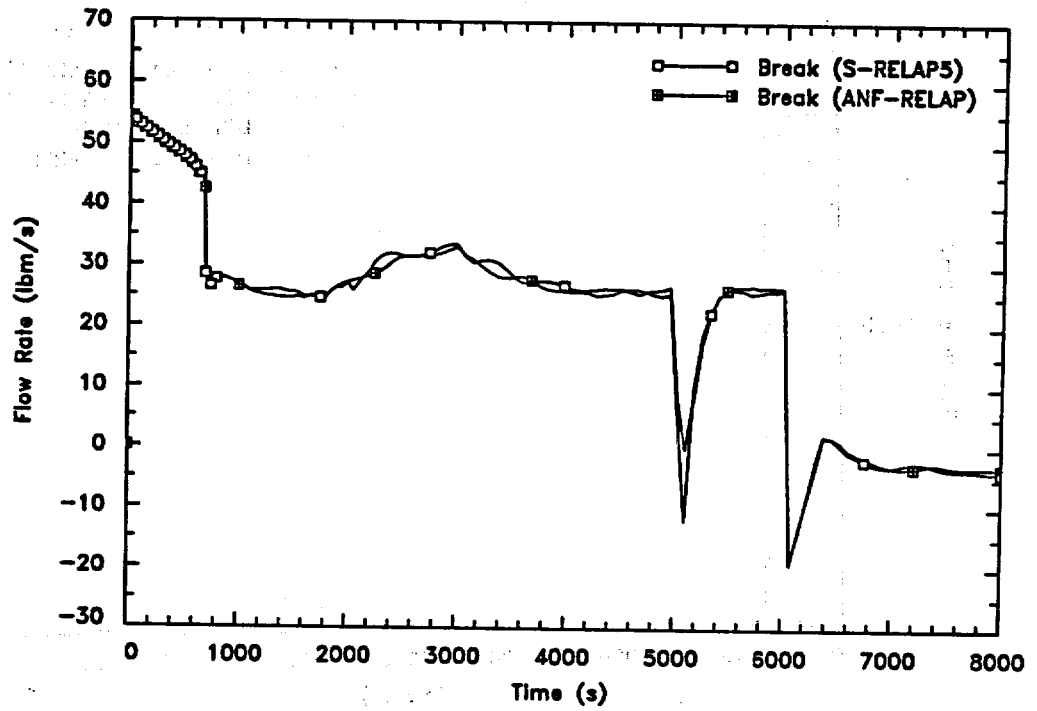


Figure 6.62 SGTR Break Flow Rate

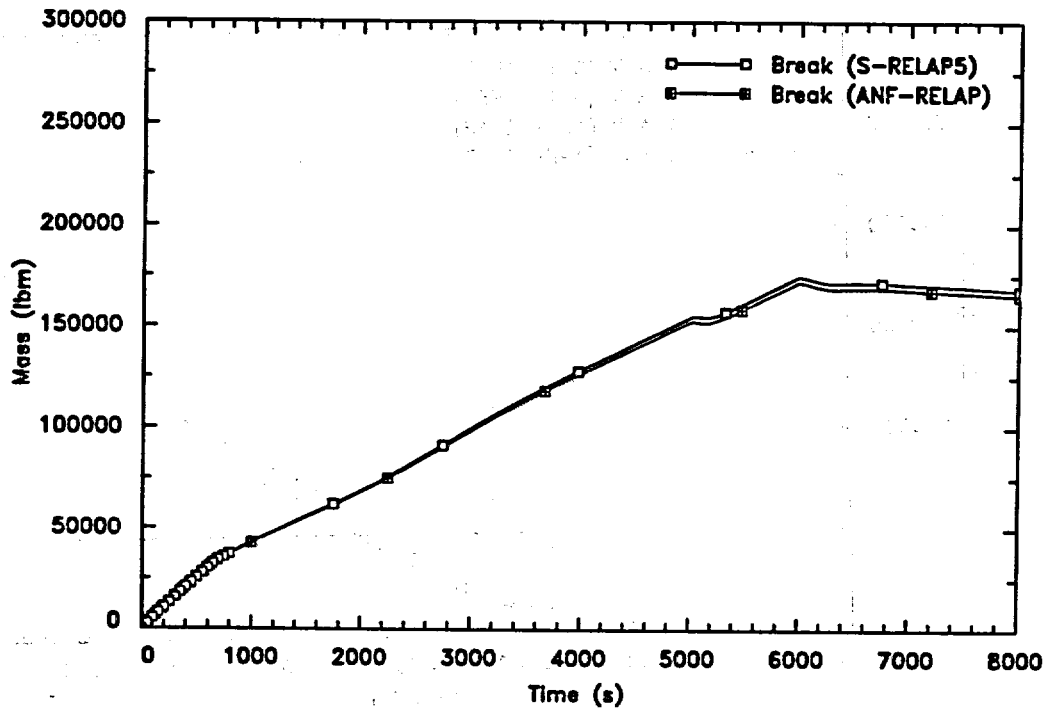


Figure 6.63 SGTR Integrated Break Flow

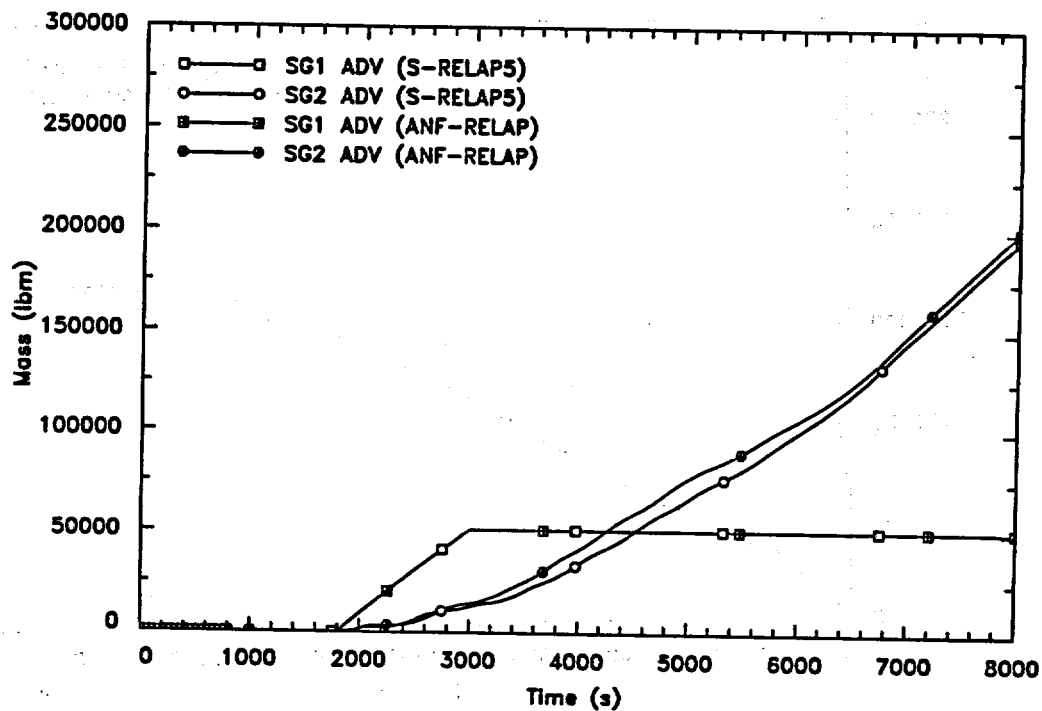


Figure 6.64 SGTR Integrated ADV Flows

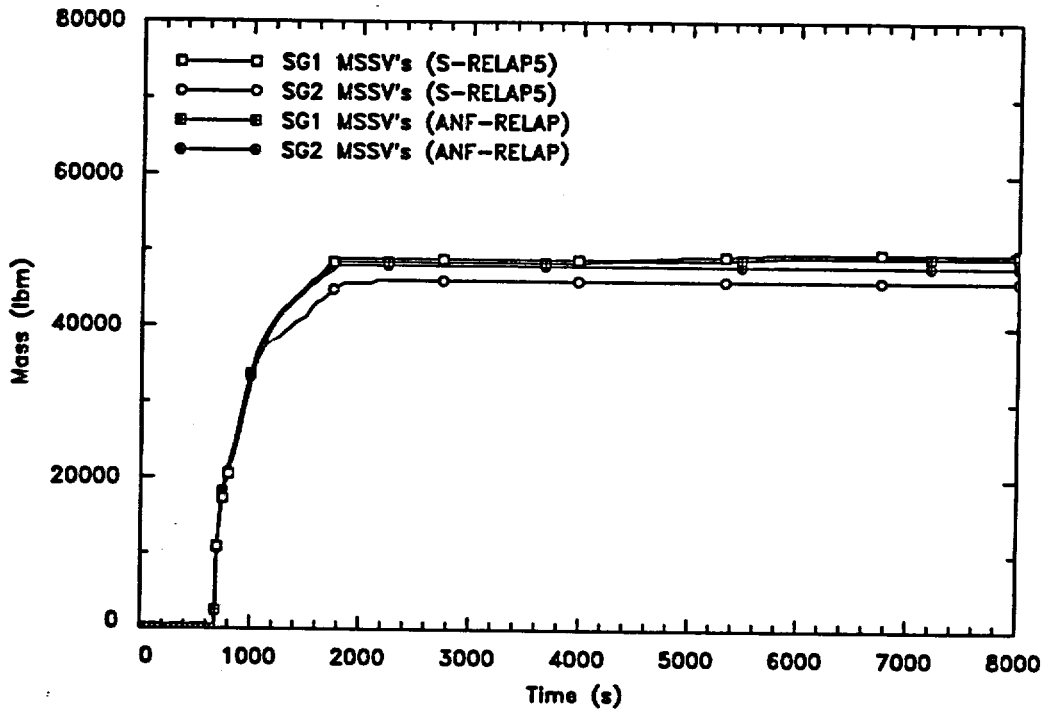


Figure 6.65 SGTR Integrated MSSV Flows

7.0 References

1. EMF-2100(P), *S-RELAP5 Models and Correlations Code Manual*, Siemens Power Corporation, November 1999.
2. NUREG-0800, *USNRC Standard Review Plan*, U.S. Nuclear Regulatory Commission, Washington, D.C. 20555, July 1981.
3. ANF-89-151(P)(A), *ANF-RELAP Methodology for Pressurized Water Reactors: Analysis of Non-LOCA Chapter 15 Events*, Advanced Nuclear Fuels Corporation, May 1992.
4. EMF-84-93(P)(A) Revision 1, *Steam Line Break Methodology for PWRs*, Siemens Power Corporation, February 1999.
5. XN-NF-82-49(P)(A) Revision 1, Supplement 1, *Exxon Nuclear Company Evaluation Model - EXEM PWR Small Break Model*, Siemens Power Company, December 1994.
6. XN-75-21(P)(A) Revision 2, *XCOBRA-IIIC: A Computer Code to Determine the Distribution of Coolant During Steady-State and Transient Core Operation*, Exxon Nuclear Company, January 1986.
7. XN-NF-81-58(P)(A) Revision 2 and Supplements 1 and 2, *RODEX2 Fuel Rod Thermal-Mechanical Response Evaluation Model*, Exxon Nuclear Company, March 1984.
8. ANF-81-58(P)(A) Revision 2 Supplements 3 and 4, *RODEX2 Fuel Rod Thermal Mechanical Response Evaluation Model*, Advanced Nuclear Fuels, June 1990.
9. NUREG/CR-0247, TREE-1208, *LOFT System and Test Description (5x5-ft Nuclear Core 1 LOCES)*, EG&G Idaho, Idaho Falls, ID 83415, July 1978.
10. NUREG/CR-1797, EGG-2067, *Experiment Data Report for LOFT Anticipated Transient Experiments L6-1, L6-2, and L6-3*, EG&G Idaho, Idaho Falls, ID 83415, December 1980.
11. NUREG/CR-1520, EGG-2045, *Experiment Data Report for LOFT Anticipated Transient Experiment L6-5*, EG&G Idaho, Idaho Falls, ID 83415, July 1980.
12. EGG-LOFT-1561, *Best Estimate Prediction for LOFT Nuclear Experiments L6-1, L6-2, L6-3, and L6-51*, EG&G Idaho, Idaho Falls, ID 83415, October 1980.
13. EGG-LOFT-5199, *Base Input for LOFT RELAP5 Calculations*, EG&G Idaho, Idaho Falls, ID 83415, July 1980.
14. EGG-LOFT-6159, *Posttest Analysis of LOFT Anticipated Transient Experiments L6-1, L6-2, L6-3, and L6-5*, EG&G Idaho, Idaho Falls, ID 83415, January 1983.
15. XN-NF-621(P)(A) Revision 1, *Exxon Nuclear DNB Correlation for PWR Fuel Designs*, Exxon Nuclear Company, September 1983.

16. EMF-92-153(P)(A) and Supplement 1, *HTP: Departure from Nucleate Boiling Correlation for High Thermal Performance Fuel*, Siemens Power Corporation, March 1994.
17. IN-1412, TID-4500, *A Correlation of Rod Bundle Critical Heat Flux for Water in the Pressure Range 150 to 725 psia*, Idaho Nuclear Corporation, July 1970.
18. L. Biasi et al., "Studies on Burnout, Part 3: A New Correlation for Round Ducts and Uniform Heating and Its Comparison with World Data," *Energia Nucleare*, Volume 14, Number 9, September 1967, pages 530 through 536.
19. ANF-84-73(P)(A) Revision 5, (Appendix B), *Advanced Nuclear Fuels Methodology For Pressurized Water Reactors: Analysis of Chapter 15 Events*, Advanced Nuclear Fuels Corporation, July 1990.
20. Regulatory Guide 1.77, *Assumptions Used for Evaluating a Control Rod Ejection Accident for Pressurized Water Reactors*, U.S. Nuclear Regulatory Commission, May 1974.
21. XN-NF-78-44(NP)(A), *A Generic Analysis of the Control Rod Ejection Transient for Pressurized Water Reactors*, Exxon Nuclear Company, October 1983.

Distribution

J. S. Holm, 26/USNRC (12)

email notification only

PWR Safety
PWR Neutronics
K. E. Carlson
H. Chow
R. E. Collingham
R. L. Feuerbacher
K. R. Greene
R. G. Grummer
S. E. Jensen
J. M. Kelly
R. P. Martin
A. B. Meginnis
L. D. O'Dell
D. W. Pruitt
R. S. Reynolds
R. I. Wescott